University Saad Dahlab of Blida 1

Faculty of Sciences

Physics Department

Master Thesis

Spinor helicity and unitarity methods for one-loop order amplitude computation

Prepared by: **Abderraouf BELALIA**

Defended on August 30, 2020 before the jury composed of:

Dr. M. SIDOUMOU	Prof.	University of Blida 1	President
Dr. S. A. YAHIAOUI	MCB	University of Blida 1	Examiner
Dr. N. BOUAYED	MCA	University of Blida 1	Co-Supervisor
Dr. A. YANALLAH	MCB	University of Blida 1	Supervisor

August 2020

Abstract

The growing precision of our experimental apparatus requires relevant advances in the accuracy of our theoretical cross-section computation. Implying that we need to be able to calculate multi-leg and/or multi-loop corrections to various amplitudes. The purpose of this thesis is to come to this aim and to demonstrate the affinity of the Spinor Helicity Formalism in dealing with *Next-to-leading order (NLO)* computations related to the QCD sector. We start by employing Helicity spinors in writing scattering amplitudes resulting in expressions with a high potential for simplifications, then introduce complex momenta to find a recursive method for building Helicity tree amplitudes and at last we used Generalized Unitarity to connect amplitudes in an order by order manner. The results were a generic one-loop formulation for Helicity amplitudes that is entirely determined through cut-coefficients along with a procedure for the extraction of box and triangle coefficients generalizable to the remaining ones. We found that cut-coefficients were built out of the product of Helicity tree amplitudes which themselves are constructed using lower-point amplitudes recursively, meaning that the NLO was ultimately linked to the kinematic 3-points of the theory and that even higher orders will necessarily employ available lower order found amplitudes.

الدقة المتزايدة لجهازنا التجريبي تتطلب تقدمًا ذو صلة في دقة الحساب النظري لمقطع التصادم. مما يعني أننا بحاجة إلى أن نكون قادرين على حساب تصحيحات متعددة الاطراف و / أو متعددة الحلقات لسعات مختلفة. الغرض من هذه المذكرة هو الوصول إلى هذا الهدف واظهار تقارب الشكلية الحلزونية السبينية في التعامل مع حسابات الترتيب التالي إلى الرائد (NLO) المتعلقة بقطاع QCD. نبدأ باستخدام السبينورات الحلزونية في كتابة السعات المتناثرة مما أدى إلى تعبيرات ذو إمكانيات عالية للتبسيط ، ثم إدخال ازخم معقدة للعثور على طريقة عودية لبناء سعات حلزونية دون حلقات وأخيرا استخدمنا الوحدودية المعممة لربط السعات بحيث كل رتبة ترتبط بالرتبة التي تليها. وكانت النتائج عبارة عن صياغة عامة ذات حلقة واحدة للسعات الحلزونية التي يتم تحديدها بالكامل من خلال معاملات القطع إلى جانب إجراء لاستخراج معامل box و triangle القابلة للتعميم على المعاملات المتبقية. وجدنا أن معاملات القطع بنيت من جداء سعات حلزونية دون حلقات التي هي بنفسها بنيت باستخدام سعات أقل رتبة بشكل عودي، وهذا يعني أن NLO كان مرتبطا في نهاية المطاف إلى 3-نقاط كينماتيكية الخاصة بالنظرية وأنه حتى الرتب الاعلى سوف توظف بالضرورة السعات المتاحة ذات الرتب الدنيا.

Keywords : High-energy physics, SM, QCD, Spinor Helicity Formalism, Helicity Amplitude, Complex momenta, Recursion formulae, NLO, Generalized Unitarity, On-shell cut-coefficients Extraction

Dedication

To my parents, who showed unconditional support and had faith in my choices.

To my grandparents, who always thought I'd achieve great things.

To my best friend and ally through life, M. ABDERRAOUF.

To the one who followed me through all the process and stood up with me at my best and worst times, H. NESRINE.

I will forever be grateful to all of you.

Contents

List of Figures

Introduction

The experimental paradigm followed for the Quantum Field Theory or QFT framework, is based on collision events and implemented in labs through the usage of particle accelerators meaning that from a theoretical perspective we are interested in cross-sections. The framework offers a computational technology for each of its sub-theories in-term of Feynman diagrams. These diagrams are used within a conventional procedural format called the "Trace method". To sum it up the method starts by drawing all possible tree diagrams contributing to a certain process and then write their contributions using the Feynman rules. We obtain the cross-section by summing over possible final states and averaging over initial ones which leads to the apparition of traces (hence the name of the method), then square the final amplitude giving us what the theorists termed the Leading Order (LO).

Seeking more precision required us to account for higher orders which ultimately would include loop-corrections. The first problem encountered there was the divergences arising from loop integrals, which was dealt with both mathematically through regularization procedures and at the phenomenological level employing renormalization schemes. But there was an even deeper problem proper to the method itself, that is, the growing complexity of intermediate step expressions compared to the simplicity of the final results. Meaning that even if the method works at some point it wouldn't be compatible with our computational capabilities putting us at standstill jokingly termed, "NLO[1] bottleneck".

The past recent years have witnessed the silent undergoing of a revolution in Quantum Field Theory, that affected our computational capabilities and opened the door for what was previously considered a tedious task. The origin of this revolution starts from wanting more compact ways to describe nature as a possible solution to deal with increasing intermediate complexity of expressions. That motivation on its own leads us to exploit the indistinguishability of Chirality, Helicity and Spin in the absence of mass[2] giving rise to Helicity formalism [1] exposed in the introductory work [2] done last year showing how this formalism offered an alternative way to compute LO amplitudes while demonstrating an outstanding efficiency. The complexity problem manifested by the Trace method was absent to the extent that one can conduct computations manually. The question that is central to our theme is, what kind of affinity can Helicity method exhibit in dealing with the NLO ?

In order to answer the previous question we start the first chapter of this work by an overview of QCD and Helicity formalism followed by concepts related to (LO) Helicity amplitudes. The second chapter will be marked by the introduction of complex momenta and probing their consequences as an implementation of on-shell ideas to internal states. The third chapter will provide the last piece to the puzzle coming from the Unitarity (both simple and generalized) constraint applied to the S-matrix linking loop and tree contributions via cut rules leading to a one-loop formulation of Helicity amplitudes in term of cut-coefficients. The fourth and final chapter will showcase all of the ideas gathered from previous chapters at work in computing one of the loop-coefficients that

---

[1] *Next-to Leading Order*

[2] See Appendix A.

is relevant to the $gg \longrightarrow gg$ process.

We supplement this work with three appendices treating of : Spinors and their related formulae, Group theoretic notions and at last Technologies used in the conduct of this project.

Chapter 1

Overview of QCD and Helicity Formalism

The usage of Helicity basis within the framework of Quantum Field Theory have lead us to step up the efficiency of our computational tools. While at first the usage was only constrained to high energy limits where the values of kinematic variables are so great that the mass becomes negligible, interesting additions supplied the formalism with a consistent way to embed mass. The application to QCD sector and especially the pure gluon processes revealed symmetries that weren't known by conventional means. All of this clues and discoveries are the temptation behind wanting to employ Helicity formalism more and more, to tackle problems which did put us at a standstill before.

1.1   Standard Model

The Standard Model has a respectable place in the realm of physics as the theory of fundamental constituents of the universe. The matter and its interactions are explained via a quantum field paradigm of packaging and exchanging information. Multiplet of states transforming under Poincare group are embedded in fields representative of what we call commonly, particles. The fermions with a half-integer spin are responsible for structure and order in nature since they obey the Pauli exclusion principle. The bosons with an integer spin are the carriers of information between fermionic structures leading them to interact within the range of action of fundamental forces. To put it bluntly, these bosons are our representation of how a fundamental force actually operates.

The model was developed in stages throughout history with the help of many physicists from both theoretic and experimental sides providing it with solid roots. One of the first motivations for it was the explanation of the strong interaction, for which CHEN NING YANG and ROBERT MILLS did extend the concept of a gauge theory from abelian to non-abelian groups, in other words, a generalization of Quantum Electrodynamics that we call a Yang-Mills theory. Later on SHELDON GLASHOW [3] unified the electromagnetic and weak interactions which was supplemented by the Higgs mechanism from STEVEN WEINBERG [4] and ABDUS SALAM [5] making the modern form of the Electroweak theory. The term "Standard Model" was used for the first time in 1975 compared to when the physicists started getting interested in the previous problems around 1954.

At the experimental level the theory was providing us with ways to single out signals corresponding to particles resulting from processes falling within the range of its predictions. The Large Hadron Collider is the arena where a lot of things played out and the reliability of the theory was tested to great extents. Passing these tests with a blatant success is one of the reasons this model is still around. One of the most known methods to compute amplitudes for events taking place in scattering experiments is the trace method based on the evaluation of tree Feynman diagrams. The calculations of leading-order contributions were easily automated and implemented both numeri-

cally and analytically, but taking the model further in its predictions requires us to access more precision by computing next-to-leading order corrections, namely the evaluation of loop diagrams correcting the previously known tree diagrams. This presented many challenges as most if not all of these loops weren't finite and thus couldn't be linked to something observable, leading us to adopt regularization procedures and renormalization schemes to deal with these infinities. Still the NLO was a very daunting task and a novel method was more than needed.

In order to present one of the most efficient methods for tackling the problem of not only the NLO but also to make LO calculations much easier, we will confine our discussion mainly with the QCD sector and use it to illustrate how the combination of Helicity formalism, On-shell and Unitarity methods along with ways to handle color, or the algebra part, combine to make our task more easier and flawless.

1.1.1 Quantum Chromodynamics Lagrangian

The Quantum Chromodynamics theory define the interaction between quarks and gluons. It is a special case of the Yang-Mills family with gauge symmetry group, $SU(3)$. While our examples will mainly involve this sector, it doesn't affect the generality of the ideas we are advancing. In what follows we will write the Lagrangian encoding all of the theory's dynamics and then extract the Feynman rules that will help us build process amplitudes which serve as a check against results we obtain through the Helicity Formalism.

The Dirac Lagrangian[1] coupled to the gluon field is given by,

$$\mathcal{L} = -\frac{1}{4}\left(F_{\mu\nu}^a\right)^2 - \frac{1}{2\xi}\left(\partial_\mu A_\mu^a\right)^2 + \left(\partial_\mu \overline{c}^a\right)\left(\delta^{ac}\partial_\mu + g_s f^{abc}A_\mu^b\right)c^c + \overline{\psi}_i\left(\delta_{ij}i\slashed{\partial} + g_s\slashed{A}^a - m\delta_{ij}\right)\psi_j. \quad (1.1)$$

The gluon strength field $F_{\mu\nu}^a$ writes in-term of the gauge fields A_μ^a, coupling constant g_s and the structure constants f^{abc} coming from the color algebra as,

$$F_{\mu\nu}^a = \partial_\mu A_\nu^a - \partial_\nu A_\mu^a + g_s f^{abc}A_\mu^b A_\nu^c. \quad (1.2)$$

The c^a and $\overline{c}^a$ are the Faddeev-Popov [7] ghosts and anti-ghosts respectively. And at last ψ_i and $\overline{\psi}_i$ are the Dirac fields for the quarks and anti-quarks.

1.1.2 Feynman rules

A Feynman diagram is an alternative way to write quantum amplitudes in the form of graphical representations. The basic components making a diagram are lines and vertices. The lines can be external when they have only one of their ends attached to a vertex or they could be internal in which case both of their ends are attached to vertices and they are termed propagators. External legs represent either incoming or outgoing particles depending on the direction of the time-flow which conventionally is taken to be from left to right. The propagators represent intermediate particles that won't show in the measurement but nonetheless they are the hidden mechanism behind the interaction represented by the diagram. The vertices are points of interaction where more than two lines representing quantum fields meet. In order to compute cross-sections we need to have the Feynman rules which are associations between a given graphical component and a factor entering in the expression of the amplitude. These rules are generally extracted from the Lagrangian of the theory. We'll just list down the ones that will be relevant to us.

---

[1]Section 26.1, [6]

- The Kinetic part of the Lagrangian provides us with the propagators[2],

$$\mathcal{L}_{kin} = -\frac{1}{4}\left(\partial_\mu A_\nu^a - \partial_\nu A_\mu^a\right)^2 - \frac{1}{2\xi}\left(\partial_\mu A_\mu^a\right)^2 + \overline{\psi}_i\left(i\not{\partial} - m\right)\psi_i - \overline{c}^a \,\square\, c^a. \tag{1.3}$$

Gluon propagator,

$$\nu, b \,\text{〰〰〰〰〰}\, \mu, a \qquad = \frac{-i}{p^2 + i\varepsilon}\left[g_{\mu\nu} - (1-\xi)\frac{p_\mu p_\nu}{p^2}\right]\delta^{ab}. \tag{1.4}$$

Ghost propagator,

$$b \,\cdots\!\!\!\rhd\!\!\!\cdots\, a \qquad = \frac{i}{p^2 + i\varepsilon}\delta^{ab}. \tag{1.5}$$

Colored spinor propagator,

$$j \,\longrightarrow\, i \qquad = \frac{i(\not{p}+m)}{p^2 - m^2 + i\varepsilon}\delta^{ij}. \tag{1.6}$$

The i, j refer to fundamental[3] color indices. The delta's force color conservation, "the color that comes in is the same as the color that comes out". We have to sum over color when these appear as intermediate states.

- We read the factors of the external legs from the solutions[4] of the Quantum fields,

$$\begin{aligned}
\psi_i(x) &= \sum_s \int \frac{d^3p}{(2\pi)^3}\frac{1}{\sqrt{2\omega_p}}\left(a_p^s u_p^s e^{-ipx} + b_p^{s\dagger} v_p^s e^{+ipx}\right) \\
\overline{\psi}_i(x) &= \sum_s \int \frac{d^3p}{(2\pi)^3}\frac{1}{\sqrt{2\omega_p}}\left(b_p^s \overline{v}_p^s e^{-ipx} + a_p^{s\dagger}\overline{u}_p^s e^{+ipx}\right)
\end{aligned} \tag{1.7}$$

In the case of quarks each external leg receives a spinor (u- or v-type) depending on the orientation of the particle flow and whether it is incoming or outgoing (unbarred or barred). The conventional direction of the particle flow is –to the right– so that antiparticles flow in the opposite direction and if arrow is entering toward the vertex of interaction then it is incoming while the opposite situation would be outgoing.

$$\begin{aligned}
&\,\longrightarrow\!\bullet && = u(p) \\
&\bullet\!\longrightarrow && = \overline{u}(p) \\
&\,\longleftarrow\!\bullet && = \overline{v}(p) \\
&\bullet\!\longleftarrow && = v(p)
\end{aligned} \tag{1.8}$$
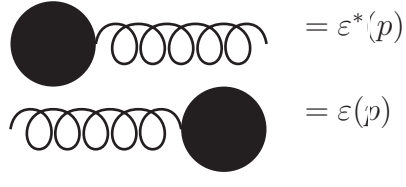
$$A_\mu^a(x) = \int \frac{d^3p}{(2\pi)^3}\frac{1}{\sqrt{2\omega_p}}\sum_{\lambda=\pm}\left(\epsilon_\mu^{a,\lambda}(p)a_{p,j}e^{-ipx} + \epsilon_\mu^{a,\lambda}(p)^* a_{p,j}^\dagger e^{+ipx}\right). \tag{1.9}$$

---

[2] Section 25.4, [6]

[3] See Appendix B

[4] Sections 23 and 8.4.2 in [6]

As for the gluons we only need to consider if the leg is incoming or outgoing.

$$= \varepsilon^*(p)$$

$$= \varepsilon(p)$$
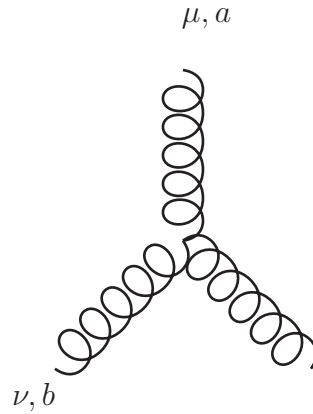
$$(1.10)$$

- The Interaction part of the Lagrangian provides us with vertices,

$$\mathcal{L}_{int} = -g f^{abc} \left(\partial_\mu A_\nu^a \right) A_\mu^b A_\nu^c - \frac{1}{4} g^2 \left(f^{eab} A_\mu^a A_\nu^b \right) \left(f^{ecd} A_\mu^c A_\nu^d \right) + g f^{abc} \left(\partial_\mu \bar{c}^a \right) A_\mu^b c^c + g A_\mu^a \overline{\psi}_i \gamma^\mu T_{ij}^a \psi_j.$$

$$(1.11)$$
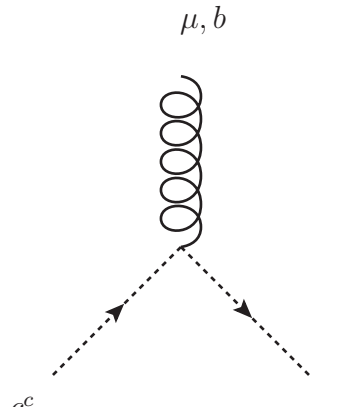
The three-gluon vertex is,

$$= g f^{abc} [g^{\mu\nu} (k-p)^\rho$$
$$+ g^{\nu\rho} (p-q)^\mu$$
$$+ g^{\rho\mu} (q-k)^\nu] \qquad .$$

$$(1.12)$$

Note that we use the convention [6] where all the momenta are incoming $k + q + p = 0$.
The ghost-antighost-gluon vertex,

$$= -g f^{abc} p^\mu.$$

$$(1.13)$$

The quark-quark-gluon vertex,

6

$$= ig\gamma^\mu T^a_{ij}.$$

(1.14)

And finally, the four-gluon vertex,

$$= -ig^2[f^{abe}f^{cde}\left(g^{\mu\rho}g^{\nu\sigma} - g^{\mu\sigma}g^{\nu\rho}\right)$$
$$+ f^{ace}f^{bde}\left(g^{\mu\nu}g^{\rho\sigma} - g^{\mu\sigma}g^{\nu\rho}\right)$$
$$+ f^{ade}f^{bce}\left(g^{\mu\nu}g^{\rho\sigma} - g^{\mu\rho}g^{\nu\sigma}\right)]$$

(1.15)

1.2   Helicity Formalism

In this section we lay the foundation upon which we'll undertake future calculations. Both the massless and the massive[5] cases are treated thoroughly. The detail behind the possibility of this formalism has been placed in Appendix A to keep the discussion lighter and the focus on relevant results. It is very important that one understands the massless formalism before proceeding with further reading as the massive case only builds on it and everything treated here could ultimately be expressed using massless spinors.

1.2.1   Massless case

The notation introduced in the Appendix A allows us to write any massless 4-momentum[6] in term of its Helicity spinors as,

---

[5] We include mass for fermions only, but the method can be generalized to bosons by updating their polarization vectors.

[6] In our calculations instead of giving different "labels", Latin symbols to momenta involved in the problem we'll adopt a format p^μ_i where the i reference which particle in the problem so that we can reduce the referencing just to i which is just an integer when using our Helicity spinors.

$$p^\mu = \frac{1}{2}\left[p\overline{\sigma}^\mu p\right\rangle = \frac{1}{2}\left\langle p\sigma^\mu p\right], \tag{1.16}$$

and its corresponding bi-spinors[7] or slashed matrices as, $p^{\alpha\dot\alpha} = p\rangle\,[p$ and $p_{\dot\alpha\alpha} = p]\,\langle p$.

The Lorentz contraction of two 4-vectors writes using both anti-symmetric inner products,

$$p \cdot q = \frac{1}{2}\left\langle pq\right\rangle\left[qp\right], \tag{1.17}$$

with $\langle pq\rangle = [qp]^\dagger$ for the case of real momenta.

A manipulation we can do with these Helicity spinors is using the fact that they are two-dimensional to write one spinor in terms of two others,

$$p\rangle = \frac{\langle pr\rangle}{\langle qr\rangle}\,q\rangle + \frac{\langle pq\rangle}{\langle rq\rangle}\,r\rangle, \tag{1.18}$$

after contraction with $\langle s$ and some rearrangements we obtain the *Shouten identity*,

$$\langle sp\rangle\langle qr\rangle + \langle sq\rangle\langle rp\rangle + \langle sr\rangle\langle pq\rangle = 0. \tag{1.19}$$

Momentum conservation generally writing as,

$$\left(\sum p\right)_{in} = \left(\sum p\right)_{out}, \tag{1.20}$$

becomes,

$$\sum_{incoming} i\rangle\,[i = \sum_{outgoing} i\rangle\,[i\,. \tag{1.21}$$

And if we take all momenta to be either "incoming" or "outgoing", it simplifies to,

$$\sum_i i\rangle\,[i = 0. \tag{1.22}$$

And in term of anti-symmetric products we have,

$$\sum_j \langle ij\rangle\,[jk] = 0. \tag{1.23}$$

By fixing the choice of whether we take external momenta all incoming or all outgoing, the *kinematic invariants* of our problem take a very simple form,

$$s_{ij} = (p_i + p_j)^2 = \overset{0}{\cancel{p_i^2}} + \overset{0}{\cancel{p_j^2}} + 2p_i \cdot p_j, \tag{1.24}$$

implying that,

$$s_{ij} = \langle ij\rangle\,[ji] = |\langle ij\rangle|^2 = |[ij]|^2\,. \tag{1.25}$$

In the case of $2 \longrightarrow 2$ scattering, the $s'_{ij}s$ will take the various values of $\{s, t, u\}$[8], satisfying the condition $s + t + u = 0$ which is another form of momentum conservation.

---

[7]See Appendix A.

[8]MandelStam variables, see [6].

8

- Dirac spinors appear when we are dealing with fermions, although the information they contain if we look at their components is just the square root of the contraction of the momentum with the sigmas which surprisingly resembles how we extract bi-spinors. We retrieve the full momentum via a product of two Dirac spinors in some fashion so that we get rid of the square root reducing the physical dimension by half. The point of this is to say that Dirac spinors can be very well handled by Helicity spinors. As the distinction between particle and antiparticles is blurred by masslessness, external physical states can either be left- or right-handed,

$$
\begin{aligned}
p\rangle &= P_L u(p) = P_L v(p) \\
p] &= P_R u(p) = P_R v(p)
\end{aligned} \tag{1.26}
$$

With a correspondence list [8] of this sort,

$$
\begin{aligned}
p\rangle &= u_-(p) = v_+(p) \\
p] &= u_+(p) = v_-(p) \\
\langle p &= \overline{u}_+(p) = \overline{v}_-(p) \\
[p &= \overline{u}_-(p) = \overline{v}_+(p)
\end{aligned} \tag{1.27}
$$

The problem we immediately notice is that while Dirac spinors are four dimensional objects the Helicity spinors are two dimensional, this leads us to look at an embedding which enables meaningful contraction with the $\gamma - matrix$ as it will appear regularly in calculations. To this issue we propose,

$$
p^-\rangle = \begin{pmatrix} p\rangle \\ 0 \end{pmatrix} \quad \langle^+ p = \begin{pmatrix} \langle p & 0 \end{pmatrix}
$$
$$
p^+\rangle = \begin{pmatrix} 0 \\ p] \end{pmatrix} \quad \langle^- p = \begin{pmatrix} 0 & [p \end{pmatrix} \tag{1.28}
$$

where the sign in the superscript refers to the Helicity projection.

A way to check if this redefinition captures essential properties, we first point out that the $\{p^-\rangle, p^+\rangle\}$ corresponding the unbarred spinors are related to the $\{\langle^- p, \langle^+ p\}$ by conjugation and multiplication by γ^0 which is what we look for in Dirac spinors[9]. The second thing is that it should reconstruct the momentum information correctly and match the position of the $\sigma's$ within the γ-matrix,

$$
p^-\rangle \langle^- p = \begin{pmatrix} 0 & p\rangle [p \\ 0 & 0 \end{pmatrix} \quad ; p^+\rangle \langle^+ p = \begin{pmatrix} 0 & 0 \\ p] \langle p & 0 \end{pmatrix}, \tag{1.29}
$$

where the Dirac matrix is given by,

$$
\gamma^\mu_{\{\alpha\dot\alpha\}} = \begin{pmatrix} 0 & \sigma^{\mu\alpha\dot\alpha} \\ \overline{\sigma}^\mu_{\dot\alpha\alpha} & 0 \end{pmatrix}. \tag{1.30}
$$

We see that the spinor indices matches correctly.

We can readily see that sandwich $\langle^+ q\gamma^\mu p^-\rangle$ vanishes and the same goes for $\langle^- q\gamma^\mu p^+\rangle$, the reason for this is the anti-diagonal form of γ. The product $\gamma^\mu\gamma^\nu$ has a diagonal form making $\langle^+ q\gamma^\mu\gamma^\nu p^-\rangle$ and $\langle^- q\gamma^\mu\gamma^\nu p^+\rangle$ different from zero. One can generalize this for product of odd-number and even-number of $\gamma's$,

$$
\begin{aligned}
\langle^+ q \{\gamma^\mu ...\}_{odd} p^-\rangle &= 0 = \langle^- q \{\gamma^\mu ...\}_{odd} p^+\rangle \\
\langle^+ q \{\gamma^\mu ...\}_{even} p^-\rangle &\neq 0 \neq \langle^- q \{\gamma^\mu ...\}_{even} p^+\rangle
\end{aligned} \tag{1.31}
$$

---

[9]See Appendix A.3

About the case where the sandwich involves similar Helicity states we have the opposite situation where it vanishes for a product of even-number of $\gamma's$, while in the case of an odd-number it doesn't,

$$\begin{aligned}\langle^+q\left\{\gamma^\mu...\right\}_{odd}p^+\rangle \neq 0 \neq \langle^-p\left\{\gamma^\mu...\right\}_{odd}q^-\rangle \\ \langle^+q\left\{\gamma^\mu...\right\}_{even}p^+\rangle = 0 = \langle^-p\left\{\gamma^\mu...\right\}_{even}q^-\rangle\end{aligned} \quad . \tag{1.32}$$

In our amplitude computation we'll make use of the convention of all "incoming" momenta, meaning that outgoing particles will have their Helicity flipped[10],

$$\begin{aligned}p\rangle : \left\{\begin{array}{c} u_-(p) : incoming \\ v_+(p) : outgoing \longrightarrow v_-(p) \end{array}\right\} \quad \langle p : \left\{\begin{array}{c} \bar{u}_+(p) : outgoing \longrightarrow \bar{u}_-(p) \\ \bar{v}_-(p) : incoming \end{array}\right\} \\ p] : \left\{\begin{array}{c} u_+(p) : incoming \\ v_-(p) : outgoing \longrightarrow v_+(p) \end{array}\right\} \quad [p : \left\{\begin{array}{c} \bar{u}_-(p) : outgoing \longrightarrow \bar{u}_+(p) \\ \bar{v}_+(p) : incoming \end{array}\right\}\end{aligned} \quad . \tag{1.33}$$

This convention associates negative Helicity $(-)$ solely with angle-brackets and positive Helicity $(+)$ with square ones,

$$\begin{aligned}p\rangle = u_-(p) = v_-(p) \\ p] = u_+(p) = v_+(p) \\ \langle p = \overline{u}_-(p) = \overline{v}_-(p) \\ [p = \overline{u}_+(p) = \overline{v}_+(p)\end{aligned} \quad , \tag{1.34}$$

leading to,

$$\begin{aligned}p^-\rangle = \left(\begin{array}{c} p\rangle \\ 0 \end{array}\right) \quad \langle^-p = \left(\begin{array}{cc} \langle p & 0 \end{array}\right) \\ p^+\rangle = \left(\begin{array}{c} 0 \\ p] \end{array}\right) \quad \langle^+p = \left(\begin{array}{cc} 0 & [p \end{array}\right)\end{aligned} \quad , \tag{1.35}$$

and

$$\begin{aligned}\langle^-q\left\{\gamma^\mu...\right\}_{odd}p^-\rangle = 0 = \langle^+q\left\{\gamma^\mu...\right\}_{odd}p^+\rangle \\ \langle^-q\left\{\gamma^\mu...\right\}_{odd}p^+\rangle \neq 0 \neq \langle^+p\left\{\gamma^\mu...\right\}_{odd}q^-\rangle\end{aligned} \quad . \tag{1.36}$$

The contribution of a fermionic line with one vertex of interaction or more will always vanish if the two external states have the same Helicities.

If we develop the object $\langle^-q\gamma^\mu p^+\rangle$ we get,

$$\langle^-q\gamma^\mu p^+\rangle = \left(\begin{array}{cc} \langle p & 0 \end{array}\right) \left(\begin{array}{cc} 0 & \sigma^\mu \\ \overline{\sigma}^\mu & 0 \end{array}\right) \left(\begin{array}{c} 0 \\ p] \end{array}\right) = \langle q\sigma^\mu p]. \tag{1.37}$$

Doing the same for $\langle^+p\gamma^\mu q^-\rangle$,

$$\langle^+p\gamma^\mu q^-\rangle = \left(\begin{array}{cc} 0 & [p \end{array}\right) \left(\begin{array}{cc} 0 & \sigma^\mu \\ \overline{\sigma}^\mu & 0 \end{array}\right) \left(\begin{array}{c} p\rangle \\ 0 \end{array}\right) = [p\overline{\sigma}^\mu q\rangle. \tag{1.38}$$

Via a simple demonstration we can show that the two previous results are equal, we summarize everything in the following identity[11],

---

[10]We need to keep in mind that the physical Helicity of outgoing particles is always the inverse of what we compute.

[11]Notice that we didn't flip any of the Helicities according to our convention we just pointed out the equivalence between the two ways of writing since the internal mechanisms we did set, select the correct sigma matrix to do the translation.

$$\left\langle^-q\gamma^\mu p^+\right\rangle = \langle q\sigma^\mu p] = [p\overline{\sigma}^\mu q\rangle = \left\langle^+p\gamma^\mu q^-\right\rangle . \tag{1.39}$$

In the case where we have a product of two of these, the result makes up for the first form of the Fierz identity,

$$\left\langle^+p\gamma^\mu q^-\right\rangle \left\langle^-r\gamma_\mu s^+\right\rangle = [p\overline{\sigma}^\mu q\rangle \langle r\sigma^\mu s] = 2 \left\langle rq\right\rangle [ps] . \tag{1.40}$$

By setting $q = p$ and $r = s$, and recalling that $p_\mu = \frac{1}{2} [p\overline{\sigma}_\mu p\rangle = \frac{1}{2} \left\langle^+p\gamma^\mu p^-\right\rangle$,

$$p \cdot s = \frac{1}{2} \left\langle^+p\gamma^\mu p^-\right\rangle \frac{1}{2} \left\langle^-s\gamma_\mu s^+\right\rangle = \frac{1}{2} \left\langle sp\right\rangle [ps] , \tag{1.41}$$

proving the consistency of the formalism[12]. Another form of the Fierz Identity is given below,

$$\gamma^\mu \left\langle^+p\gamma_\mu q^-\right\rangle = 2 \left\{ q^-\right\rangle \left\langle^+p + p^+\right\rangle \left\langle^-q \right\} , \tag{1.42}$$

which one can employ to have the representation of the *slashed* momentum,

$$\cancel{k} = \gamma \cdot k = \frac{1}{2}\gamma^\mu \left\langle^+k\gamma_\mu k^-\right\rangle \Longrightarrow \cancel{k} = \left[k^-\right\rangle \left\langle^+k + k^+\right\rangle \left\langle^-k \right] , \tag{1.43}$$

so that,

$$\langle p\cancel{k}q] = \langle pk\rangle [kq] . \tag{1.44}$$

- Polarization vectors arise in amplitudes when bosons appear on the external legs. Helicity states for external bosons coincide with circular polarizations. These polarizations satisfy the following physical conditions,

$$\begin{array}{c} \varepsilon_\mu(p) \left(\varepsilon^\mu(p)\right)^* = -1 \\ p^\mu \varepsilon_\mu(p) = 0 \end{array} . \tag{1.45}$$

Polarization vectors are objects with a space-time index and for a fixed momentum $p^\mu = (E, 0, 0, E)$ they write as,

$$\varepsilon_+^\mu = \frac{1}{\sqrt{2}} (0, 1, i, 0) \quad \varepsilon_-^\mu = \frac{1}{\sqrt{2}} (0, 1, -i, 0) . \tag{1.46}$$

For these to accept a conversion, not only they have to fulfill the physical polarization conditions being normalization $\varepsilon^* \cdot \varepsilon = -1$ and transversality $p \cdot \varepsilon = 0$, but also $\varepsilon \cdot \varepsilon = 0$.

In order to decompose polarizations we introduce another light-like momenta r^μ, called the reference momentum which is "arbitrary"[13] except that it shouldn't be aligned with p^μ,

$$\varepsilon_\mu^+(p;r) = \frac{\langle r\gamma_\mu p]}{\sqrt{2}\langle rp\rangle} \quad \varepsilon_\mu^-(p;r) = \frac{[r\gamma_\mu p\rangle}{\sqrt{2}[pr]} . \tag{1.47}$$

The corresponding bi-spinors are,

$$\begin{array}{c} \left[\varepsilon_p^-(r)\right]^{\alpha\dot\alpha} = \sqrt{2}\frac{p\rangle[r}{[pr]} \\ \left[\varepsilon_p^+(r)\right]^{\alpha\dot\alpha} = \sqrt{2}\frac{r\rangle[p}{\langle rp\rangle} \end{array} . \tag{1.48}$$

At this point we can use all the tools previously developed to handle polarizations through their new form.

---

[12] Confirming what we previously did set in the "Momentum" section.

[13] It is convenient to choose the reference momentum as another momentum in the problem and best exploit its arbitrariness to make simplifications.

Since all indices are contracted within an amplitude, no vector or spinor can be found with a free index. In order to prepare for upcoming computations in the next section we work out various contractions that can appear,

$$
\begin{aligned}
\varepsilon_p^+(r) \cdot \varepsilon_q^+(s) &= \frac{\langle rs \rangle [qp]}{\langle rp \rangle \langle sq \rangle} \\
\varepsilon_p^-(r) \cdot \varepsilon_q^-(s) &= \frac{\langle pq \rangle [sr]}{[pr][qs]} \quad , \\
\varepsilon_p^-(r) \cdot \varepsilon_q^+(s) &= \frac{\langle ps \rangle [qr]}{[pr]\langle sq \rangle}
\end{aligned}
\tag{1.49}
$$

$$
\begin{aligned}
\varepsilon_p^-(r) \cdot q &= \frac{1}{\sqrt{2}} \frac{\langle pq \rangle [qr]}{[pr]} \\
\varepsilon_p^+(r) \cdot q &= \frac{1}{\sqrt{2}} \frac{[pq]\langle qr \rangle}{\langle rp \rangle}
\end{aligned} \quad .
\tag{1.50}
$$

$$
\begin{aligned}
\not{\varepsilon}_p^+(r) &= \frac{\sqrt{2}}{\langle rp \rangle}\, [r\rangle\, [p + p\, \langle r] \\
\not{\varepsilon}_p^-(r) &= \frac{\sqrt{2}}{[pr]}\, [p\rangle\, [r + r\, \langle p]
\end{aligned}
\tag{1.51}
$$

1.2.2 Massive case

While the Helicity formalism requires masslessness in order to be of effect, there is a way to encode the mass information using a technique called Light Cone Decomposition, or LCD [9]. In this, we employ two massless 4-vectors in order to construct a massive one, our requirement is that this massive[14] 4-vector's norm should be equal to the mass squared. Under a generic form [10]leaving the space-time indices implicit we'd have,

$$
p_I = \alpha p_i + \beta \eta_I.
\tag{1.52}
$$

Where the p_I is the massive 4-vector, p_i its *associated* massless 4-vector and η_I, the *reference* vector which has to fulfill $p_i \cdot \eta_I \neq 0$ other than that, it is arbitrary. α and β are left for us to set in order to embed the mass. In what follows we set both of these to $\alpha = 1$ and $\beta = \frac{m^2}{2p_i \cdot \eta_I}$ as this choice appear in many references [10][11][12].

$$
p_I = p_i + \frac{m^2}{2p_i \cdot \eta_I} \eta_I,
\tag{1.53}
$$

Squaring up this quantity we obtain $p_I^2 = m_I^2$.

With the mass back, few of the simplifications we had won't be of effect anymore. First, spin states will not coincide with Helicity states anymore. Second, particles and antiparticles are now distinguishable and instead of just 4 possible states, we have 8. At last, the dimensionality of the spinors should revert back to four, since mass will mix between left- and right-handed states.

Starting from the Dirac equation [11],

$$
(\not{p}_I - m_I)\, u_\pm(p_I) = 0.
\tag{1.54}
$$

We seek solutions that account for both mass signs and use the reference momentum as the axis along which the two spin states are taken. A nice format was proposed in [10],

$$
\begin{aligned}
u_\mp(p_I) &= \frac{(\not{p}_I + m_I)\left|\eta_I^\pm\right\rangle}{\left\langle \mp i | \eta_I^\pm \right\rangle} & \overline{u}_\pm(p_I) &= \frac{\left\langle \mp \eta_I \right| (\not{p}_I + m_I)}{\left\langle \mp \eta_I | i^\pm \right\rangle} \\
v_\pm(p_I) &= \frac{(\not{p}_I - m_I)\left|\eta_I^\pm\right\rangle}{\left\langle \mp i | \eta_I^\pm \right\rangle} & \overline{v}_\mp(p_I) &= \frac{\left\langle \mp \eta_I \right| (\not{p}_I - m_I)}{\left\langle \mp \eta_I | i^\pm \right\rangle}
\end{aligned} \quad .
\tag{1.55}
$$

---

[14]The massive 4-vectors will be denoted using a capitalized index label.

We can easily check that these solutions gets annihilated via the Dirac operator as the product $(\not{p}_I - m_I)(\not{p}_I + m_I)$ vanishes due to $\not{p}_I^2 = p_I^2 = m_I^2$.

If we explicit [12] the solutions by replacing p_I with its expression involving its associated momentum and reference momentum then substituting for their slashed versions we get,

$$
\begin{aligned}
|I_+\rangle &= \begin{pmatrix} |i\rangle \\ \frac{m}{[i\eta_I]}|\eta_I] \end{pmatrix} = u_-(p_I) & |I_+] &= \begin{pmatrix} \frac{m}{\langle i\eta_I\rangle}|\eta_I\rangle \\ |i] \end{pmatrix} = u_+(p_I) \\
[_+I| &= \begin{pmatrix} \frac{m}{\langle \eta_I i\rangle}\langle \eta_I| & [i| \end{pmatrix} = \overline{u}_-(p_I) & \langle_+I| &= \begin{pmatrix} \langle i| & \frac{m}{[\eta_I i]}[\eta_I| \end{pmatrix} = \overline{u}_+(p_I) \\
|I_-\rangle &= \begin{pmatrix} |i\rangle \\ \frac{-m}{[i\eta_I]}|\eta_I] \end{pmatrix} = v_+(p_I) & |I_-] &= \begin{pmatrix} \frac{-m}{\langle i\eta_I\rangle}|\eta_I\rangle \\ |i] \end{pmatrix} = v_-(p_I) \\
[_-I| &= \begin{pmatrix} \frac{-m}{\langle \eta_I i\rangle}\langle \eta_I| & [i| \end{pmatrix} = \overline{v}_+(p_I) & \langle_-I| &= \begin{pmatrix} \langle i| & \frac{-m}{[\eta_I i]}[\eta_I| \end{pmatrix} = \overline{v}_-(p_I)
\end{aligned}
\tag{1.56}
$$

The subscript $\pm$ is the mass sign corresponding to the two possible signs of mass associated with particles and antiparticles. The two spin states are referred to in the notation as the angle-/square-bracket decorations.

Now that we have our basic objects we need to workout their products. Unlike what we had previously the massive products [11] count four kinds which are all related to massless anti-symmetric products,

$$
\begin{aligned}
\langle IJ\rangle &= \langle ij\rangle \\
[IJ] &= [ij] \\
\langle IJ] &= \left(\frac{m_I}{s_{i\eta}} + \frac{m_J}{s_{j\eta}}\right)\langle i\eta j] , \\
[IJ\rangle &= \left(\frac{m_I}{s_{i\eta}} + \frac{m_J}{s_{j\eta}}\right)[i\eta j\rangle
\end{aligned}
\tag{1.57}
$$

where we choose $\eta_I = \eta_J = \eta$ for simplicity.

We previously employed the spinors associated to a momentum in order to write it using a spinor chain involving the $\gamma - matrix$, in this fashion, $k^\mu = \frac{1}{2}[k\gamma^\mu k\rangle$ where k^μ is a massless 4-vector. If our mass embedding is correct, we should be able to do the same and employing one of the Fierz identities check if the norm amount the mass squared with the appropriate mass sign. We start with, $K^\mu = \frac{1}{2}[_\pm K\gamma^\mu K_\pm\rangle$ and attempt to write it using only its massless constituents,

$$
[_\pm K\gamma^\mu K_\pm\rangle = \frac{1}{2}\left\{\pm\frac{m_K^2}{s_{\eta k}}[\eta\gamma^\mu\eta\rangle + [k\gamma^\mu k\rangle\right\},
\tag{1.58}
$$

with η being the reference vector and k the associated vector. Computing k^2 implies the contraction of the previous formula with itself where the only term that survives is $\pm\frac{m^2}{s_{\eta k}}[\eta\gamma^\mu\eta\rangle[k\gamma_\mu k\rangle$ preceded with a factor of 2, leading to $K^2 = \pm m_K^2$.

The fact that objects of this form $[\square\gamma^\mu\square\rangle$ in the massive case reduce to an expression in term of their massless counterparts, we can seek the most general form involving different massive spinors which efficiently reduce to the previous known results. In doing that we find,

$$
[_\pm P\gamma^\mu K_\pm\rangle = \frac{(\pm m_P)(\pm m_K)}{\langle\eta_P p\rangle[k\eta_K]}[\eta_K\gamma^\mu\eta_P\rangle + [p\gamma^\mu k\rangle ,
\tag{1.59}
$$

with the same freedom in writing, $[_\pm P\gamma^\mu K_\pm\rangle = \langle_\pm K\gamma^\mu P_\pm]$ as we had in the massless case. The first Fierz identity for the massive case is a bit more complicated due to the addition of reference momenta. While this looks daunting we can induce a lot of simplification with a good choice of reference,

$$
\begin{aligned}
\left[{}_{\pm}P\gamma^\mu K_\pm\right\rangle\left\langle{}_{\pm}S\gamma^\mu R_\pm\right] =& \frac{(\pm m_P)\,(\pm m_K)\,(\pm m_S)\,(\pm m_R)}{\langle\eta_P p\rangle\,[k\eta_K]\,\langle\eta_S s\rangle\,[r\eta_R]}\,\langle\eta_S\eta_P\rangle\,[\eta_K\eta_R] \\
&+ \frac{(\pm m_P)\,(\pm m_K)}{\langle\eta_P p\rangle\,[k\eta_K]}\,\langle r\eta_P\rangle\,[\eta_K s] \\
&+ \frac{(\pm m_S)\,(\pm m_R)}{\langle\eta_S s\rangle\,[r\eta_R]}\,\langle\eta_S k\rangle\,[p\eta_R] \\
&+ \langle rk\rangle\,[ps]
\end{aligned}
\tag{1.60}
$$

The second form of the Fierz is a contraction with a $\gamma - matrix$,

$$
\begin{aligned}
\gamma_\mu\left[{}_{\pm}P\gamma^\mu K_\pm\right\rangle =& 2\frac{(\pm m_P)\,(\pm m_K)}{\langle\eta_P p\rangle\,[k\eta_K]}\,(\eta_P\rangle\,[\eta_K + \eta_K]\,\langle\eta_P) \\
&+ 2\,(k\rangle\,[p + p]\,\langle k)
\end{aligned}
\tag{1.61}
$$

We so far worked using the convention that all momenta are taken to be incoming and that lead us to readjust the polarizations for outgoing ones,

$$
\left\{
\begin{array}{c}
u_-(p_I) : incoming \\
v_+(p_I) : outgoing \longrightarrow v_-(p_I) \\
u_+(p_I) : incoming \\
v_-(p_I) : outgoing \longrightarrow v_+(p_I)
\end{array}
\right\}
\left\{
\begin{array}{c}
\bar u_+(p_I) : outgoing \longrightarrow \bar u_-(p_I) \\
\bar v_-(p_I) : incoming \\
\bar u_-(p_I) : outgoing \longrightarrow \bar u_+(p_I) \\
\bar v_+(p_I) : incoming
\end{array}
\right\}.
\tag{1.62}
$$

So that the list gets rewritten this way,

$$
\begin{aligned}
|I_+\rangle = \begin{pmatrix} |i\rangle \\ \frac{m}{[i\eta_I]}|\eta_I] \end{pmatrix} = u_-(p_I) && |I_+] = \begin{pmatrix} \frac{m}{\langle i\eta_I\rangle}|\eta_I\rangle \\ |i] \end{pmatrix} = u_+(p_I) \\
[{}_+I| = \begin{pmatrix} \frac{m}{\langle\eta_I i\rangle}\langle\eta_I| & [i| \end{pmatrix} = \overline{u}_+(p_I) && \langle{}_+I| = \begin{pmatrix} \langle i| & \frac{m}{[\eta_I i]}[\eta_I| \end{pmatrix} = \overline{u}_-(p_I) \\
|I_-\rangle = \begin{pmatrix} |i\rangle \\ \frac{-m}{[i\eta_I]}|\eta_I] \end{pmatrix} = v_-(p_I) && |I_-] = \begin{pmatrix} \frac{-m}{\langle i\eta_I\rangle}|\eta_I\rangle \\ |i] \end{pmatrix} = v_+(p_I) \\
[{}_-I| = \begin{pmatrix} \frac{-m}{\langle\eta_I i\rangle}\langle\eta_I| & [i| \end{pmatrix} = \overline{v}_+(p_I) && \langle{}_-I| = \begin{pmatrix} \langle i| & \frac{-m}{[\eta_I i]}[\eta_I| \end{pmatrix} = \overline{v}_-(p_I)
\end{aligned}
\tag{1.63}
$$

The very last consistency check we need to perform is recovering the closure formula[15]. The relevance of this – while still obscure right now – is of capital importance to ensure that the embedding doesn't violate Unitarity and is compatible with the recursion-procedure[16], as the sum over polarizations should reconstruct the numerator of the the propagator correctly[17],

$$
\sum_{s=\pm} u_s(p)\overline{u}_s(p) = \not{p}_I + m.
\tag{1.64}
$$

Using the explicit forms of the $u - spinors$,

---

[15]See Appendix A.
[16]Subject of the next Chapter.
[17]Page 460, [6].

$$\sum_{s=\pm} u_s(p_I)\overline{u}_s(p_I) = |I_+\rangle\,[I_+| + |I_+]\,\langle I_+|$$

$$= \begin{pmatrix} |i\rangle \\ \frac{m}{[i\eta_I]}|\eta_I] \end{pmatrix} \begin{pmatrix} \frac{m}{\langle \eta_I i\rangle}\langle \eta_I| & [i| \end{pmatrix}$$

$$+ \begin{pmatrix} \frac{m}{\langle i\eta_I\rangle}|\eta_I\rangle \\ |i] \end{pmatrix} \begin{pmatrix} \langle i| & \frac{m}{[\eta_I i]}[\eta_I| \end{pmatrix} \qquad (1.65)$$

$$= \begin{pmatrix} \left\{ \frac{m}{\langle \eta_I i\rangle}|i\rangle\langle \eta_I| + \frac{m}{\langle i\eta_I\rangle}|\eta_I\rangle\langle i| \right\} & \left\{ |i\rangle[i| + \frac{m^2}{\langle i\eta_I\rangle[\eta_I i]}|\eta_I\rangle[\eta_I| \right\} \\ \left\{ \frac{m^2}{[i\eta_I]\langle \eta_I i\rangle}|\eta_I]\langle \eta_I| + |i]\langle i| \right\} & \left\{ \frac{m}{[i\eta_I]}|\eta_I][i| + \frac{m}{[\eta_I i]}|i][\eta_I| \right\} \end{pmatrix}$$

We can readily identify the anti–diagonal with $\not{p}_I$ recalling that, $p_I = p_i + \frac{m^2}{2 p_i\cdot \eta_I}\eta_I$. While the diagonal part should be identified with $m\mathcal{I}$[18] written as,

$$m\begin{pmatrix} 1 & 0 \\ 0 & 1 \end{pmatrix} = m\begin{pmatrix} \frac{1}{\langle \eta_I i\rangle}|i\rangle\langle \eta_I| + \frac{1}{\langle i\eta_I\rangle}|\eta_I\rangle\langle i| & 0 \\ 0 & \frac{1}{[i\eta_I]}|\eta_I][i| + \frac{1}{[\eta_I i]}|i][\eta_I| \end{pmatrix}. \qquad (1.66)$$

Implying two things,

1. $\frac{1}{\langle \eta_I i\rangle}|i\rangle\langle \eta_I| + \frac{1}{\langle i\eta_I\rangle}|\eta_I\rangle\langle i| = 1$.

2. $\frac{1}{[i\eta_I]}|\eta_I][i| + \frac{1}{[\eta_I i]}|i][\eta_I| = 1$.

Making sense of these two implications requires us to put them in a context and see if we can get something meaningful. We choose to inject the 1 inside the anti-symmetric products likewise,

$$\begin{array}{l} \langle j1k\rangle = \frac{1}{\langle \eta_I i\rangle}\langle ji\rangle\langle \eta_I k\rangle + \frac{1}{\langle i\eta_I\rangle}\langle j\eta_I\rangle\langle ik\rangle \\ [j1k] = \frac{1}{[i\eta_I]}[j\eta_I][ik] + \frac{1}{[\eta_I i]}[j\eta_I][ik] \end{array} \qquad (1.67)$$

And this is without mistake the two version of the Shouten identity both for left- and right-handed cases.

1.3 Helicity Amplitudes

Helicity amplitudes result from the translation of the expressions we get via Feynman rules[19] in term of Helicity spinors. The generic structure of a QCD amplitude is comprised of a color algebra part and an kinematic part. From the next chapter and on, we'll make use of a technique explained in Appendix B to handle the color algebra, while in this chapter we deal with it in the conventional way to make the need of an alternative evident. The kinematic part can contain momenta, Dirac spinors and Polarization vectors. All of which accept a form involving Helicity spinors. In this section, we'll take as an object of study the LO contribution of $gg \longrightarrow gg$, pure gluon process to emphasize properties behind the efficiency of calculation as we'll be able to produce the cross-section in just few steps.

---

[18]$\mathcal{I}$ is the 4x4 matrix made with two diagonal blocks of 2x2 identity matrices.
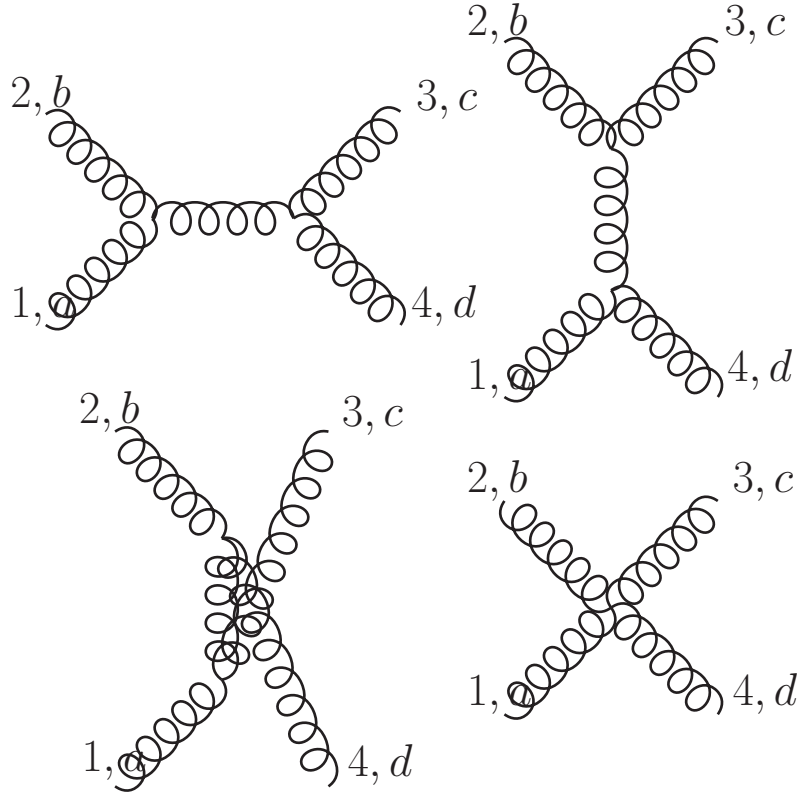
[19]See the first section of this chapter.

Figure 1.1: All tree diagrams contributing to the LO with a clockwise ordering of labels.

$$
\begin{aligned}
i\mathcal{A}_s^{tree}(1,2,3,4) &= -i\frac{g_s^2}{s}f^{abe}f^{cde}\left[(\varepsilon_1\cdot\varepsilon_2)(p_1-p_2)_\mu - 2(\varepsilon_1)_\mu(\varepsilon_2\cdot p_1) + 2(\varepsilon_2)_\mu(\varepsilon_1\cdot p_2)\right] \\
&\quad\times\left[(\varepsilon_3\cdot\varepsilon_4)(p_3-p_4)^\mu - 2(\varepsilon_3)^\mu(\varepsilon_4\cdot p_3) + 2(\varepsilon_4)^\mu(\varepsilon_3\cdot p_4)\right] \\
i\mathcal{A}_t^{tree}(1,2,3,4) &= -i\frac{g_s^2}{t}f^{ade}f^{cbe}\left[(\varepsilon_1\cdot\varepsilon_4)(p_1-p_4)_\mu + 2(\varepsilon_4)_\mu(\varepsilon_1\cdot p_4) - 2(\varepsilon_1)_\mu(\varepsilon_4\cdot p_1)\right] \\
&\quad\times\left[(\varepsilon_2\cdot\varepsilon_3)(p_3-p_2)^\mu + 2(\varepsilon_2)^\mu(\varepsilon_3\cdot p_2) - 2(\varepsilon_3)^\mu(\varepsilon_2\cdot p_3)\right] \\
i\mathcal{A}_u^{tree}(1,2,3,4) &= -i\frac{g_s^2}{u}f^{ace}f^{dbe}\left[(\varepsilon_1\cdot\varepsilon_3)(p_1-p_3)_\mu + 2(\varepsilon_3)_\mu(\varepsilon_1\cdot p_3) - 2(\varepsilon_1)_\mu(\varepsilon_3\cdot p_1)\right] \\
&\quad\times\left[(\varepsilon_2\cdot\varepsilon_4)(p_4-p_2)^\mu + 2(\varepsilon_2)^\mu(\varepsilon_4\cdot p_2) - 2(\varepsilon_4)^\mu(\varepsilon_2\cdot p_4)\right] \\
i\mathcal{A}_{4-p}^{tree}(1,2,3,4) &= -ig_s^2\{f^{bce}f^{ade}\left((\varepsilon_1\cdot\varepsilon_2)(\varepsilon_3\cdot\varepsilon_4) - (\varepsilon_2\cdot\varepsilon_4)(\varepsilon_1\cdot\varepsilon_3)\right) \\
&\quad +f^{bae}f^{cde}\left((\varepsilon_2\cdot\varepsilon_3)(\varepsilon_1\cdot\varepsilon_4) - (\varepsilon_2\cdot\varepsilon_4)(\varepsilon_1\cdot\varepsilon_3)\right) \\
&\quad +f^{bde}f^{cae}\left((\varepsilon_2\cdot\varepsilon_3)(\varepsilon_1\cdot\varepsilon_4) - (\varepsilon_1\cdot\varepsilon_2)(\varepsilon_3\cdot\varepsilon_4)\right)\}
\end{aligned}
\tag{1.68}
$$

1.3.1 Maximum Helicity Violating Amplitudes

We start by noticing something about these amplitudes, that is, every term contains at least one contraction of two polarizations. If suppose we take all Helicities positive and recalling that,

$$
\varepsilon_p^+(r)\cdot\varepsilon_q^+(s) = \frac{\langle rs\rangle[qp]}{\langle rp\rangle\langle sq\rangle},
\tag{1.69}
$$

which is the term that will at least appear once in every term. We can choose all reference momenta to be same and the previous product vanishes in all previous amplitudes. And since two amplitudes related by parity conjugation have the exact same contribution needless to say that we'd have the same result if all Helicities were negative. Interestingly this holds for an arbitrary number of legs and one can see that by considering the fact that the contributing bits to make

16

these diagrams are 3-point vertex, 4-point vertex, adding to it the fact that the 3-point vertex contributes with just one factor of momentum in each terms where the 4-point vertex provides with none, we always have fewer vertices than external legs in a diagram, there would naturally be at least one polarization contraction in each term guaranteeing the vanishing of the amplitude for any number of legs.

If one of the Helicities is negative while all others are positive we'd have $\varepsilon_p^+(r) \cdot \varepsilon_q^+(s)$ and $\varepsilon_p^-(r) \cdot \varepsilon_q^+(s)$ with,

$$\varepsilon_p^-(r) \cdot \varepsilon_q^+(s) = \frac{\langle ps \rangle \, [qr]}{[pr] \, \langle sq \rangle}. \tag{1.70}$$

If "reference momentum" for the positive Helicity is set to be the "momentum" of the negative Helicity, the previous vanishes, and so for us to have every term vanish we set all reference momenta except that of the negative[20] Helicity polarization to equal its momentum. We can generalize[21] this by saying that, amplitudes with all but one positive (or all but one negative) Helicity vanish at tree level for any number of external legs greater than three[22].

Starting from two Helicities that are negative while the rest is positive and on, we'd have terms involving $\varepsilon_p^+(r) \cdot \varepsilon_q^+(s)$, $\varepsilon_p^-(r) \cdot \varepsilon_q^+(s)$ and $\varepsilon_p^-(r) \cdot \varepsilon_q^-(s)$. And by a simple reasoning one can tell that there is no possible choice that makes all the terms vanish at the same time. Our conclusion is that starting from having "all but two Helicities" situations the amplitudes won't vanish, and they make what we call "Maximum Helicity Violating" amplitudes, $MHV's$. Beyond this case we get to what is called Next-to-Maximum Helicity Violating[23], $NMHV$. We can think of it as spectrum where at first we have the vanishing amplitudes that we spoke about as being "all" and "all but one" situations. Then, $MHV's$ being the first non-vanishing kind of amplitudes, "all but two" and then different "orders" that for the sake of clarity are referred to in the literature as $NMHV$: "all but three", N^2MHV : "all but four", etc.

To sum up all we have to compute for the pure gluon scattering are the MHV amplitudes. The diagrams will have contributions with the exception of the 4-point diagram since we can always find a choice of reference momenta to make it vanish.

1.3.2 Crossing symmetry

An interesting symmetry that originates from our deliberate choice of labeling the external legs, enables us to link the different amplitude expressions by moving the labels around. The s, t and u channels can now be related via what we call "crossing symmetry",

1. $s \leftrightarrow t$, colors : $b \leftrightarrow d$, polarizations :$2 \leftrightarrow 4$.

2. $s \leftrightarrow u$, colors : $b \leftrightarrow c$, polarizations : $2 \leftrightarrow 3$.

3. $t \leftrightarrow u$, colors : $d \leftrightarrow c$, polarizations: $3 \leftrightarrow 4$.

With the Mandelstam variables written explicitly as follows,

---

[20]There is no need to choose a reference momentum for the negative polarization since its term vanishes just because of our choice regarding the positive polarization

[21]Section 27.2, [6].

[22]The 3-point amplitude with all but one configuration doesn't vanish in the case of complex momenta, refer to the next chapter.

[23]Another note I want to add is that these situations cannot arise except if a certain number of external legs is available. An example, would be suppose we are looking for the $NMHV$ in a four-leg process well there is no way to get it because that would be just the trivially vanishing "all but one" situation.

$$
\begin{aligned}
s &= (p_1 + p_2)^2 \\
t &= (p_1 + p_4)^2 \\
u &= (p_1 + p_3)^2
\end{aligned}
. \tag{1.71}
$$

Such property reduces the workload as we only have to compute fewer amplitudes and then generate the remaining ones by moving the labels around.

1.3.3 Application

Now to the different $MHVs$, we can have: $\{(--++),(-+-+),(-++-)\}$ and their parity conjugate which as we said before provide the same contribution.

We'll first work $\mathcal{A}^{tree}_{gg \longrightarrow gg}(1^-, 2^-, 3^+, 4^+)$ where,

$$
\mathcal{A}^{tree}_{gg \longrightarrow gg}(1,2,3,4) = \mathcal{A}^{tree}_s(1,2,3,4) + \mathcal{A}^{tree}_t(1,2,3,4) + \mathcal{A}^{tree}_u(1,2,3,4). \tag{1.72}
$$

We choose our reference momenta to be $r_1 = r_2 = p_4$ and $r_3 = r_4 = p_1$. This choice kills all contractions except $\varepsilon_2^- \cdot \varepsilon_3^+$.

The $s - channel$ diagram, has only one surviving term,

$$
i\mathcal{A}^{tree}_s(1^-, 2^-, 3^+, 4^+) = i\frac{4g_s^2}{s} f^{abe} f^{cde} \left[\left(\varepsilon_1^- \cdot p_2 \right) \left(\varepsilon_4^+ \cdot p_3 \right) \left(\varepsilon_2^- \cdot \varepsilon_3^+ \right) \right],
$$

and using the previous relations,

$$
\begin{aligned}
\varepsilon_1^- (4) \cdot p_2 &= \tfrac{1}{\sqrt{2}} \tfrac{\langle 12 \rangle [24]}{[14]} \\
\varepsilon_4^+ (1) \cdot p_3 &= \tfrac{1}{\sqrt{2}} \tfrac{[43]\langle 31 \rangle}{\langle 14 \rangle} \\
\varepsilon_2^- (4) \cdot \varepsilon_3^+ (1) &= \tfrac{\langle 21 \rangle [34]}{[24]\langle 13 \rangle}
\end{aligned}
,
$$

with $s = \langle 12 \rangle [21]$.

We plug these into the amplitude,

$$
\mathcal{A}^{tree}_s(1^-, 2^-, 3^+, 4^+) = 2g_s^2 f^{abe} f^{cde} \frac{\langle 21 \rangle [34]^2}{[21][14]\langle 14 \rangle}. \tag{1.73}
$$

To write everything in-term of $\langle ... \rangle$ we use $\sum_j \langle ij \rangle [jk] = 0$ for $2 \longrightarrow 2$ scattering with i, j, k all different,

$$
\langle 21 \rangle [14] = -\langle 23 \rangle [34] \implies \frac{[34]}{[14]} = -\frac{\langle 21 \rangle}{\langle 23 \rangle}.
$$

For the second ratio which has no leg common we use $s_{12} = s_{34}$ with $s_{ij} = (p_i + p_j)^2 = \langle ij \rangle [ji]$ giving us,

$$
\langle 12 \rangle [21] = \langle 34 \rangle [43] \implies \frac{[34]}{[21]} = -\frac{\langle 12 \rangle}{\langle 34 \rangle}.
$$

Plugging both identities we get,

$$
\mathcal{A}^{tree}_s(1^-, 2^-, 3^+, 4^+) = -2g_s^2 f^{abe} f^{cde} \frac{\langle 12 \rangle^4}{\langle 12 \rangle \langle 23 \rangle \langle 34 \rangle \langle 41 \rangle}. \tag{1.74}
$$

We turn to the $t-channel$ with our choice of momenta we only look for $\varepsilon_2^- \cdot \varepsilon_3^+$ pairs since they are the only ones to survive, but notice that the whole first factor vanishes making everything vanish with it,

$$\mathcal{A}_t^{tree}(1^-, 2^-, 3^+, 4^+) = 0. \tag{1.75}$$

The $u-channel$ is related to the $s-channel$ by $2 \leftrightarrow 3$ and $b \leftrightarrow c$ and we can affirm that it doesn't vanish,

$$\mathcal{A}_u^{tree}(1^-, 2^-, 3^+, 4^+) = \frac{4g_s^2}{u} f^{ace} f^{bde} \left[\left(\varepsilon_3^+ \cdot \varepsilon_2^- \right) \left(p_3 \cdot \varepsilon_1^- \right) \left(p_2 \cdot \varepsilon_4^+ \right) \right], \tag{1.76}$$

with,

$$\begin{aligned} \varepsilon_3^+(1) \cdot \varepsilon_2^-(4) &= \frac{\langle 21 \rangle [34]}{[24] \langle 13 \rangle} \\ p_3 \cdot \varepsilon_1^-(4) &= \frac{1}{\sqrt{2}} \frac{\langle 13 \rangle [34]}{[14]} \\ p_2 \cdot \varepsilon_4^+(1) &= \frac{1}{\sqrt{2}} \frac{[42] \langle 21 \rangle}{\langle 14 \rangle} \end{aligned} \quad ,$$

and $u = \langle 13 \rangle [31]$,

$$\mathcal{A}_u^{tree}(1^-, 2^-, 3^+, 4^+) = -2g_s^2 f^{ace} f^{bde} \left[\frac{\langle 21 \rangle^2 [34]^2}{[14] \langle 14 \rangle \langle 13 \rangle [31]} \right],$$

using $\langle 24 \rangle [34] = -\langle 21 \rangle [31]$ and $\frac{[34]}{[14]} = -\frac{\langle 21 \rangle}{\langle 23 \rangle}$,

$$\mathcal{A}_u^{tree}(1^-, 2^-, 3^+, 4^+) = -2g_s^2 f^{ace} f^{bde} \frac{\langle 21 \rangle^4}{\langle 14 \rangle \langle 42 \rangle \langle 23 \rangle \langle 31 \rangle}. \tag{1.77}$$

With this we accounted for all contributions to the matrix element for $(--++)$ polarization signature,

$$\mathcal{A}_{gg \rightarrow gg}^{tree}\left(1^-, 2^-, 3^+, 4^+\right) = -2g_s^2 \left[f^{abe} f^{cde} \frac{\langle 12 \rangle^4}{\langle 12 \rangle \langle 23 \rangle \langle 34 \rangle \langle 41 \rangle} + f^{ace} f^{bde} \frac{\langle 21 \rangle^4}{\langle 14 \rangle \langle 42 \rangle \langle 23 \rangle \langle 31 \rangle} \right]. \tag{1.78}$$

To get the cross-section we have to perform color sums and square the matrix elements. We start by squaring,

$$\sum_{colors} \left[\mathcal{A}_{gg \rightarrow gg}^{tree}\left(1^-, 2^-, 3^+, 4^+\right) \right]^2 = \left[\mathcal{A}_s^{tree}(1^-, 2^-, 3^+, 4^+) + \mathcal{A}_u^{tree}(1^-, 2^-, 3^+, 4^+) \right]^2$$

$$= \left[\mathcal{A}_s^{tree}(1^-, 2^-, 3^+, 4^+) \right]^2 + \left[\mathcal{A}_u^{tree}(1^-, 2^-, 3^+, 4^+) \right]^2$$
$$+ 2 \left[\mathcal{A}_s^{tree}(1^-, 2^-, 3^+, 4^+) \mathcal{A}_u^{tree}(1^-, 2^-, 3^+, 4^+) \right].$$

We see that we have to square amplitudes independently and do the product of them. Focusing again with only the spin part,

$$\begin{aligned} \left[\frac{\langle 12 \rangle^4}{\langle 12 \rangle \langle 23 \rangle \langle 34 \rangle \langle 41 \rangle} \right]^2 &= \frac{s^2}{t^2} \\ \left[\frac{\langle 21 \rangle^4}{\langle 14 \rangle \langle 42 \rangle \langle 23 \rangle \langle 31 \rangle} \right]^2 &= \frac{s^4}{t^2 u^2} \\ \frac{\langle 12 \rangle^4}{\langle 12 \rangle \langle 23 \rangle \langle 34 \rangle \langle 41 \rangle} \frac{\langle 21 \rangle^4}{\langle 14 \rangle \langle 42 \rangle \langle 23 \rangle \langle 31 \rangle} &= \frac{s^3}{t^2 u} \end{aligned} \quad , \tag{1.79}$$

19

$$\sum_{colors} \left[\mathcal{A}_{gg \longrightarrow gg}^{tree} \left(1^-, 2^-, 3^+, 4^+ \right) \right]^2 = 4g_s^4 [\left(f^{abe} f^{cde} \right)^2 \frac{s^2}{t^2}$$

$$+ \left(f^{ace} f^{bde} \right)^2 \frac{s^4}{t^2 u^2} + 2 \left(f^{abe} f^{cde} \right) \left(f^{acg} f^{bdg} \right) \frac{s^3}{t^2 u}] \qquad (1.80)$$

The color part here is given[24] by,

$$\begin{aligned} \left(f^{abe} f^{cde} \right)^2 &= N^2 \left(N^2 - 1 \right) \\ \left(f^{abe} f^{cde} \right) \left(f^{acg} f^{bdg} \right) &= \tfrac{1}{2} N^2 \left(N^2 - 1 \right) \end{aligned}, \qquad (1.81)$$

leading to,

$$\sum_{colors} \left[\mathcal{A}_{gg \longrightarrow gg}^{tree} \left(1^-, 2^-, 3^+, 4^+ \right) \right]^2 = 4g_s^4 N^2 \left(N^2 - 1 \right) \left\{ \frac{s^2}{t^2} + \frac{s^4}{t^2 u^2} + \frac{s^3}{t^2 u} \right\}$$

$$= 4g_s^4 N^2 \left(N^2 - 1 \right) \left\{ \frac{s^2}{t^2} + \frac{s^4}{t^2 u^2} + \frac{s^2(-t - u)}{t^2 u} \right\}.$$

$$= 4g_s^4 N^2 \left(N^2 - 1 \right) \left\{ \frac{s^4}{t^2 u^2} - \frac{s^2}{tu} \right\}$$

What is remaining for us to compute is $\{(-+-+), (-++-)\}$ which both are related to $(--++)$ through crossing symmetry,

1. $(--++) \longrightarrow (-+-+)$ via $s \leftrightarrow u$.

2. $(--++) \longrightarrow (-++-)$ via $s \leftrightarrow t$.

Which is enough for us to know the full cross-section, and it makes sense that we have only these, any other contribution would require another permutation but the result we got previously is manifestly symmetric under $t \leftrightarrow u$ which means we cannot draw further information from what we computed previously and that we have enough to define our problem entirely.

Of course we need to not forget multiplying by 2 for each polarization in our sum to account for configurations that are related to the ones we have by parity conjugation,

$$\sum_{colors, polarizations} \left| \mathcal{A}_{gg \longrightarrow gg}^{tree} \right|^2 = 2 \left\{ \begin{aligned} & \sum_{colors} \left[\mathcal{A}_{gg \longrightarrow gg}^{tree} \left(1^-, 2^-, 3^+, 4^+ \right) \right]^2 \\ & + \sum_{colors} \left[\mathcal{A}_{gg \longrightarrow gg}^{tree} \left(1^-, 2^+, 3^-, 4^+ \right) \right]^2 \\ & + \sum_{colors} \left[\mathcal{A}_{gg \longrightarrow gg}^{tree} \left(1^-, 2^+, 3^+, 4^- \right) \right]^2 \end{aligned} \right\}, \qquad (1.82)$$

$$\sum_{colors, polarizations} \left| \mathcal{A}_{gg \longrightarrow gg}^{tree} \right|^2 = 4g_s^4 N^2 \left(N^2 - 1 \right) [2 \left(\frac{s^4}{t^2 u^2} - \frac{s^2}{tu} \right)$$

$$+ 2 \left(\frac{u^4}{t^2 s^2} - \frac{u^2}{ts} \right) + 2 \left(\frac{t^4}{s^2 u^2} - \frac{t^2}{su} \right)], \qquad (1.83)$$

which after some work gives us,

---

[24]Section 27.3, [6].

$$\sum_{colors,polarizations} \left|\mathcal{A}^{tree}_{gg\longrightarrow gg}\right|^2 = 4g_s^4 N^2 \left(N^2 - 1\right) \frac{\left(s^2 + t^2 + u^2\right)\left(s^4 + t^4 + u^4\right)}{s^2 t^2 u^2}. \qquad (1.84)$$

At last we average over initial states, that is to divide by $4 * \left(N^2 - 1\right)^2$ taking into account spin and color,

$$\frac{1}{4 * \left(N^2 - 1\right)^2} \sum_{colors,polarizations} \left|\mathcal{A}^{tree}_{gg\longrightarrow gg}\right|^2 = \frac{N^2}{\left(N^2 - 1\right)} g_s^4 \frac{\left(s^2 + t^2 + u^2\right)\left(s^4 + t^4 + u^4\right)}{s^2 t^2 u^2}, \qquad (1.85)$$

then we set $N = 3$,

$$\begin{aligned}
\frac{1}{256} \sum_{colors,polarizations} \left|\mathcal{A}^{tree}_{gg\longrightarrow gg}\right|^2 &= \frac{9}{8} g_s^4 \frac{\left(s^2 + t^2 + u^2\right)\left(s^4 + t^4 + u^4\right)}{s^2 t^2 u^2} \\
&= \frac{9}{2} g_s^4 \left[\frac{1}{4} \frac{\left(s^2 + t^2 + u^2\right)\left(s^4 + t^4 + u^4\right)}{s^2 t^2 u^2}\right]
\end{aligned}, \qquad (1.86)$$

and this result agrees with the known cross-section[25],

$$\frac{1}{256} \sum_{colors,polarizations} \left|\mathcal{A}^{tree}_{gg\longrightarrow gg}\right|^2 = \frac{9}{2} g_s^4 \left(3 - \frac{su}{t^2} - \frac{ut}{s^2} - \frac{st}{u^2}\right). \qquad (1.87)$$

---

[25] Eq (27.74), [6]

Chapter 2

On-shell method and Recursion Formulae

The power of any formalism comes from its independence with regard to external inputs. In the previous chapter we showcased the possibility to translate QCD amplitudes into Helicity ones, along with the employment of symmetry and analytical properties to reduce the workload to just few manageable computations. For the formalism to achieve independence, it needs to construct the amplitude expressions in a way that isn't based on Feynman diagrams. Fortunately, the introduction of complex momenta combined with on-shell method ideas will probe some structures and rules that will make for a convenient alternative to the traditional ways of extracting LO contributions.

2.1 Kinematic 3-points

So far we only applied Helicity formalism to external states, and we want to generalize its use to internal states too, but that will require $p^2 = m^2$ (massive case) or $p^2 = 0$ (massless case) on internal lines which isn't generally the case. To handle this problem we introduce the usage of complex momenta. Then, we discuss the consequences on lower-point amplitudes and how this give us a way to write them entirely using complex-spinors.

2.1.1 GGG-vertex

As we've seen before, after writing down the amplitudes and squaring, we get functions of kinematic invariants s_{ij}. And if we take a look at the pure gluon 3-point kinematic for real momenta we find that [13],
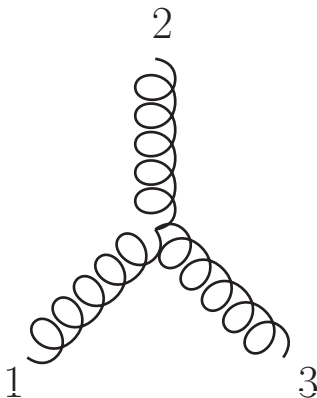

Figure 2.1: Pure gluon 3-vertex.

$$p_1^\mu + p_2^\mu + p_3^\mu = 0$$
$$p_1^2 = p_2^2 = p_3^2 = 0 \qquad (2.1)$$

Through a simple analysis we notice that invariants vanish altogether $s_{12} = (p_1 + p_2)^2 = p_3^2 = 0$, so that 3-point amplitudes generally vanish. If the momenta are real, then $\langle ij \rangle = [ij] = 0$ since they are related by conjugation and the solutions to the previous equation are parallel 4-vectors. If we have complex momenta, then $\langle ij \rangle$ and $[ij]$ aren't related anymore, but we'd still have $s_{ij} = \langle ij \rangle [ji] = 0$. If we think about it then it has to be that some of the Helicity products are non zero while $s_{ij} = 0$. Giving us two possible chiraly conjugate solutions,

1. All $[ij] = 0$ while $\langle ij \rangle \neq 0 \Longrightarrow p_1^{\dot\alpha} \propto p_2^{\dot\alpha} \propto p_3^{\dot\alpha}$.

2. The inverse.

The thing here is that we can't expect the amplitude to be a continuous function of the invariants, the solutions we have for the amplitude to be non-vanishing are discrete. The kinematical region defined by a 3-point amplitudes in the case of complex momenta is made of two points related by parity conjugation. We also notice (1.) and (2.) cannot be at the same time so each solution excludes the other.

Now to find the solutions, we'll use little-group[1] scaling as it is the only constraint we dispose at this time on pure gluonic amplitudes. The rule to follow is that when counting the number of occurrences of some label with a certain helicity we need to find that for negative helicities there must be a factor of two and for a positive one there must be a factor of minus two[2].

For the case of $(+++)$,

$$\mathcal{A}_{GGG}\left(1^{a+}, 2^{b+}, 3^{c+}\right) = \mathcal{C}^{abc}\left[[12][23][31] \, or \, \frac{1}{\langle 12 \rangle \langle 23 \rangle \langle 31 \rangle}\right]. \qquad (2.2)$$

The second proposition diverges in the real limit. Thus we naturally select the first proposition. Now by doing dimensional analysis we find that while the amplitude has mass dimension 1, $[12][23][31]$ has mass dimension 3 and the structure constants should be dimensionless, so that the only solution out is $\mathcal{C}^{abc} = 0$.

For the MHV situation, the allowed forms by little group scaling are either of this form $\frac{\langle ... \rangle \langle ... \rangle \langle ... \rangle}{\langle ... \rangle^4}$ or $\frac{\langle ... \rangle^4}{\langle ... \rangle \langle ... \rangle \langle ... \rangle}$ and the same for right-handed brackets, where in the limit of real momenta the first case diverges faster than it vanishes, so that we turn to the second form [6],

$$\mathcal{A}_{GGG}\left(1^{a+}, 2^{b+}, 3^{c-}\right) = \mathcal{C}^{abc}\frac{[12]^3}{[23][31]}$$
$$\overline{\mathcal{A}}_{GGG}\left(1^{a-}, 2^{b-}, 3^{c+}\right) = \overline{\mathcal{C}}^{abc}\frac{\langle 12 \rangle^3}{\langle 23 \rangle \langle 31 \rangle} \qquad , \qquad (2.3)$$

which has the correct physical dimension[3]. When we put things into context then we require amplitudes to be symmetric under the interchange of two particles since we are dealing with bosons, taking into consideration the anti-symmetric nature of the Helicity products we require $\mathcal{C}^{abc}$ (and $\overline{\mathcal{C}}^{abc}$) to be anti-symmetric too to compensate for the sign. Also it is important to outline again that when $\mathcal{A}_{3-point}$ is non-vanishing, $\overline{\mathcal{A}}_{3-point}$ is (vanishing), and vice versa. The values of the color factors[4] $\mathcal{C}^{abc}$ and $\overline{\mathcal{C}}^{abc}$ are the same and equal to $ig_s\sqrt{2}f^{abc}$.

---

[1] See Appendix B.

[2] Pg. 540-541, [6].

[3] The previous equation went through a simplification as originally it looked like $\frac{\langle 12 \rangle^4}{\langle 12 \rangle \langle 23 \rangle \langle 31 \rangle}$. The remark about this form is that the legs with the "majoritarian" polarization are written in the numerator and the labels follow on cyclically (clockwise, see the diagram).

[4] These factors are dealt with in Appendix B, so we'll drop them for now and get back to them when needed.

2.1.2 GQQ-vertex

In order to construct processes involving quarks whether as external states or propagating internally we need to consider the vertex coupling them to a gluon,
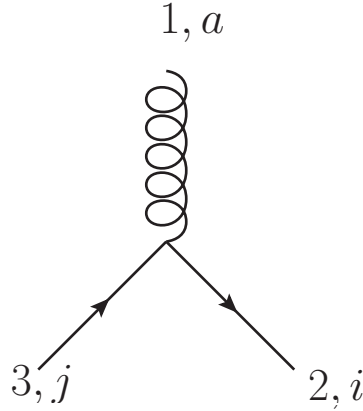
Figure 2.2: The Gluon-Quark-Quark 3-vertex.

$$\mathcal{A}_{GQQ}\left(1^a, 2_i, 3_j\right) = C_{ij}^a \frac{i}{\sqrt{2}} \varepsilon^\mu(1)\overline{f}(2)\gamma_\mu f(3), \tag{2.4}$$

with $C_{ij}^a = \sqrt{2}g T_{ij}^a$ and f being either a u- or v-spinor.

This diagram unlike what we saw previously is directed and its orientation changes its interpretation. The form of the amplitude changes accordingly leading to various expressions for the same vertex. If we list all the possible ways we can orient it, we notice that due to time flowing from left to right, a horizontal mirror operation will not affect our interpretation. Leading to a set of four basic forms illustrated below.

(a) Vertical orientation

(b) Horizontal orientation

Figure 2.3: Different orientations of the GQQ-vertex

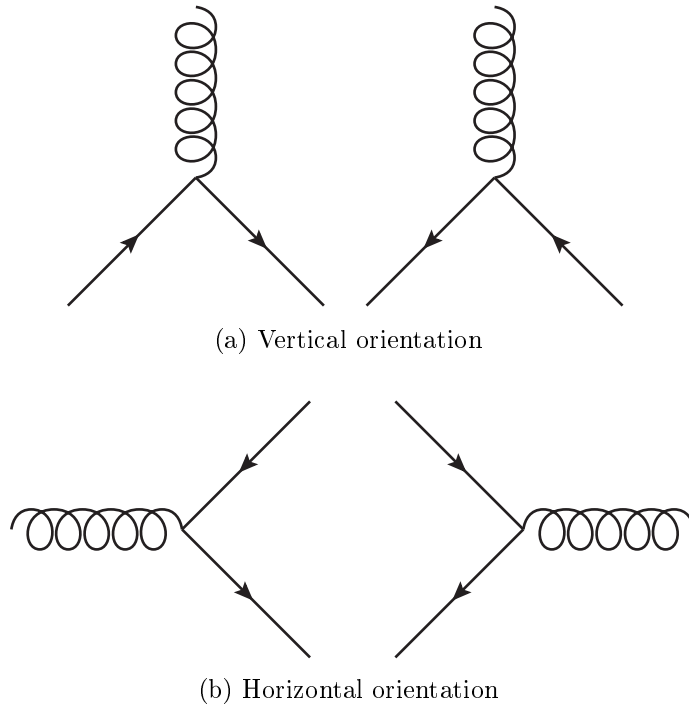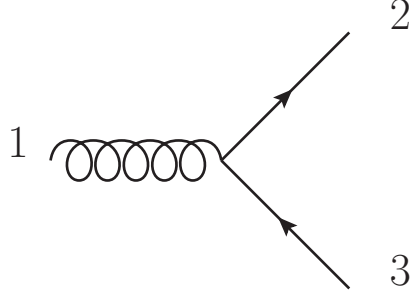In the sub-figure (a), the interaction point being neither to the left or the right both fermionic legs flow to either of these directions uniformly. If the flow goes to the right, then we are speaking about incoming and outgoing particles [6]. While the opposite direction is for antiparticles. The sub-figure (b) contains two diagrams where at first the interaction is to the left with respect to the fermionic legs and then we have the opposite situation. When the fermionic legs are to the right, the incoming is an antiparticle and the outgoing is a particle and the inverse happen when they are to the left.

To write the partial amplitudes[5] associated to each possible vertex we just have to add external states corresponding to each leg according to the prescription given in [10] so that we have,

$$\begin{aligned} \widetilde{\mathcal{A}}_{GQQ}(1^\lambda, 2_q^-, 3_{\bar{q}}^-) &= \tfrac{i}{\sqrt{2}} \left\langle {}_+2 \not{\epsilon}^\lambda(1) 3_- \right\rangle \\ \widetilde{\mathcal{A}}_{GQQ}(1^\lambda, 2_q^-, 3_{\bar{q}}^+) &= \tfrac{i}{\sqrt{2}} \left\langle {}_+2 \not{\epsilon}^\lambda(1) 3_- \right] \end{aligned}$$
(2.5)

The rest of possible diagrams could be obtained in a similar manner. Likewise for the other possible polarization configurations which are just chiraly conjugate to these. Developing the previous expressions in term of massless components will not reveal anything interesting beyond this point. Although there is an interesting case to consider for this vertex, that is the massless limit where the possible amplitudes reduce to only two chiraly conjugate formulae given below,

$$\begin{aligned} \widetilde{\mathcal{A}}_{GQQ}(1^\lambda, 2^+, 3^-) &= \tfrac{i}{\sqrt{2}} \left\langle 3 \not{\epsilon}^\lambda(1) 2 \right] \\ \widetilde{\mathcal{A}}_{GQQ}(1^\lambda, 2^-, 3^+) &= \tfrac{i}{\sqrt{2}} \left[3 \not{\epsilon}^\lambda(1) 2 \right\rangle \end{aligned}$$
(2.6)

2.2   Recursion formula

The evocation of complex numbers in general bring with them the idea of computing integrals using residues. In our study of complex momenta there is yet another way to exploit them via a certain transformation or *shifts* described for the massless particles in the reference [14] which later on got generalized to massive ones in [15]. These shifts will provide us with a rule capable of combining Kinematic 3-points from the previous section into QCD diagrams with the correct amplitude expression. In what follows we will only derive the rule for the massless case knowing that the generalization only requires few additions and is given in [16].

---

[5]Meaning amplitudes stripped from the color factor. (See Appendix B)
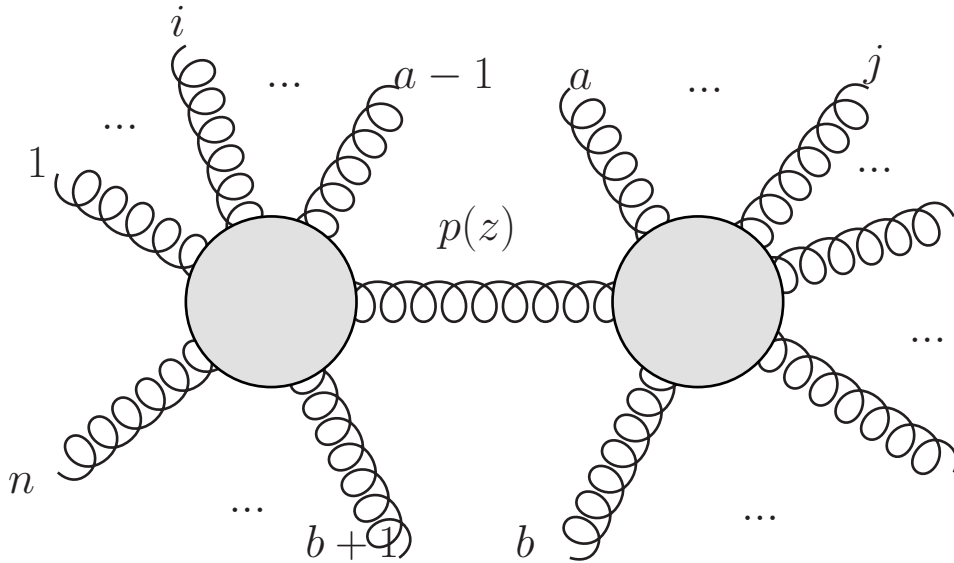
2.2.1 BCFW-shifts

Figure 2.4: Illustration of the mechanism behind the recursion procedure.

The procedure starts by shifting two spinors of the gluons i and j,

$$\begin{aligned} [[\to i] &= [i + z\,[j \\ [j \to]\rangle &= j\rangle - z\,i\rangle \end{aligned}, \tag{2.7}$$

where z is some complex number. The momenta bi-spinors get affected by the shifts,

$$\begin{aligned} p_{[\to i]} &= i\rangle\,[[\to i] \\ p_{[j\to]} &= [j\to]\rangle\,[j \end{aligned}. \tag{2.8}$$

This procedure respects masslessness $p_{[\to i]}^2 = p_{[j\to]}^2 = 0$ and overall momentum conservation meaning that, $p_{[\to i]} + p_{[j\to]} = p_i + p_j$.

With these shifts, we can think of the amplitude $\mathcal{A}^{tree}$ as a function of z where the physical amplitude is given by $\mathcal{A}^{tree}[0] = \mathcal{A}^{tree}[z]\big|_{z=0}$. If this function is well behaved at infinity then we can relate its behavior at $z = 0$ with its residues at finite values of z (singularities). If $\mathcal{A}^{tree}[z] \longrightarrow 0$ at $z \longrightarrow \infty$ then we have [13, 6],

$$0 = \oint_C \frac{dz}{2\pi i}\frac{1}{z}\mathcal{A}^{tree}[z] = \mathcal{A}^{tree}[0] + \sum_k Res\left\{\frac{\mathcal{A}^{tree}[z]}{z}\right\}\bigg|_{z=z_k}, \tag{2.9}$$

where C is the circle at infinity, and the z_k are the locations of the factorization singularities in the $z - plane$. To know the origin of the poles we start by drawing a picture that leads to the emergence of the complex parameter. We had a momentum proportional to z being subtracted and added to two external lines, thus tracing z over the diagram it comes in from i and out through j, implying that only a "propagator" along this line can contribute with poles.

Suppose that this propagator has momentum $\widehat{P}(z)$, the pole is at $\widehat{P}^2(z) = 0$ which puts this line on-shell. This procedure splits the diagram into two on-shell sub-diagrams related by a propagator with complex momentum, giving us a pole when we put it on-shell. Each pole we might have splits the diagram into two, so basically we can apply this procedure again and again on the sub-diagrams until we end up with indivisible blocks. Reverting the process we can recursively build tree-level amplitudes.

Now let's see how this is done mathematically, we choose $\widehat{P}$ to be going from right to left so that $\{a...b\}$ are on the right as shown in the previous figure. Momentum conservation at the vertex on the right considering all momenta incoming with $\widehat{P}$ outgoing leads to $\left(-\widehat{P}(z)\right) + \sum_{k=a}^{b} p_k = 0$ recalling that j is on that side we get,

$$\widehat{P}(z) = \sum_{k=a}^{b} k\rangle \left[k - z\, i\right\rangle [j . \tag{2.10}$$

The pole is at $\widehat{P}^2(z_{a,b}) = 0$,

$$0 = \left(\sum_{k=a}^{b} k\rangle \left[k - z_{a,b}\, i\right\rangle [j\right)^2 = \left(\sum_{k=a}^{b} p_k\right)^2 - z_{a,b} \sum_{k=a}^{b} \langle ik\rangle [kj] \tag{2.11}$$

$$\implies z_{a,b} = \frac{\left(\sum_{k=a}^{b} p_k\right)^2}{\sum_{k=a}^{b} \langle ik\rangle [kj]}, \tag{2.12}$$

implying that we'll get a $z_{a,b}$ for each partition of the diagram by a, b.

Now if we apply $\mathcal{A}^{tree}[0] = -\sum_k Res\left\{\frac{\mathcal{A}^{tree}[z]}{z}\right\}\Big|_{z=z_k}$ where we have one pole at $z_{a,b}$,

$$\mathcal{A}^{tree}[0] = -\frac{1}{z_{a,b}} Res\left\{\mathcal{A}_{left}^{tree}[z]\, \frac{1}{\left(\sum_{k=a}^{b} p_k\right)^2 - z \sum_{k=a}^{b} \langle ik\rangle [kj]}\, \mathcal{A}_{right}^{tree}[z]\right\}\Bigg|_{z \longrightarrow z_{a,b}}$$

$$= \mathcal{A}_{left}^{tree}[z_{a,b}]\, \frac{1}{\left(\sum_{k=a}^{b} p_k\right)^2}\, \mathcal{A}_{right}^{tree}[z_{a,b}] . \tag{2.13}$$

The generalization leads to the "BCFW [14] recursion formula",

$$\mathcal{A}^{tree}(1, ...n) = \sum_{a<b,h} \mathcal{A}_{left}^{tree}\left(1, ...a-1, \widehat{P}^h, b+1, ...n\right)[z_{a,b}]\, \frac{1}{\left(\sum_{k=a}^{b} p_k\right)^2}\, \mathcal{A}_{right}^{tree}\left(-\widehat{P}^{-h}, a, ...b\right)[z_{a,b}] . \tag{2.14}$$

The presence of $[z_{a,b}]$ implies that the evaluation should be done with the shift that gave us this pole, namely $\left\{\; [[\to i] = [i + z\,[j \quad [j \to]\rangle = j\rangle - z\, i\rangle \;\right\}$. The Helicity must be summed over[6], and the convention of incoming momenta forces h flip from the left to the right.

The only requirement for the BCFW-recursion formula to work is to have a well behaved $z \longrightarrow \infty$ limit, which is generally true except for some choices of shifts. There are some general rules[7] for $2 \longrightarrow 2$ scatterings, the Helicity combinations $(i, j) = (+, +), (-, -)\, or\, (-, +)$ are good, while $(+, -)$ is bad.

2.2.2 Parke-Taylor Formula

The combination of Kinematic 3-points and BCFW-recursion formula realizes the independence of the Helicity formalism and produces a generative power that surpasses conventional methods

---

[6] This sum encodes the closure formula over polarizations that will produce the numerator of the propagator. One of the reasons that this rule generalizes to massive quarks too.

[7] Section 27.6, [6].

leading to the discovery of previously unknown patterns. One of these patterns is about $MHVs$ of pure n-gluon processes which writes as follow [17, 6],

$$\mathcal{A}_{MHV}^{tree}\left(1^{+}, ..., k^{-}...l^{-}, ...n^{+}\right) = \frac{\langle kl \rangle^{4}}{\langle 12 \rangle \, ... \, \langle n1 \rangle}. \tag{2.15}$$

We call it the Parke-Taylor formula [18].It provides us with a simple analytic expression that we can use to express the amplitude of any high-multiplicity pure gluon diagram.
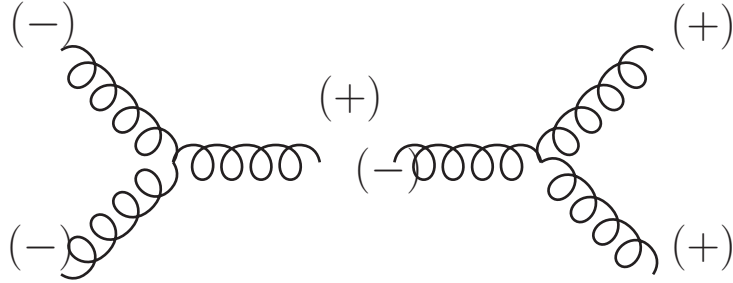
(a) The first MHV diagram
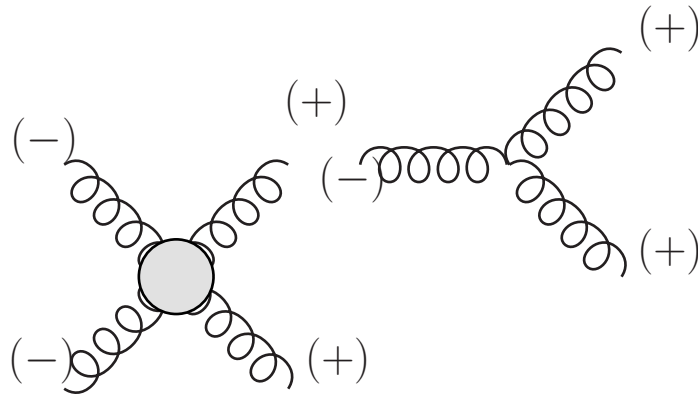
(b) The second MHV diagram

Figure 2.5: Composing MHV amplitudes for gluons.

The proof of this formula will not be given here as there is enough literature about it. Although we illustrate in the figure the first steps of the recursion which clearly show that we can use BCFW-recursion in order to derive the formula.

2.3 Application

In the following section we show how to perform BCFW-recursion employing the two packages[8] S@M and SpinorsExtras under Mathematica. The discussion about loading these has been differed to the Appendix C along with a list of the functions we employed throughout this document.

---

[8]Refer to Appendix C for further information.

2.3.1 Massless case

As a first application we intend to construct the s-channel contribution of a pure gluon process with external helicity configuration $(-, -, +, +)$ and a momentum labeling illustrated below.
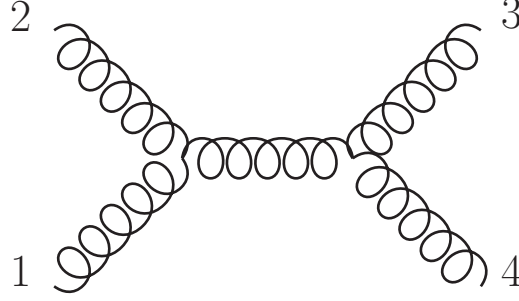

Figure 2.6: S-channel diagram for the $gg \rightarrow gg$ with $(-, -, +, +)$ polarization.

This diagram factorizes to two GGG-vertices, so we start by defining their expression.

```
In[1]:=   GGG[{a_,+1},{b_,+1},{c_,-1}]:=Spbb[a,b]^3/(Spbb[b,c]*Spbb[c,a])
          GGG[{a_,-1},{b_,-1},{c_,+1}]:=Spaa[a,b]^3/(Spaa[b,c]*Spaa[c,a])
```

The next step is a straight forward one since we have to declare the objects that represent the momenta of our problem. S@M interprets integer labels as Helicity spinors even without declaring them leaving the necessity to only declare the label for the transfer momentum. In fact we need two labels, because symbols in S@M are treated contextually and thus could be treated as vectors or spinors leading to a confusion whether $-P$ is to be interpreted as $-P$ (as a vector) or $\pm iP$ (as a spinor). So we just add another label and then replace when the context is clear.

```
In[2]:=   DeclareSpinor[P,mP]
```

```
          {P,mP} added to the list of spinors
```

We solve to find the value of the shift parameter z that puts the propagator on-shell.

```
In[3]:=   OnShellCond=Solve[ShiftBA[1,4,z][s[1,2]]== 0,z] //ExpandSToSpinors //
          SpOpen // Flatten
```

$$Out[3]= \quad \{z \rightarrow -\frac{[2|1]}{[4|2]}\}$$

Then, we construct the amplitude according to the formula given in the previous section and apply the substitution $mP \longrightarrow +iP$ as things would turn out the same if instead we applied $mP \longrightarrow -iP$ because we'd have a factor of $(\pm i)^2 = -1$.

```
In[4]:=   AmplitudeExpression= GGG[{1,-1},{2,-1},{P,+1}]*(1/s12)*
          GGG[{3,+1},{4,+1},{mP,-1}]/.mP→+I P
```

$$Out[4]= \quad \frac{\langle 1|2 \rangle^3 \quad [4|3]^3}{s12 \; \langle P|1 \rangle \; \langle P|2 \rangle \quad [3|P] \; [4|P]}$$

Since the transfer momentum is an object that is only clearly defined within a spinor chain, we transform the expression so that we find it that way,

In[5]:=   `AmplitudeExpressionStep1 =SpClose[AmplitudeExpression,P]`

Out[5]= $\dfrac{\langle 1|2\rangle^{3}\ \ [4|3]^{3}}{\text{s12}\ \langle 1|P|3\rangle\ \langle 2|P|4\rangle}$

And perform the shift on the expression while substituting for the value of P in term of external momenta and z for the value that we previously computed.

In[6]:=   `AmplitudeExpressionStep2 =ShiftBA[1,4,z][AmplitudeExpressionStep1`
        `/.P`$\to$` Sm[3]+Sm[4]]/.OnShellCond`

Out[6]= $\dfrac{\langle 1|2\rangle^{3}\ \ [4|3]^{2}}{\text{s12}\ \langle 1|4\rangle\ \langle 2|3|4\rangle}$

At last we perform a series of manipulation in order to obtain an expression that is solely in terms of angle-brackets.

In[7]:=   `AmplitudeExpressionStep3=AmplitudeExpressionStep2 /.s12`$\to$`s[1,2]//`
        `ExpandSToSpinors // SpOpen // Simplify`

Out[7]= $-\dfrac{\langle 1|2\rangle^{2}\ \ [4|3]}{\langle 1|4\rangle\ \langle 2|3\rangle\ [2|1]}$

In[8]:=   `AmplitudeSChannel=AmplitudeExpressionStep3/.Spbb[4,3]`$\to$
        `(Spaa[1,2]*Spbb[2,1]/Spaa[3,4])`

Out[8]= $-\dfrac{\langle 1|2\rangle^{3}}{\langle 1|4\rangle\ \langle 2|3\rangle\ \langle 3|4\rangle}$

Now to check that our result is correct we need to compare if the expression we obtained through BCFW-shifts yields the same numerical results as the expression we obtain from the standard Feynman-diagram procedure.

We start by generating massless external momenta that satisfy the constraint $p_1+p_2+p_3+p_4 = 0$ using the command,

In[9]:=   `GenMomenta[{1,2,3,4}]`

        `Momenta for the spinors 1, 2, 3, 4 generated.`

Then we declare four new spinors to use them in the construction of the expression of s-channel found in[9]with the same choice of reference momenta.

In[10]:=   `DeclareSpinor[a,b,c,d]`

        `{a,b,c,d} added to the list of spinors`

---

[9]Section 27.3, [6].

In[11]:= `Amplitude[`$a\_$`,`$b\_$`,`$c\_$`,`$d\_$`]` `=-2*(1/s[a,b])(ExpandPolVec[MP[PolVec[a,+1],b]]*`
`ExpandPolVec[MP[PolVec[d,-1],c]]*`
`ExpandPolVec[MP[PolVec[b,+1],PolVec[c,-1]]])/.{SpRef[a]`→ `d,SpRef[b]`→ `d,`
`SpRef[c]`→ `a,SpRef[d]`→ `a}`

Out[11]= $-\dfrac{\langle a|b\rangle}{s_{ab}}\dfrac{\langle a|b|d]}{\langle a|c\rangle}\dfrac{\langle a|c|d]}{\langle a|d\,\rangle}\dfrac{[d|c]}{[d|a]\ [d|b]}$

We finally find,

In[12]:= `Amplitude[1,2,3,4]//N`

Out[12]= `19.1846+3.39786 i`

In[13]:= `AmplitudeSChannel//N`

Out[13]= `19.1846+3.39786 i`

Both expressions give the same result although issued from completely different methods, implying that BCFW-shifts pass the test when it comes to pure gluonic processes.

2.3.2 Massive case

In this part we'll compute the t-channel amplitude for the $qq \longrightarrow qq$ process with polarization configuration $(-,+,+,-)$.
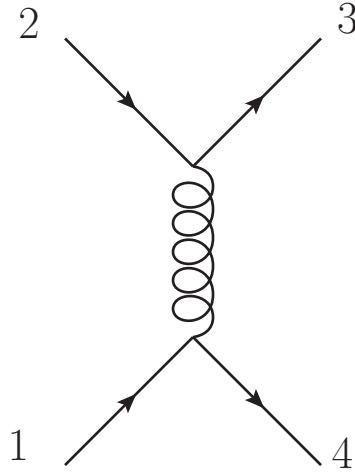
Figure 2.7: T-channel diagram for the $qq \to qq$ with $(-,+,+,-)$ polarization.

This diagram is composed of two GQQ-vertices to which we define the expression for relevant helicity configurations as follow,

In[14]:= `GQQMassive[{`$a\_$`,+1},{`$b\_$`,-1},{`$c\_$`,-1}]:=`$\dfrac{\text{I}}{\sqrt{2}}$ `*`
`Spaa[SpM[`b`,+1],PolVec[`a`,-1],SpM[`c`,+1]]`
`GQQMassive[{`$a\_$`,-1},{`$b\_$`,-1},{`$c\_$`,-1}]:=`$\dfrac{\text{I}}{\sqrt{2}}$ `*`

$$\text{GQQMassive}[\{a\_,+1\},\{b\_,+1\},\{c\_,+1\}]:=\frac{\text{I}}{\sqrt{2}} \quad * \quad \frac{\text{Spaa}[\text{SpM}[b,+1],\text{PolVec}[a,+1],\text{SpM}[c,+1]]}{\text{Spbb}[\text{SpM}[b,+1],\text{PolVec}[a,-1],\text{SpM}[c,+1]]}$$

$$\text{GQQMassive}[\{a\_,-1\},\{b\_,+1\},\{c\_,+1\}]:=\frac{\text{I}}{\sqrt{2}} \ * \ \text{Spbb}[\text{SpM}[b,+1],\text{PolVec}[a,+1],\text{SpM}[c,+1]]$$

We declare the transfer momentum and the massive external momenta.

In[15]:=   `DeclareSpinor[P,mP]`

      `{P,mP} added to the list of spinors`

In[16]:=   `DeclareLVector[p1,p2,p3,p4]`

      `{p1,p2,p3,p4} added to the list of Lorentz vectors`

We specify the masses.

In[17]:=   `MP[p1,p1]^=MP[p2,p2]^=MP[p3,p3]^=MP[p4,p4]^=m^2;`
      `$Assumptions=m>0;`

We write the two expressions contributing to the formula as terms of the sum over internal helicities within a table.

In[18]:=   `AmplitudeTable= Table[GQQMassive[{P,+1},{p3,+1},{p2,+1}]` $\ast\frac{1}{\text{s14}}\ast$
      `GQQMassive[{mP,-1},{p4,-1},{p1,-1}],{l,{-1,+1}}]`

Out[18]= $\{\dfrac{\langle {}_{+}\text{p1}|\epsilon^{-}(\text{mP})|{}_{+}\text{p4} \, \rangle \ \ [{}_{+}\text{p3}|\epsilon^{+}(\text{P})|{}_{+}\text{p2}]}{2 \ \text{s14}},\dfrac{\langle {}_{+}\text{p1}|\epsilon^{+}(\text{mP})| \ {}_{+}\text{p4} \, \rangle \ \ [{}_{+}\text{p3}|\epsilon^{-}(\text{P})|{}_{+}\text{p2}]}{2 \ \text{s14}}\}$

Then we apply the LCD on the final state while expanding for the explicit expression of the polarizations.

In[19]:=   `AmplitudeLCDFinal=LightConeDecompose[AmplitudeTable,p3|p4]//`
      `ExpandPolVec`

We replace mP for its possible values in the context of a spinor or a vector using appropriate functions.

In[20]:=   `ReplaceLVector[AmplitudeLCDFinal,mP→-P];`
      `AmplitudePOnly=ReplaceSpinor[%,mP→ ±I P]`

Then we explicit the reference vectors for the momenta we intend to shift.

In[21]:=   `AmplitudeExplicitRef=ExplicitRef[AmplitudePOnly,p2|p1]/.`
      `{SpRef[p1]→SpAssoc[p2,p1],SpRef[p2]→SpAssoc[p1,p2]}`

At this point we require the value of z that puts the propagator on-shell.

In[22]:= `ShiftBA[p1,p2,z][MP2[p2+p3]==0]`
`OnShellCond=Solve[%,z]//Flatten`

Out[22]= $2\ m^2 + 2\ (MP[p2,p3] + \frac{1}{2}\ z\ \ \langle p1^{p2}|p3|p2^{p1}]) == 0$

Out[23]= $\{z \to -\frac{2\ (m^2 + MP[p2,p3])}{\langle p1^{p2}|p3|p2\ ^{p1}]}\}$

Then we shift the amplitudes via,

In[24]:= `AmplitudeShifted=AmplitudeExplicitRef//ShiftBA[p1,p2,z]/.OnShellCond`

and apply LCD on the remaining massive vectors along with some remapping of the associate vectors.

In[25]:= `AmplitudeShifted//LightConeDecompose//Refine;`
`AmplitudeLCDAll=%/.{SpAssoc[p1,SpAssoc[p2,p1]]→SpAssoc[p1,p2],`
`SpAssoc[p2,SpAssoc[p1,p2]]→SpAssoc[p2,p1]}`

The final form of the amplitude is obtained by simplifying the reference momenta to find the most compact form.

In[26]:= `FinalAmplitude=RefSimplify[#,SpRef[P|mP]]&/@AmplitudeLCDAll/.`
`s14→s[p1,p4]//Total//Simplify`

Out[26]= $\dfrac{m^2\ \ (\dfrac{\langle p4^\flat|\ p1^{p2}\rangle\ \ [p2^{p1}|p3^\flat]}{\langle p1^{p2}|\ p2^{p1}\rangle[p2^{p1}|p1^{p2}]} - \dfrac{\langle p1^{p2}\ |q_{p3}\rangle\ \ [q_{p4}|p2^{p1}]}{\langle p3^\flat|q_{p3}\rangle[q_{p4}|p4^\flat]})}{s_{p1p4}}$

Now to the numerical check, we need to set the mass along with generating the momenta

In[27]:= `N[m]=.5`

In[28]:= `Module[`
`{`
`v1=RandomReal[{-100,100},3],`
`v2=RandomReal[{-100,100},3],`
`v1Sq,v2Sq,`
`eQ`
`}`
`,`

`{v1Sq,v2Sq}=Total[`$\#^2$`]&/@{v1,v2};`
`v2=`$\sqrt{\dfrac{v1Sq}{v2Sq}}$`v2;`
`{eQ,eQ}=`$\sqrt{v1Sq+N[\#]^2}$`&/@{m,m};`

`DeclareLVectorMomentum[p1,Flatten[{eQ,v1}]];`
`DeclareLVectorMomentum[p2,Flatten[{eQ,-v1}]];`
`DeclareLVectorMomentum[p3,Flatten[{-eQ,-v2}]];`
`DeclareLVectorMomentum[p4,Flatten[{-eQ,+v2}]];`
`]`

Then we set the values of the reference and associate vectors.

In[29]:= `DeclareSpinorMomentum/@SpRef/@{p3,p4};`

In[30]:= `DeclareSpinorMomentum/@{SpAssoc[p1,p2],SpAssoc[p2,p1],`
          `SpAssoc[p3],SpAssoc[p4]};`

Next we write the expression of the amplitude as given from the Feynman-rules.

In[31]:= `GammaVec={Gamma0,Gamma1, Gamma2, Gamma3};`

In[32]:= $\frac{1}{\text{s14}}$`MP[`$\frac{\text{I}}{\sqrt{2}}$ `Spbb[SpM[p3,1],#,SpM[p2,1]]&/@GammaVec,`
          $\frac{\text{I}}{\sqrt{2}}$ `Spaa[SpM[p4,1],#,SpM[p1,1]]&/@GammaVec];`
          `LightConeDecompose[%,{p2`→`p1,p1`→`p2,p3,p4}]//Refine;`
          `StandardAmplitude=%/.s14`→`s[p1,p4]`

At last we evaluate both expressions,

In[33]:= `FinalAmplitude//N`
          `StandardAmplitude//N`

Out[33]= `-9.65801*10^-6+8.92161*10^-6 i`

Out[34]= `-9.65801*10^-6+8.92161*10^-6 i`

And again we see that both results agree.

Chapter 3

Unitarity method and Cut coefficients

The real test to any amplitude computation method happens during its encounter with loop-amplitudes, or NLO contributions. The previous chapters were marked by a success to obtain tree amplitudes in a very elegant and compact manner. And in order to tackle the test, our formalism will employ a consequence coming from the notion of Unitarity ; a notion that is proper to the QFT paradigm as a whole. This chapter is the core of this thesis and within its boundaries we will attempt to unravel a technical synergy stemming from the compatibility of the previously developed method with Generalized Unitarity, in order to develop a one-loop formulation that employs information coming from tree-level expressions. Thus, putting to use the solutions offered by the formalism we built throughout the previous chapters.

3.1   Cutkosky rules

The imposition of Unitarity constraint in the simple straight forward sense seems to reveal a very interesting relation between LO and NLO contributions. This link will be of extreme importance as it will help us tackle loop-amplitudes in an indirect way.

Let's start by putting that condition under mathematical terms,

$$S^\dagger S = 1, \tag{3.1}$$

with $S = 1 + i\mathcal{T}$, where the first term is the trivial-part which only survives if for the sandwich $\langle f \left| S \right| i \rangle$, $|i\rangle = |f\rangle$ meaning that nothing happens, and the second term which is the non-trivial one, also called the Transfer-matrix contributes for $|i\rangle \neq |f\rangle$, namely when something actually happened (interactions).

Unitarity of the S-matrix tells us that,

$$i \left(\mathcal{T}^\dagger - \mathcal{T} \right) = \mathcal{T}^\dagger \mathcal{T}. \tag{3.2}$$

A strange equality between a difference and a product, which can only be explained if the left-hand side is interpreted as a loop amplitude and the right-hand one as a product of two conjugate tree amplitudes.This must hold order-by-order in perturbation theory, meaning that it relates LOs to NLOs. Another read leads us to say that imaginary parts of loop amplitudes are determined by tree-level amplitudes,

$$2Im[\mathcal{T}] = \mathcal{T}^\dagger \mathcal{T}. \tag{3.3}$$

To draw further conclusions we go back to discussing Feynman propagators and more precisely evaluating the imaginary part[1] of a propagator,

$$Im\frac{1}{p^2 - m^2 + i\varepsilon} = \frac{1}{2i}\left[\frac{1}{p^2 - m^2 + i\varepsilon} - \frac{1}{p^2 - m^2 - i\varepsilon}\right] = \frac{-\varepsilon}{(p^2 - m^2)^2 + \varepsilon^2}. \tag{3.4}$$

This vanishes as $\varepsilon \longrightarrow 0$, except near $p^2 = m^2$(at the pole). If we integrate over p^2 we get,

$$\int_0^\infty dp^2 \left[\frac{-\varepsilon}{(p^2 - m^2)^2 + \varepsilon^2}\right] = -\pi. \tag{3.5}$$

So that we have $Im\frac{1}{p^2-m^2+i\varepsilon} = -\pi\delta(p^2 - m^2)$, saying that "the propagator is real except for when the particle goes on-shell", meaning we have imaginary parts arising and if this propagator is a part of a loop, then the imaginary parts of loop amplitudes come from intermediate particles going on-shell. Thus, we can put this conclusion in a procedural format by what is known as the "Cutting rules" formulated first by Cutkosky [19]:

1. Cut through the diagram in any way that can put all of the cut propagators on-shell without violating momentum conservation.

2. For each cut, replace $\frac{1}{p^2-m^2+i\varepsilon} \longrightarrow -2i\pi\delta\left(p^2 - m^2\right)\theta\left(p^0\right)$.

3. Sum over all cuts (shown in the example treated in pg. 457, [6]).

4. The result is the discontinuity of the diagram, where $Disc\left[\mathcal{T}\right] = 2Im\left[\mathcal{T}\right]$.

The discontinuity of a diagram refers to the amplitude difference for when the energies are given small positive and small negative imaginary parts[2]. Put more formally as,

$$Disc\left[\mathcal{T}(p^0)\right] = \mathcal{T}(p^0 + i\varepsilon) - \mathcal{T}(p^0 - i\varepsilon) = 2Im\left[\mathcal{T}(p^0)\right].$$

3.2   One-Loop formulation of Helicity amplitudes

We previously studied the simple form of Unitarity which only speaks about the $S - matrix$, $S = 1 + i\mathcal{T}$ being unitary leading us to a procedure determining imaginary parts of loops deduced from the following relation,

$$Disc\left(\mathcal{T}\right) = \mathcal{T}^\dagger\mathcal{T}. \tag{3.6}$$

The previous equation holds order by order in the perturbation theory, where suppose $\mathcal{T}_n^{(L)}$ is the L-loop n-gluons amplitude then,

$$\begin{aligned} \mathcal{T}_4 &= g^2\mathcal{T}_4^{(0)} + g^4\mathcal{T}_4^{(1)} + g^6\mathcal{T}_4^{(2)} + ... \\ \mathcal{T}_5 &= g^3\mathcal{T}_5^{(0)} + g^5\mathcal{T}_5^{(1)} + g^7\mathcal{T}_5^{(2)} + ... \end{aligned}. \tag{3.7}$$

The different terms of these developments can combine to provide imaginary parts of the higher-loop amplitudes through the application of Cut-rules,

---

[1]page 456, [6]

[2]Pg. 459, [6].

$$Disc\left(\mathcal{T}_4^{(0)}\right) = 0$$
$$Disc\left(\mathcal{T}_4^{(1)}\right) = \mathcal{T}_4^{(0)\dagger}\mathcal{T}_4^{(0)}$$
$$Disc\left(\mathcal{T}_4^{(2)}\right) = \mathcal{T}_4^{(0)\dagger}\mathcal{T}_4^{(1)} + \mathcal{T}_4^{(1)\dagger}\mathcal{T}_4^{(0)} + \mathcal{T}_5^{(0)\dagger}\mathcal{T}_5^{(0)} \qquad (3.8)$$

Tree amplitudes have no branch cuts. The discontinuities of one loop amplitudes are given by the product[3] of tree amplitudes with the intermediate states always consisting of particles that are re-scattering, "two-particle cuts". The two-loops involve beside two-particle cuts three particle-cuts given by higher multiplicity amplitudes, etc.

To understand the whole Unitarity method bundle we need to put in perspective all the ideas we accumulated so far:

1. The previous relations are derived assuming real momenta for both external and internal lines. Trying to solve on-shell conditions for complex loop momenta leads us to "Generalized Unitarity".

2. Since in our case Unitarity is applied perturbatively we can use the properties of perturbation theory that is Feynman diagram expansion leading us to represent loop amplitudes as a linear combination of a basic set of Feynman integrals, called "master integrals", multiplied by coefficient functions.

The Unitarity method combines (1) and (2), namely that the information we get from (1) can be compared with (2) to yield the coefficients. If all possible integral coefficients are determined , then the amplitude itself is completely determined.

The method we outline here starts by dividing the loop contribution that is dimensionally regularized into its cut parts which are consequences of Unitarity plus rational parts which comes in to complete[4] the full answer,

$$\mathcal{A}_n^{1-loop} = C_n + R_n. \qquad (3.9)$$

The cut parts are given through the extension of Unitarity to the case of complex loop momenta and solving for the conditions that makes these on-shell. This extension has the consequence of raising the number of cuts available to perform on a loop. Since we are in four dimensions $\epsilon = 0$, meaning that the loop momentum l has four unknown components requiring us four equations to be exactly solvable, we can make up to "four" cuts in total where each cut imposes a constraint of the form $(l - K)^2 = 0$ where K is a momenta cluster, namely some combination of external momenta in this fashion $K = \sum p$.

The solutions in this case are discrete and we cannot have in this situation a fifth cut because we'd end up with more equations than unknowns which is too constrained and this is partly the reason why at this level we won't see pentagonal (5-point) integrals. For the case where we perform 3, 2 or 1 cut(s), we end up with less equations than unknowns and thus we'd have parameterized solutions with one or more complex variables.

Performing a certain number of cuts on a loop diagram would require an equal number of propagators available to conduct the cuts, implying that each – quadruple, triple, ... –cuts would yield an information about the diagram with a – box, triangle, ...–like loop. If we have a close look at the contribution of these loops at the amplitude level we see that we can isolate each time an – 4,3, ...–point integral arising from that loop. Adding to this the fact [13] that we can't have

---

[3]There is an implicit discrete sum over the helicities which lie between the two $\mathcal{T}$ matrices and there is a continuous integral over intermediate phase states.

[4]The cuts give us only imaginary parts.

37

quintuple cuts meaning that pentagon-like loop information cannot be captured in four dimensions but luckily there is a systematic way to reduce pentagon and higher order loop integrals in terms of – box, triangle, ... –integrals making them somehow a good basis of decomposition to our problem.
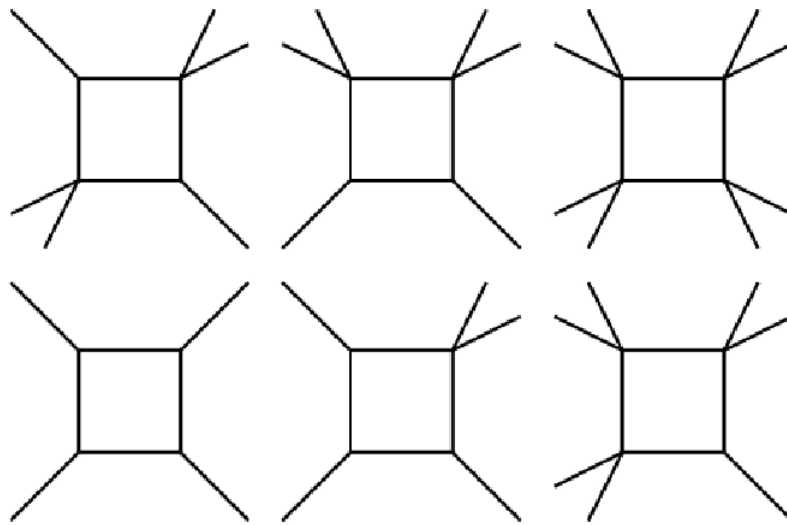
This was the point that (2) was trying to make; leading us to,

$$C_n = \sum_i d_i \mathcal{I}_{4-point}^i + \sum_i c_i \mathcal{I}_{3-point}^i + \sum_i b_i \mathcal{I}_{2-point}^i + \sum_i a_i \mathcal{I}_{1-point}^i, \qquad (3.10)$$

with,

$$\mathcal{I}_{m-point}^i = \mu^{2\epsilon} \int \frac{d^{4-2\epsilon} l}{(2\pi)^{4-2\epsilon}} \frac{1}{\prod_{n=1}^m l_n^2}, \qquad (3.11)$$
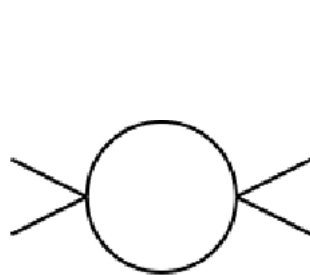
and the coefficients $\{d_i, c_i, b_i, a_i\}$ are independent of the loop momentum and only function of kinematic invariants. These coefficients are read off diagrams represented below.
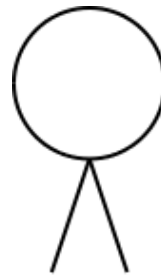

(a) Box diagrams
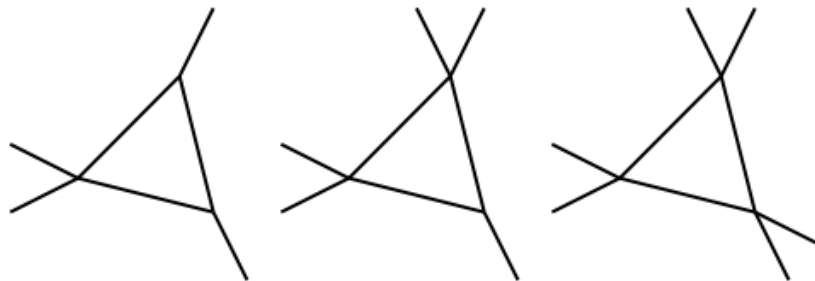

(b) Triangle diagrams

(c) Bubble diagram

(d) Tadpole diagram

Figure 3.1: Loop diagram basis

3.2.1 Conventions

The loop amplitude we are describing can have n-external legs which can be distributed in sets all around the loop. These sets are located at the points of the integrals thus a box integral can have 4-sets, a triangle can have 3, etc. We name these sets "clusters" and are the same $K's$ that arise in the cut constraints.

It is clear that we can have as much clusters as there are "points" in the integral and the fact that they are just combinations of external momenta, we can have many arrangements of these using the momenta of the problem. The cluster can be massless if it contains just one momentum or massive if it is a sum of two or more momenta. Each arrangement gives us a different contribution which is the information stocked in the the kinematic coefficients $d_i, c_i, ...$ so that each i corresponds to a possible partition of external momenta into 4,3, ... sets. We will refer to these clusters by a set $\{K_1, K_2, ...\}$ and take loop momentum to be flowing counter-clockwise as a convention. While we might have a number of propagators in the loop only the loop momentum is needed to characterize them all, making it the only variable we are integrating on. The propagator's momenta are functions of the loop momentum and the clusters of external momenta.
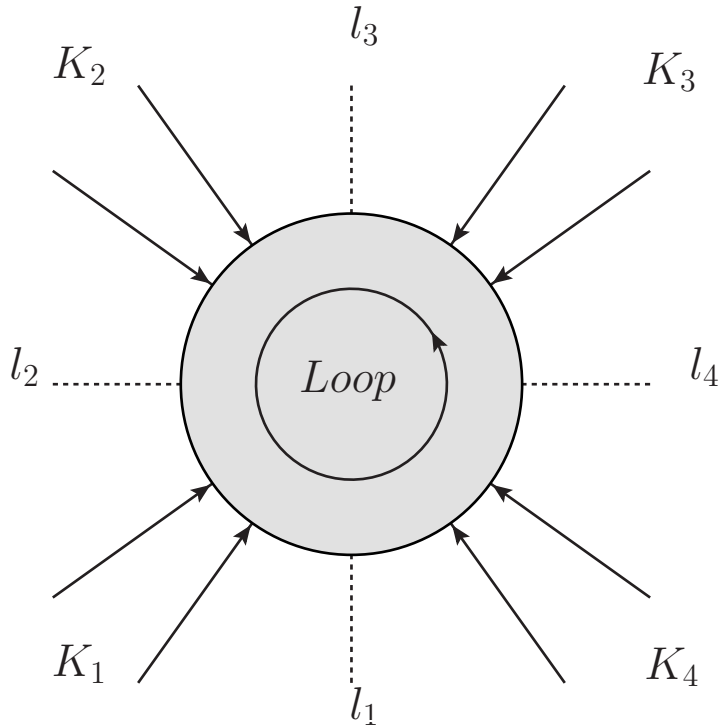
3.3 Cut coefficients and Rational terms

The determination of the cut coefficients starts with the process of solving cut conditions in order to have an expression for the loop momenta appearing in the tree amplitudes combining to yield the coefficients themselves. Solving such system of equations is quite tedious and goes far beyond the scope of this thesis. I will use results from previously done calculations in other research papers [20, 21], while making sure to translate them into our convention correctly. Even though there is a total of four coefficients to extract we'll interest ourselves with only two, box and triangle. The reason for this, is that the extraction of the remaining coefficients reuses ideas that are introduced to solve the first two cases.

3.3.1 Box coefficients

Extracting the coefficient corresponding to some box diagram with a specific partition of the clusters starts with solving the on-shell conditions and the determination of the loop momentum. The generic diagram representing a quadruple cut looks like,
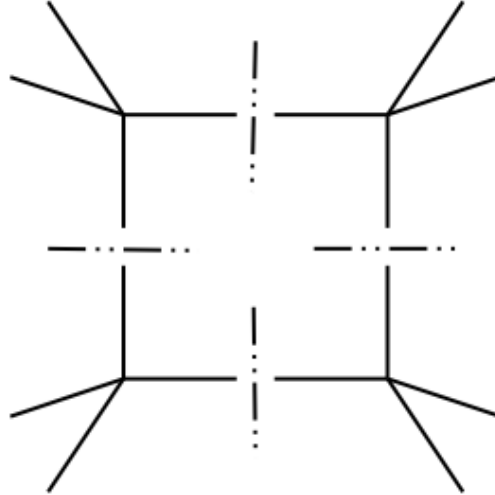

Figure 3.2: Generic quadruple-cut diagram.

Sticking with our convention of labeling momenta clockwise, we start from the bottom-left for the clusters and from bottom for the cut loop momenta (propagators on which we did draw the cuts). Recalling that we chose the loop momentum to flow counter-clockwise meaning that cut loop momenta will be directed likewise. We explicit their form in term of the loop momentum and clusters we have,

$$
\begin{aligned}
l_1 &= l \\
l_2 &= l_1 - K_1 = l - K_1 \\
l_3 &= l_2 - K_2 = l - K_1 - K_2 \\
l_4 &= l_3 - K_3 = l_1 + K_4 = l + K_4
\end{aligned}
\quad ,
\tag{3.12}
$$

with $K_1 + K_2 + K_3 + K_4 = 0$. The quadruple cut (massless) conditions write as $l_i^2 = 0$ with $i = \{1, 2, 3, 4\}$. The explicit system of equations in term of the massless loop momentum is,

$$
\begin{aligned}
l^2 &= 0 \\
(l - K_1)^2 &= 0 \\
(l - K_1 - K_2)^2 &= 0 \\
(l + K_4)^2 &= 0
\end{aligned}
\quad .
\tag{3.13}
$$

As it has been reported in the papers [21, 22], we have two possible solutions. These can be obtained by choosing a parametrization of the loop momentum in term of massless momenta,

$$
l^\mu = \sum_{i=1}^{4} A_i \alpha_i^\mu.
\tag{3.14}
$$

Although different parametrizations, $\{A_i, \alpha_i^\mu\}$ have been given in each paper, they are identical and yield the same numerical results. For the purpose of this document we'll employ the

parametrization which uses $\left\{ K_1^\mu, K_2^\mu, K_4^\mu, \epsilon_{\mu\nu\rho\lambda} K_1^\nu K_2^\rho K_4^\lambda \right\}$ as its α_i's , the coefficients A_i along with the full solutions which are given in [20] and simplified in a rather useful manner in another paper [21]. By taking the first cluster to be massless, that is, containing one leg only leading to $K_1^2 = 0$ the two solutions for the on-shell conditions are given as,

$$
\begin{aligned}
\left(l_1^{(\pm)} \right)^\mu &= \frac{\langle \pm 1 | K_2 K_3 K_4 \gamma^\mu | 1^\pm \rangle}{2 \langle \pm 1 | K_2 K_4 | 1^\pm \rangle} \\
\left(l_2^{(\pm)} \right)^\mu &= -\frac{\langle \pm 1 | \gamma^\mu K_2 K_3 K_4 | 1^\pm \rangle}{2 \langle \pm 1 | K_2 K_4 | 1^\pm \rangle} \\
\left(l_3^{(\pm)} \right)^\mu &= \frac{\langle \pm 1 | K_2 \gamma^\mu K_3 K_4 | 1^\pm \rangle}{2 \langle \pm 1 | K_2 K_4 | 1^\pm \rangle} \\
\left(l_4^{(\pm)} \right)^\mu &= -\frac{\langle \pm 1 | K_2 K_3 \gamma^\mu K_4 | 1^\pm \rangle}{2 \langle \pm 1 | K_2 K_4 | 1^\pm \rangle}
\end{aligned} \quad . \tag{3.15}
$$

To further check the validity of these solutions we need to make sure that they are massless and enable us to extract cluster information following from momentum conservation.

Since all loop momenta are built from $\left(l_1^{(\pm)} \right)^\mu$ it is only sufficient to check this one for masslessness,

$$
\left(l_1^{(\pm)} \right)^\mu \left(l_1^{(\pm)} \right)_\mu \propto \langle \mp K_4 | \gamma^\mu | 1^\pm \rangle \langle \mp K_4 | \gamma_\mu | 1^\pm \rangle \propto \langle 11 \rangle^0 \tag{3.16}
$$

Recall that,

$$
\begin{aligned}
l_2 - l_3 &= K_2 \\
l_3 - l_4 &= K_3 \\
l_4 - l_1 &= K_4
\end{aligned} \quad . \tag{3.17}
$$

Checking the first equation we get,

$$
\left(l_2^{(\pm)} - l_3^{(\pm)} \right)^\mu = -\frac{\langle \pm 1 | \{ K_2, \gamma^\mu \} K_3 K_4 | 1^\pm \rangle}{2 \langle \pm 1 | K_2 K_4 | 1^\pm \rangle} = -K_2^\mu \frac{\langle \pm 1 | K_3 K_4 | 1^\pm \rangle}{\langle \pm 1 | K_2 K_4 | 1^\pm \rangle},
$$

where we applied $\{\gamma^\mu, \gamma^\nu\} = 2g^{\mu\nu}$ and then fraction reduces to -1 by using $K_3 = -k_1 - K_2 - K_4$, confirming the relations and checking effectively that our solutions are consistent.

The coefficient of any box topology is given as the superposition of the two coefficients evaluated from each solution $d_i = \frac{1}{2} \sum_{\sigma = \pm} d_i^\sigma$,

$$
d_i^\sigma = \mathcal{A}_1^{tree} \mathcal{A}_2^{tree} \mathcal{A}_3^{tree} \mathcal{A}_4^{tree} |_{l_i \longrightarrow l_i^\sigma}, \tag{3.18}
$$

with $\mathcal{A}_i^{tree} = \mathcal{A}^{tree} \left(-l_i, \{K_i\}, l_{i+1} \right)$ and $\{K_i\}$ refer to the list of external momenta forming the cluster K_i.

3.3.2 Triangle Coefficient

At this point of calculation we'll run into our first complication as it is clear that a triple cut will not allow us to fully determine the loop momentum. There will be a remaining degree of freedom having the interesting consequence of making the triangle coefficients that we read directly from the triangle topology not pure, that is receiving box contributions. All this is due to that unfixed parameter in the loop momentum. Unlike what we had before where the quadruple-cut provided information that is purely box-coefficient related, the triple-cut contains a mixture of information between box contributions and triangle ones.
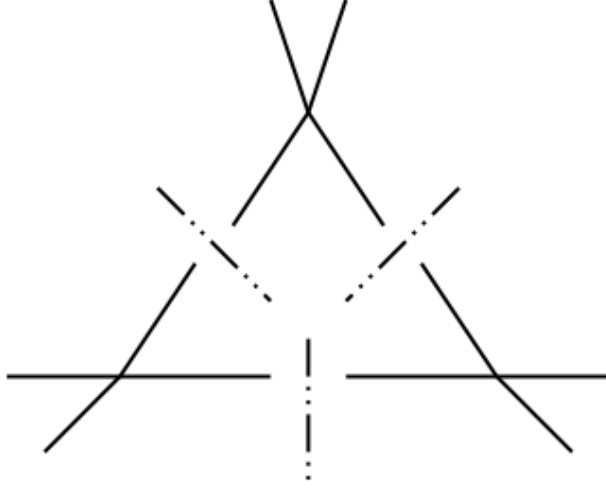
Figure 3.3: Generic triple-cut diagram.

The cut conditions used $\left\{ l(t)^2 = 0, (l(t) - K_1)^2 = 0, (l(t) + K_2)^2 = 0 \right\}$ to obtain $l^\mu(t)$ where t is a complex parameter are solved to give us [13],

$$ l^\mu(t) = \tilde{K}_1^\mu + \tilde{K}_3^\mu + \frac{t}{2} \left\langle {}^+ \tilde{K}_1 | \gamma^\mu | \tilde{K}_3^- \right\rangle + \frac{1}{2t} \left\langle {}^+ \tilde{K}_3 | \gamma^\mu | \tilde{K}_1^- \right\rangle, \tag{3.19} $$

with,

$$ \begin{aligned} \tilde{K}_1^\mu &= \gamma \alpha \frac{\gamma K_1^\mu + S_1 K_3^\mu}{\gamma^2 - S_1 S_3} \\ \tilde{K}_3^\mu &= -\gamma \alpha' \frac{\gamma K_3^\mu + S_3 K_1^\mu}{\gamma^2 - S_1 S_3} \end{aligned}, \tag{3.20} $$

and,

$$ \begin{aligned} \alpha &= \frac{S_3(S_1 - \gamma)}{S_1 S_3 - \gamma^2} \\ \alpha' &= \frac{S_1(S_3 - \gamma)}{S_1 S_3 - \gamma^2} \\ \gamma = \gamma_\pm &= -K_1 \cdot K_3 \pm \sqrt{\Delta} \\ \Delta &= (K_1 \cdot K_3)^2 - K_1^2 K_3^2 \end{aligned}, \tag{3.21} $$

where $S_1 = K_1^2$ and $S_3 = K_3^2$. Keeping in mind that we have to sum over two solutions corresponding to $\gamma_\pm$ in order to determine the coefficients. We write the "uncleaned" triangle coefficients as $\widetilde{c}_i = 1/2 \sum_{\sigma = \pm} \widetilde{c}_i^\sigma$ with,

$$ \widetilde{c}_i^\sigma = \mathcal{A}_1^{tree} \mathcal{A}_2^{tree} \mathcal{A}_3^{tree} \big|_{l_i = l_i^\sigma(t)}. \tag{3.22} $$

The box contribution comes in for some finite values of t, namely regions where the topology looks like a box one. We of course are only interested in the triangle information requiring us to cleanse the triple-cut from box information first. Doing that requires us to know the values of the parameter for which the unneeded information steps in.
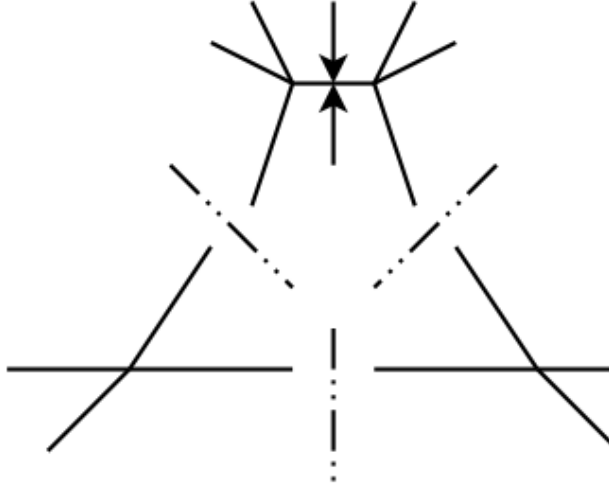
Figure 3.4: Illustration of "pinching" process.

To paint a picture about the cleansing process, we imagine ourselves "pinching" one point of the triangle until it splits in two making its structure look like a box. The "pinching" will expose a new loop propagator and impose a fourth-condition, a condition for which the new propagator vanishes or more appropriately goes on-shell. This condition will fix $t = t_0$, a finite value for which the propagator blows up making that value a pole. Finding all the poles amount to finding all the values for which we have a box contribution. This can be put mathematically in a rather elegant manner that was first introduced by Forde [23],

$$\mathcal{A}_1^{tree}(t)\mathcal{A}_2^{tree}(t)\mathcal{A}_3^{tree}(t) = \left[Inf_t\mathcal{A}_1^{tree}\mathcal{A}_2^{tree}\mathcal{A}_3^{tree}\right](t) + \sum_{\{k\}}\left[\frac{Res_{t=t_k}\mathcal{A}_1^{tree}\mathcal{A}_2^{tree}\mathcal{A}_3^{tree}}{t - t_k}\right]. \qquad (3.23)$$

The second term here account for all the box contributions as residues for finite t_k that put the pinched-out propagator on-shell. The first term is a contribution at infinity formally defined as,

$$lim_{t\longrightarrow\infty}\left(\left[Inf_t\mathcal{A}_1^{tree}\mathcal{A}_2^{tree}\mathcal{A}_3^{tree}\right](t) - \mathcal{A}_1^{tree}(t)\mathcal{A}_2^{tree}(t)\mathcal{A}_3^{tree}(t)\right) = 0. \qquad (3.24)$$

The pole structure, or polology[5] of the "uncleaned" triangle coefficient is composed of both finite and infinite singularities with the finite ones giving those box impurities. The contributions at infinity are free from finite singularities and can be written as a power series,

$$\left[Inf_t\mathcal{A}_1^{tree}\mathcal{A}_2^{tree}\mathcal{A}_3^{tree}\right](t) = \sum_{n=0}^{m}e_nt^n, \qquad (3.25)$$

with m being taken to be 3 for renormalizable theories, justified by the fact that there can be at most 3 momenta in the numerator of triangle integrals [13].

Subtracting the residues corresponding the box contributions from the "uncleaned" triangle coefficient, tells us that the pure triangle contributions come from $[Inf_t]$, namely terms at infinity. Recalling that the coefficients we are trying to compute are parameter-independent requiring us to sum over any free continuous index we obtain it by integrating over t after properly cleansing the integrand leading us to,

---

[5]It is a constructed term(p.471, [6]) that refers to the study of the pole structure of complex functions.

$$c_i^\sigma = i\,(-2\pi i)^3 \int \frac{dt}{(2\pi)^4} J_t \left(\left[Inf_t \mathcal{A}_1^{tree} \mathcal{A}_2^{tree} \mathcal{A}_3^{tree} \right] (t) \right) |_{l_i = l_i^\sigma(t)}, \tag{3.26}$$

where the J_t is the Jacobian of the transformation from an integral over $d^4 l$ to one over the remaining parameter dt.

Using the polynomial form the integrand we find ourselves in need to construct a table of integrals for $i\,(-2\pi i)^3 \int \frac{dt}{(2\pi)^4} J_t t^n$, which gives 1 for $n = 0$ and vanishes for the $n > 0$ [22]. The previous confirms the independence from the parameter leading us to write at last,

$$c_i^\sigma = - \left(\left[Inf_t \mathcal{A}_1^{tree} \mathcal{A}_2^{tree} \mathcal{A}_3^{tree} \right] (t) \right) |_{t=0}. \tag{3.27}$$

The last formula tells us that all that is missing to have the answer is to find the poles and subtract their residues and then put $t = 0$ to remove the dependence on it.

3.3.3 Bubble and Tadpole Coefficients

In addition to the previous coefficients, the full 1-loop answer requires coefficients from two lower-point topologies depicted below.

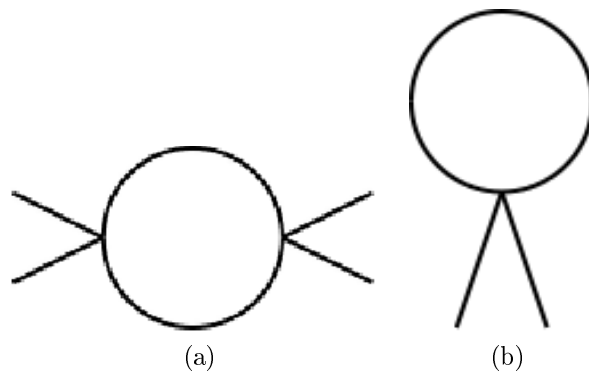(a) (b)

Figure 3.5: A bubble and tadpole topology.

We again recognize the same problem that we had with the triangle topology, where the triple-cut didn't impose enough constraints to exactly determine the loop momentum. Moreover the appearance of contributions from higher-point topologies at some specific regions lead us to consider a *cleaning* procedure to extract the information of interest.

(a)   (b)
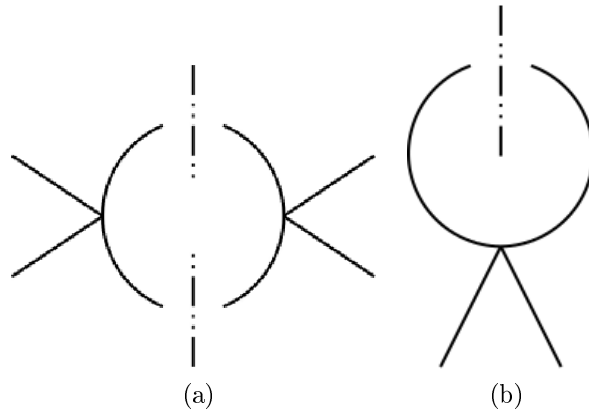
Figure 3.6: Double and One-cut

The same dilemma is to be encountered here where a double or a one-cut provide us with clearly not enough constraints to solve the cut conditions leading us to have more than one free parameter. In addition we get to have contributions from triangle and box coefficients mixed within at some specific values of the parameters. The good thing here is that it won't require us more than what we already exposed to have our coefficients, it will only require more work.

3.3.4   Rational terms

Cuts will not capture all the information relevant to the one-loop problem and this was indicated when we first mentioned "simple" Unitarity and worked out that the application of the cut rules only provide us with the imaginary part of the amplitude. The rational terms are the parts of the amplitude that aren't captured by the cut procedure,

$$R_n = \mathcal{A}_n^{1-loop}|_{\mathcal{I}_{m-point}^i \longrightarrow 0}. \tag{3.28}$$

There are so far many methods to get these terms and the common point between all of these methods is that they require us to know all the cut coefficients. Most of these methods [24, 25] have been implemented both numerically and analytically.

Chapter 4

One-Loop Helicity amplitude Application

Now that we have a one-loop formulation for Helicity amplitudes, it is of interest to showcase the extraction process of Kinematic (cut) coefficients for a given one-loop topology. In the previous chapter we were able to find the exact analytical solutions for the box-coefficients. The triangle-coefficients presented some complications where they had to be distilled from box-contributions before obtaining the pure triangle ones and the same complications are encountered at lower-point topologies where we follow the same procedure to resolve. That procedure emphasizes the fact that all coefficients relate to the highest-point one. In this chapter, we'll compute the box-coefficients related to pure gluon box-diagram correcting the LO for the $gg \longrightarrow gg$ process.

4.1   Box-Loop corrections to $gg \longrightarrow gg$

Among the numerous one-loop diagrams contributing at the next-to-leading order we only have two that correspond to a 4-point topology.

(a) pure gluonic diagram

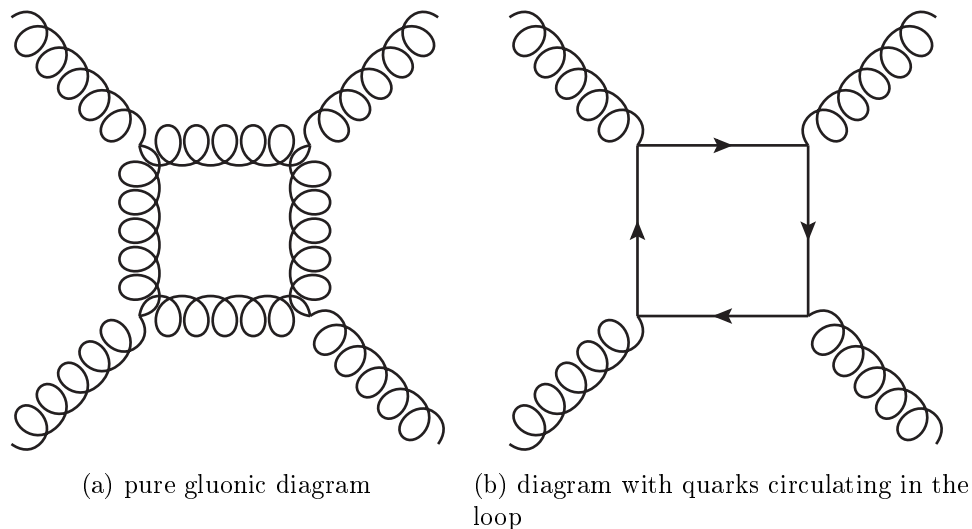(b) diagram with quarks circulating in the loop

Figure 4.1: One-loop diagrams with a box-shape loop.

Both of these are involved in the complete determination of the d_i[1] coefficients since they are the

---

[1]Refer to chapter 4 subsection 3.1.

only diagrams providing four propagators to cut. In order to illustrate the procedure of extraction we choose to work with the diagram in sub-fig (a) of Fig 4.1. We start with a computer-assisted derivation of the analytical expressions using Mathematica/S@M and then perform a check against a numerical algorithm presented in [11].

4.2 Pure-gluon box-coefficient

This section will deal with the extraction of the box-coefficient related to the previously selected diagram with external polarization $(+ + --)$. And since the interest is mainly directed towards treating the kinematic part of the amplitude we separate the color from the rest of the expression as it can be handled with similar tools presented in Appendix B[2].

To conduct our task, we'll make use of a formula given in the previous chapter that tells us, box-coefficients are obtained by cutting through each propagator in a way that puts it on-shell and then do the product of the resulting tree-amplitudes likewise,

$$d_i = \frac{1}{2} \sum_{\sigma=1,2} \left(\mathcal{A}_1^{tree} \mathcal{A}_2^{tree} \mathcal{A}_3^{tree} \mathcal{A}_4^{tree} \big|_{l_i \longrightarrow l_i^{(\sigma)}} \right). \tag{4.1}$$
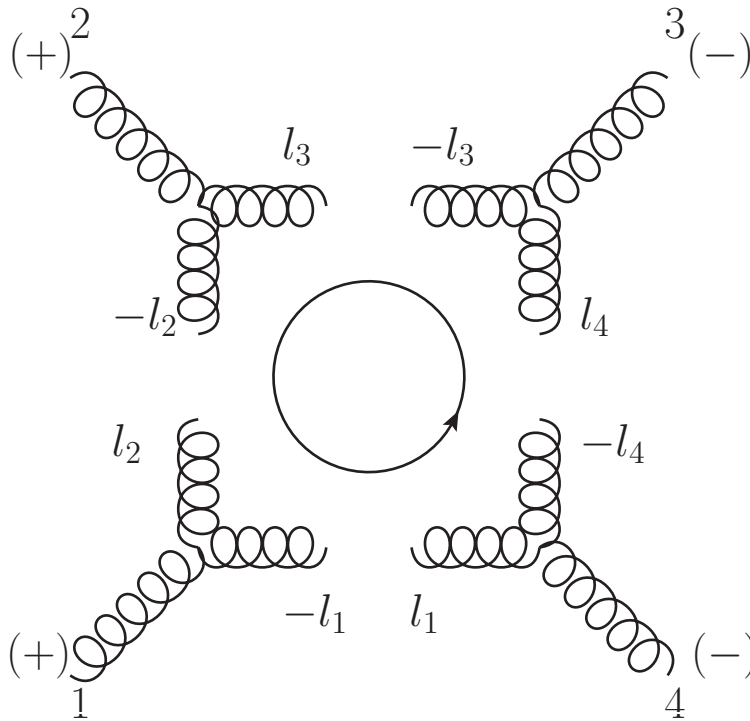
Figure 4.2: Quadruple-cut performed on the box-shape loop diagram.

In this diagram[3] the clusters are massless implying that we have only one possibility for the arrangement of momenta leading us to have just one coefficient to compute in this case. Another effect of this is that the tree amplitudes at each corner are just GGG-vertices. Making the generic form of the coefficient contribution looking like,

---

[2]See also [26], pg. 11-12.

[3]The directed circle indicates the loop momentum flow.

$$d = \widetilde{\mathcal{A}}_{GGG|1}^{tree}\left(-l_1, 1, l_2\right) \widetilde{\mathcal{A}}_{GGG|2}^{tree}\left(-l_2, 2, l_3\right) \widetilde{\mathcal{A}}_{GGG|3}^{tree}\left(-l_3, 3, l_4\right) \widetilde{\mathcal{A}}_{GGG|4}^{tree}\left(-l_4, 4, l_1\right).$$

We can readily see that the spinor associated with each momentum appears an even number of times in the amplitude[4]. If one of momenta is inverted, for example if we have $-p$ instead of p then the corresponding spinors either angled (or square) are related by a phase $\pm i$. In the case where we have an occurrence that is equal to 4 or one of its powers then all the phases produced factor up to unity, which is what we have in our generic expression, thus we can remove the $(-)$ from the labels and write it in a direct manner,

$$d = \widetilde{\mathcal{A}}_{GGG|1}^{tree}\left(l_1, 1, l_2\right) \widetilde{\mathcal{A}}_{GGG|2}^{tree}\left(l_2, 2, l_3\right) \widetilde{\mathcal{A}}_{GGG|3}^{tree}\left(l_3, 3, l_4\right) \widetilde{\mathcal{A}}_{GGG|4}^{tree}\left(l_4, 4, l_1\right). \tag{4.2}$$

Recalling the expressions of $3 - point$ color-stripped amplitudes,

$$\begin{aligned}
\widetilde{\mathcal{A}}_{GGG}^{tree}\left(1^+, 2^+, 3^-\right) &= \frac{[12]^3}{[23][31]}\\
\widetilde{\mathcal{A}}_{GGG}^{\sim tree}\left(1^-, 2^-, 3^+\right) &= \frac{\langle 12\rangle^3}{\langle 23\rangle\langle 31\rangle}
\end{aligned} \tag{4.3}$$

The final coefficient is obtained by summing over possible internal Helicity configurations and averaging the result obtained from both loop momentum solutions,

$$\begin{aligned}
\left(l_1^{(1)}\right)^{\alpha\dot{\alpha}} &= \frac{[23]\langle 34\rangle}{[24]\langle 41\rangle}|4\rangle[1|\\
\left(l_1^{(2)}\right)^{\alpha\dot{\alpha}} &= \frac{\langle 23\rangle[34]}{\langle 24\rangle[41]}|1\rangle[4|
\end{aligned} \tag{4.4}$$

4.2.1 Color-stripped coefficient

We start this part by defining the basic amplitudes we'll be using along with declaring the spinor variables of our problem as follows,

```
In[35]:=    GGG[{a_,+1},{b_,+1},{c_,-1}]:=
            Spbb[a,b]^3/(Spbb[b,c]*Spbb[c,a])
            GGG[{a_,-1},{b_,-1},{c_,+1}]:=
            Spaa[a,b]^3/(Spaa[b,c]*Spaa[c,a])

In[36]:=    DeclareSpinor[l1,l2,l3,l4]

            {l1,l2,l3,l4} added to the list of spinors
```

There are in total six possible internal Helicity configurations. This count is obtained by considering the constraint that Helicity should be the opposite on the different side of the same propagator cut[5], meaning that we have either $(+-)$ or $(-+)$ along the same propagator and we have 4 propagators implying that we should have $C_4^2 = 6$ possible configurations. We'll adopt a compact way to refer[6] to each configuration based on the kind of contributing GGG-vertices (either $\mathcal{A}$ or $\overline{\mathcal{A}}$).

- The first internal configuration, $\mathcal{A}\overline{\mathcal{A}}\mathcal{A}\overline{\mathcal{A}}$.

---

[4]Mainly because the form of the amplitude is dictated by little group scaling.
[5]Consequence of on-shell methods presented in chapter 2.
[6]The referencing follows a clockwise ordering starting from the bottom left corner.
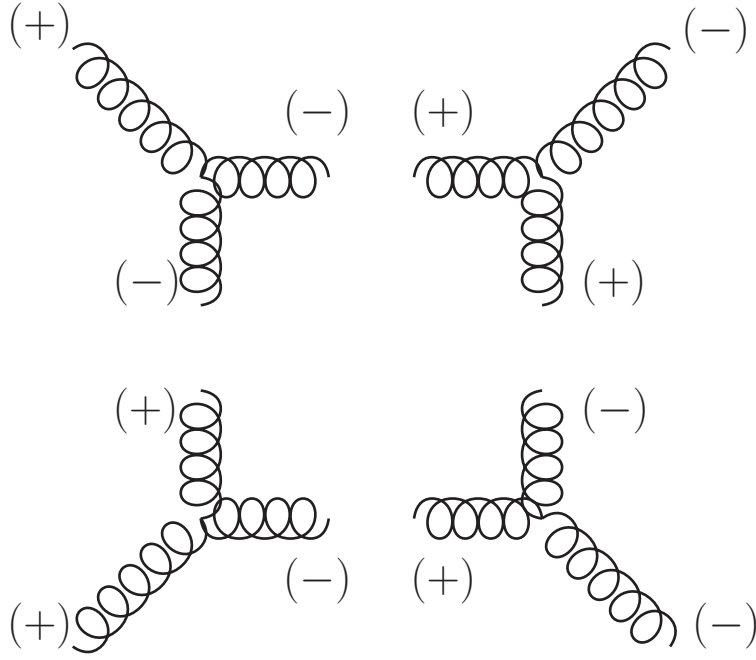
Figure 4.3: $\mathcal{A}\overline{\mathcal{A}}\mathcal{A}\overline{\mathcal{A}}$

We start by putting down the corresponding product of amplitudes,

In[37]:= `AaAa=GGG[{1,+1},{l2,+1},{l1,-1}]*`
`GGG[{l3,-1},{l2,-1},{2,+1}]*`
`GGG[{l4,+1},{l3,+1},{3,-1}]*`
`GGG[{l4,-1},{4,-1},{l1,+1}] //`
` SpClose`

Out[37]= $\dfrac{\langle 4|l4|l3|l2|1]^3}{\langle 2|l3|3]\quad \langle 4|l1|1]\quad \langle 2|l2|l1|l4|3]}$

and then write l_2, l_3 and l_4 in term of l_1.

In[38]:= `xAaAa=AaAa/.{l2→l1-Sm[1],`
`l3→l1-Sm[1]-Sm[2],`
`l4→ l1+Sm[4]}`

Out[38]= $-\dfrac{(-\langle 4|l1|1|l1|1]-\langle 4|l1|2|l1|1])^{\;3}}{(\langle 2|l1|3]-\langle 2|1|3])\;\langle 4|l1|1]\quad\langle 2|1|l1|4|3]}$

At last we substitute for the solutions of the loop momenta, starting with $l_1^{(1)}$

In[39]:= `dAaAa=xAaAa/.l1 →` $\dfrac{[2|3]\langle 3|4\rangle}{[2|4]\langle 4|1\rangle}$`SmBA[4,1]`

to obtain,

$$\dfrac{\langle 34\rangle^4\,\langle 1|2|4]^3\,[32]^4\,[41]^2}{\langle 14\rangle^2\,\langle 1|4|3]\,\langle 2|1|4]\,[42]^4\left(-\langle 2|1|3]+\frac{\langle 12\rangle\langle 34\rangle[32][43]}{\langle 14\rangle[42]}\right)} \qquad (4.5)$$

while the second solution $l_1^{(2)}$ annihilate the expression,

49

In[40]:= `Numerator[xAaAa]/.l1 →` $\dfrac{\langle 2|3\ \rangle[3|4]}{\langle 2|4\rangle[4|1]}$`SmBA[1,4]`

Out[40]= 0

Here we used the ***Numerator[...]*** function to isolate the numerator, since Mathematica doesn't understand that the amplitudes composing our expression are made so that they vanish faster than they diverge and interprets them as just divergent.

- The second internal configuration, $\mathcal{A}\overline{\mathcal{A}\mathcal{A}}\mathcal{A}$.
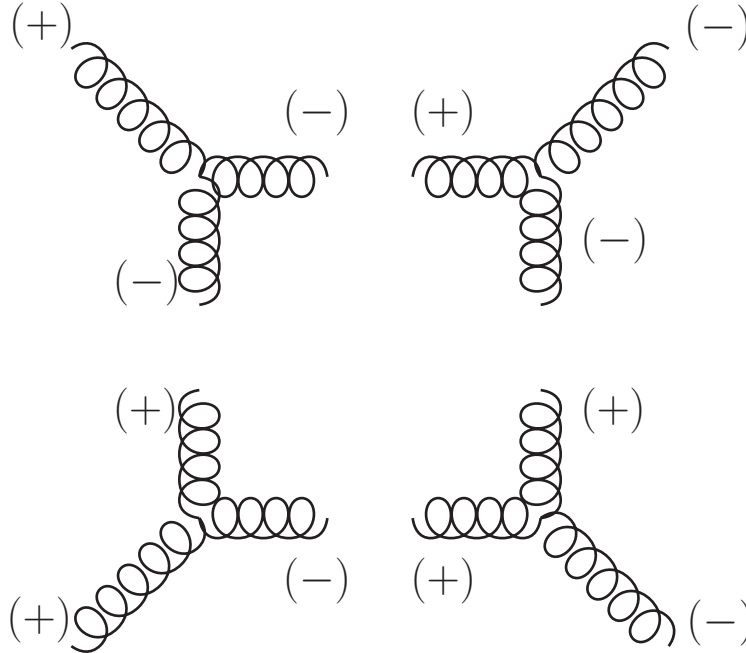
Figure 4.4: $\mathcal{A}\overline{\mathcal{A}\mathcal{A}}\mathcal{A}$

The input for the corresponding contribution writes like,

In[41]:=
```
AaaA=GGG[{1,+1},{l2,+1},{l1,-1}]*
GGG[{l3,-1},{l2,-1},{2,+1}]*
GGG[{3,-1},{l4,-1},{l3,+1}]*
GGG[{l1,+1},{l4,+1},{4,-1}] //
 SpClose
```

Out[41]= $\dfrac{\langle l3|l2|1]^{3}\ \ \langle 3|l4|l1]^{3}}{\langle l3|2\rangle\ \ \langle l3|3\rangle\ \langle l3|l4|4]\ \langle 2|l2|l1]\ [1|l1]\ [4|l1]}$

We notice that the loop momenta appears at the extremities of the spinor chains which prevents us from proceeding further. If we attempt to substitute every loop momentum in term of l_1 we obtain an error as these objects are only defined as slashed matrices that could only exist within a chain and not at the ends of it. A work around is to multiply by $\langle 3|l1\rangle^{3}[l3|1]^{3}$ and divide by it so that it amounts to unity. The effect of this trick is to remove the loop spinors from extremities by surrounding them with external momenta spinors allowing us perform the substitution.

```
In[42]:=   Numerator[AaaA]Spbb[l3,1]^3*
           Spaa[3,l1]^3 //SpClose;
           xAaaANum=%/.{l2→l1-Sm[1],
           l3→l1-Sm[1]-Sm[2],
           l4→ l1+Sm[4]}
```

Out[42]= $\langle 3|l1|4|3\rangle^3$ $[1|2|l1|1]^3$

```
In[43]:=   xAaaANum/.l1 →
```
$$\frac{\langle 2|3\rangle[3|4]}{\langle 2|4\rangle[4|1]}\text{SmBA}[1,4]$$

Out[43]=   0

```
In[44]:=   xAaaANum/.l1 →
```
$$\frac{[2|3]\langle 3|4\rangle}{[2|4]\langle 4|1\rangle}\text{SmBA}[4,1]$$

Out[44]=   0

The freedom to choose the anti-symmetric product to complete the chain provides us with a control over the vanishing of the contribution.

- The third ($\overline{\mathcal{A}}\mathcal{A}\mathcal{A}\overline{\mathcal{A}}$), fourth ($\mathcal{A}\mathcal{A}\overline{\mathcal{A}\mathcal{A}}(1)$) and fifth ($\mathcal{A}\mathcal{A}\overline{\mathcal{A}\mathcal{A}}(2)$) internal signatures present the same situation as the second one and in the same way they will not contribute.

The code implementing calculations for all of the three diagrams discussed in the previous paragraph is given below.
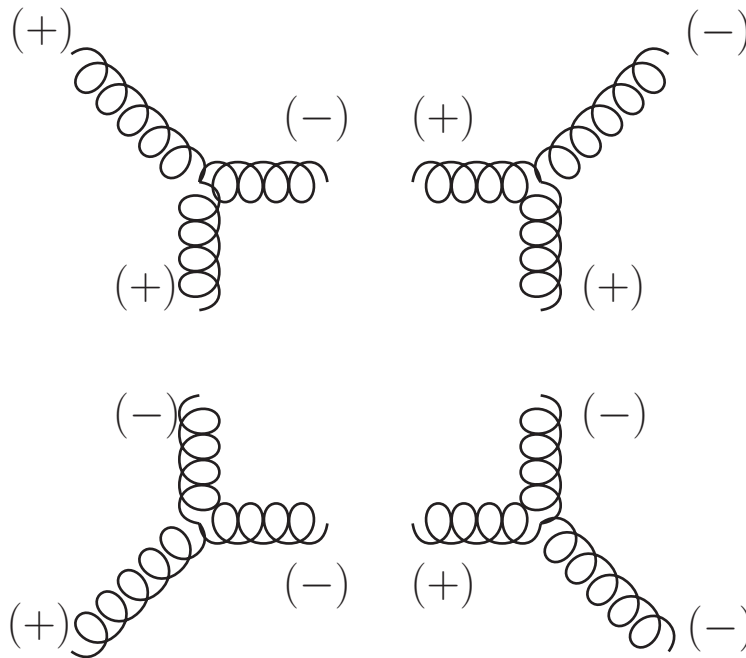
Figure 4.5: $\overline{\mathcal{A}}\mathcal{A}\mathcal{A}\overline{\mathcal{A}}$

```
In[45]:=   aAAa =GGG[{l2,-1},{l1,-1},{1,+1}]*
           GGG[{l2,+1},{2,+1},{l3,-1}]*
           GGG[{l4,+1},{l3,+1},{3,-1}]*
           GGG[{l4,-1},{4,-1},{l1,+1}] //
           SpClose
```

51

Out[45]= $$\frac{\langle l1|l2|2]^3 \quad \langle 4|l4|l3]^3}{\langle l1|1\rangle \quad \langle l1|4\rangle \quad \langle l1|l4|3] \quad \langle 1|l2|l3] \quad [2|l3] \quad [3|l3]}$$

In[46]:= `Numerator[aAAa]Spaa[l3,1]^3*`
`Spbb[3,l1]^3 //SpClose;`
`xaAAaNum=%/.{l2→l1-Sm[1],`
`l3→l1-Sm[1]-Sm[2],`
`l4→ l1+Sm[4]}`

Out[46]= $-\langle 1|2|l1|4\rangle^3 \; [3|l1|1|2]^3$

In[47]:= `xaAAaNum/.l1` $\rightarrow \dfrac{\langle 2|3\rangle[3|4]}{\langle 2|4\rangle[4|1]}$ `SmBA[1,4]`

Out[47]= 0

In[48]:= `xaAAaNum/.l1` $\rightarrow \dfrac{[2|3]\langle 3|4\rangle}{[2|4]\langle 4|1\rangle}$ `SmBA[4,1]`

Out[48]= 0
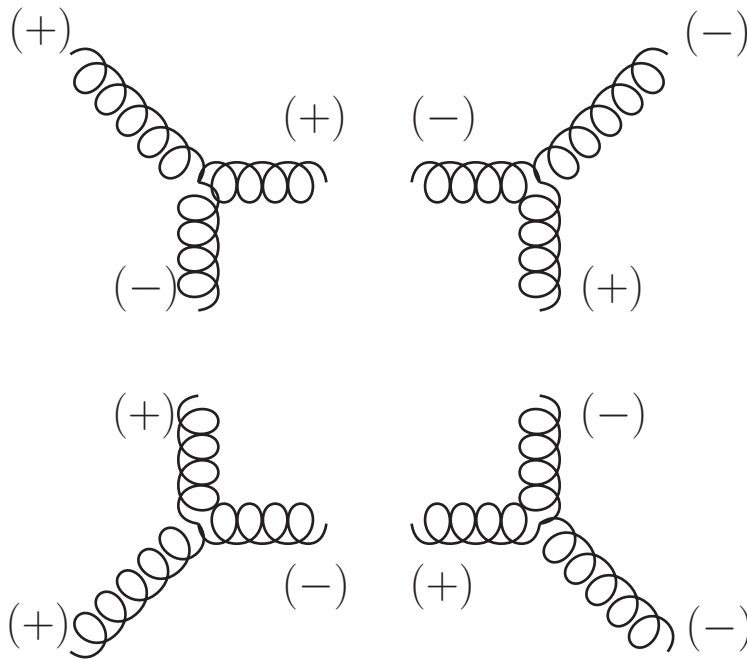
Figure 4.6: $\mathcal{A}\mathcal{A}\overline{\mathcal{A}\mathcal{A}}(1)$

In[49]:= `AAaa1 =GGG[{1,+1},{l2,+1},{l1,-1}]*`
`GGG[{2,+1},{l3,+1},{l2,-1}]*`
`GGG[{l3,-1},{3,-1},{l4,+1}]*`
`GGG[{l4,-1},{4,-1},{l1,+1}] //`
`SpClose`

Out[49]= $$\frac{\langle l4|4\rangle^3 \quad \langle 3|l3|2]^3 \quad [1|l2]^3}{\langle l4|3\rangle \quad \langle l4|l1|l2] \quad \langle l4|l3|l2] \quad \langle 4|l1|1] \quad [2|l2]}$$

In[50]:= `Numerator[AAaa1]Spaa[12,4]^3*`
`Spbb[4,14]^3 //SpClose;`
`xAAaa1Num=%/.{12→11-Sm[1],`
`13→11-Sm[1]-Sm[2],`
`14→ 11+Sm[4]}`

Out[50]= $(\langle 3|11|2] - \langle 3|1|2])^3 \quad \langle 4|11|4|11|1]^3$

In[51]:= `xAAaa1Num/.11` $\rightarrow \dfrac{\langle 2|3\rangle[3|4]}{\langle 2|4\rangle[4|1]}$`SmBA[1,4]`

Out[51]= 0

In[52]:= `xAAaa1Num/.11` $\rightarrow \dfrac{[2|3]\langle 3|4\rangle}{[2|4]\langle 4|1\rangle}$`SmBA[4,1]`

Out[52]= 0
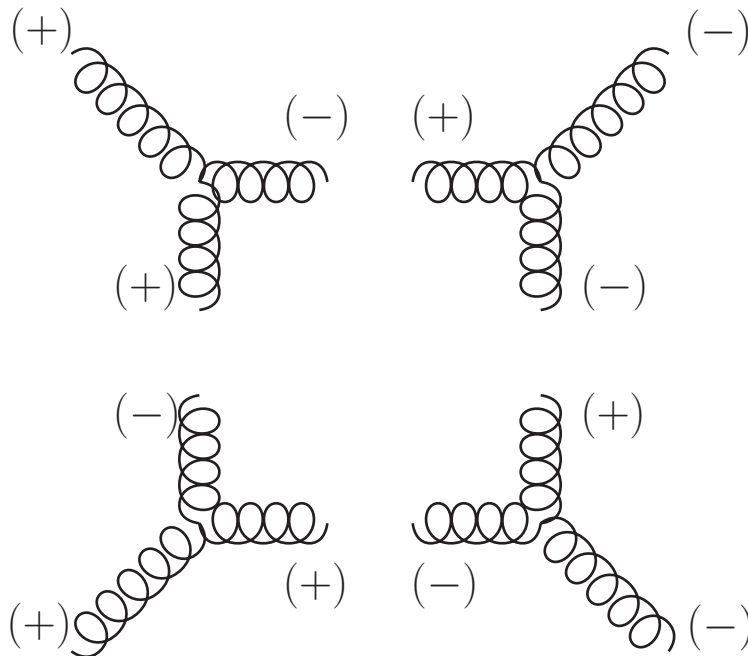
Figure 4.7: $\mathcal{A}\mathcal{A}\overline{\mathcal{A}\mathcal{A}}(2)$

In[53]:= `AAaa2=GGG[{11,+1},{1,+1},{12,-1}]*`
`GGG[{12,+1},{2,+1},{13,-1}]*`
`GGG[{3,-1},{14,-1},{13,+1}]*`
`GGG[{4,-1},{11,-1},{14,+1}] //`
`SpClose`

Out[53]= $\dfrac{\langle 14|3\rangle^3 \quad \langle 4|11|1]^3 \quad [2|12]^3}{\langle 14|4\rangle \ \langle 14|11|12] \ \langle 14|13|12] \ \langle 3|13|2] \ [1|12]}$

In[54]:= `Numerator[AAaa2]Spaa[12,4]^3*`
`Spbb[4,14]^3//SpClose;`

```
          xAAaa2Num=%/.{12→11-Sm[1],
          13→11-Sm[1]-Sm[2],
          14→ 11+Sm[4]}
```

Out[54]= $\langle 4|11|1]^3$ $(\langle 3|11|4|11|2] - \langle 3|11|4|1|2])^3$

In[55]:=   `xAAaa2Num /.11 →` $\dfrac{\langle 2|3\rangle[3|4]}{\langle 2|4\rangle[4|1]}$ `SmBA[1,4]`

Out[55]=   0

In[56]:=   `xAAaa2Num /.11 →` $\dfrac{[2|3]\langle 3|4\rangle}{[2|4]\langle 4|1\rangle}$ `SmBA[4,1]`

Out[56]=   0

- The sixth internal signature, $\overline{\mathcal{A}}\mathcal{A}\overline{\mathcal{A}}\mathcal{A}$.

Figure 4.8: $\overline{\mathcal{A}}\mathcal{A}\overline{\mathcal{A}}\mathcal{A}$

The last contribution gets implemented as follow,
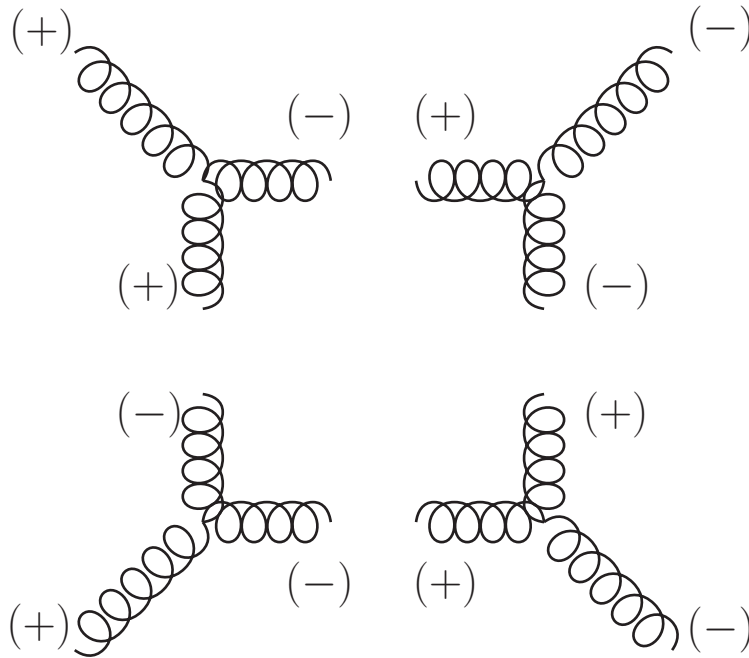
In[57]:=   `aAaA=GGG[{12,-1},{11,-1},{1,+1}]*`
          `GGG[{12,+1},{2,+1},{13,-1}]*`
          `GGG[{3,-1},{14,-1},{13,+1}]*`
          `GGG[{11,+1},{14,+1},{4,-1}] //`
          `SpClose`

Out[57]= $\dfrac{\langle 3|14|11|12|2]^3}{\langle 1|11|4]\quad \langle 3|13|2]\ \langle 1|12|13|14|4]}$

54

In[58]:= `xaAaA=aAaA/.{l2→l1-Sm[1],`
`l3→l1-Sm[1]-Sm[2],`
`l4→ l1+Sm[4]}`

So that we get the opposite situation with respect to the first signature. The expression vanishes for $l_1^{(1)}$,

In[59]:= $\texttt{Numerator[xaAaA]/.l1} \rightarrow \dfrac{[2|3]\langle 3|4\rangle}{[2|4]\langle 4|1\rangle}\texttt{SmBA[4,1]}$

Out[59]= 0

while for $l_1^{(2)}$,

In[60]:= $\texttt{daAaA=xaAaA /.l1} \rightarrow \dfrac{\langle 2|3\ \rangle[3|4]}{\langle 2|4\rangle[4|1]}\texttt{SmBA[1,4]}$

we obtain,

$$\frac{\langle 3|4|1]^3\,\langle 4|1|2]^3}{\langle 14\rangle^2\,\langle 4|2|1]\,[41]^2\left(-\langle 3|1|2]+\frac{\langle 23\rangle\langle 34\rangle[21][43]}{\langle 24\rangle[41]}\right)}. \tag{4.6}$$

As a final result we give the box-coefficient to be,

$$\begin{aligned} d_{gluon-box-loop} = &\frac{1}{2}[\frac{\langle 34\rangle^4\,\langle 1|2|4]^3\,[32]^4\,[41]^2}{\langle 14\rangle^2\,\langle 1|4|3]\,\langle 2|1|4]\,[42]^4\left(-\langle 2|1|3]+\frac{\langle 12\rangle\langle 34\rangle[32][43]}{\langle 14\rangle[42]}\right)} \\ &+\frac{\langle 3|4|1]^3\,\langle 4|1|2]^3}{\langle 14\rangle^2\,\langle 4|2|1]\,[41]^2\left(-\langle 3|1|2]+\frac{\langle 23\rangle\langle 34\rangle[21][43]}{\langle 24\rangle[41]}\right)}] \end{aligned} \tag{4.7}$$

4.2.2 Numerical check

Now that we have our analytical expression we start to implement the numerical verification.

We first generate massless external momenta so that their sum equals zero[7].

In[61]:= `SeedRandom[1111]`
`GenMomenta[{1,2,3,4}]`

`Momenta for the spinors 1, 2, 3, 4 generated.`

Then solve the system of cut-conditions for the components of the loop momentum so that we obtain two solutions.

In[62]:= `DeclareLVectorMomentum[L,{L0,L1,L2,L3}]`

`Four Momentum L set to {L0,L1,L2,L3}.`

In[63]:= `l11=L`
`l12 = L-Sp[1]`
`l13 = l12-Sp[2]`
`l14 = l13-Sp[3]`

---

[7]All taken to be incoming.

```
In[64]:=    solutions=Solve[{
            MP2[l11]==0,
            MP2[l12]== 0,
            MP2[l13]== 0,
            MP2[l14]==0
            }//N,{L0,L1,L2,L3}]
```

```
Out[64]=    {{L0→2.22727-3.30852 i,L1→1.78302-4.97181  i,L2→-2.20165+1.34759
            i,L3→3.73505+1.19483 i},{L0→2.22727+3.30852  i,L1→1.78302+4.97181
            i,L2→-2.20165-1.34759 i,L3→3.73505-1.19483 i}}
```

We start by constructing the loop spinors given by the first solution and extract the value of the coefficient for the first signature as it is the only one contributing at this level.

```
In[65]:=    DeclareSpinorMomentum[p1l1,
            Num4V[l11]/.solutions[[1]] ]
            DeclareSpinorMomentum[m1l1,
             -Num4V[l11]/.solutions[[1]] ]
            (...)
```

```
In[66]:=    d1 = (GGG[{1,+1},{p1l2,+1},{m1l1,-1}]*
            GGG[{p1l3,-1},{m1l2,-1},{2,+1}]*
            GGG[{p1l4,+1},{m1l3,+1},{3,-1}]*
            GGG[{m1l4,-1},{4,-1},{p1l1,+1}] )// N
```

```
Out[66]=    -44.3725+383.834 i
```

with (...) meaning that the command was truncated for readability.
The second solution gets contributions from the sixth signature as follows,

```
In[67]:=    DeclareSpinorMomentum[p2l1,
             Num4V[l11]/.solutions[[2]] ]
            DeclareSpinorMomentum[m2l1,
             -Num4V[l11]/.solutions[[2]] ]
            (...)
```

```
In[68]:=    d2=(GGG[{p2l2,-1},{m2l1,-1},{1,+1}]*
            GGG[{m2l2,+1},{2,+1},{p2l3,-1}]*
            GGG[{3,-1},{p2l4,-1},{m2l3,+1}]*
            GGG[{p2l1,+1},{m2l4,+1},{4,-1}] )//N
```

```
Out[68]=    -44.3725+383.834 i
```

Summing both contributions and comparing them to the result given from the previously computed analytical expressions we get,

```
In[69]:=    d=dAaAa+daAaA
```

```
In[70]:=    d1+d2
```

```
Out[70]=    -88.7451+767.667 i
```

56

4.3   Discussion

In this chapter we aimed at illustrating the procedure of box-coefficient extraction for a process that we already showed interest in previously, namely $gg \rightarrow gg$. The calculations were for a specific external polarization but we can easily work all possible ones as the ingredient we'll use for computation will always be the GGG-vertices.

Once the external polarizations fixed, the remaining was the internal ones since the cuts gave us four sub-diagrams and the propagators going on-shell will have to carry polarizations too. The same propagator will be shared between two sub-diagrams and according to a result from chapter 3, depending on the loop momentum flow if the loop momentum is incoming with a specific polarization on some sub-diagram, it will be outgoing and the polarization flips in the second sub-diagram. This constrains the possible configurations we can have reducing the possibilities by a fair number (only six in our case).

We further noticed that since we have four sub-diagrams and loop momenta will participate with two legs out of three in the GGG-vertex, meaning that half of total number will have outgoing loop momenta (4 out of 8) then we simplified it using the fact that $(\pm i)^4 = 1$, to say that we'd have the same result if we consider everything incoming and drop the minuses from the labels. This remark applies for any pure gluonic structure with a box-shape loop. The reason behind this is due to the form of amplitudes being totally constrained by Little-group scaling so that each label with a certain polarization must count two factors that doesn't get simplified which makes the previous count valid in all cases.

The process of calculation consisted of writing the correct product of GGG-vertices, then transform the expression into its close form where everything was gathered in compact spinor chains (or just one big spinor chain if possible). We substitute three of the loop momenta in term of a remaining fourth one and then evaluate for its solutions satisfying the four cut-constraints. The previous was repeated for all six possibilities and we encountered two situations :

1. loop momenta appearing within the spinor chain, e.g. $\langle k...l_i...s]$ with k and s being external momenta.

2. loop momenta appearing at the ends of the spinor chain, e.g. $\langle l_i...l_k]$.

The problem was how to deal with (2) since following the steps we announced earlier will just end up in an error (max iteration limit). That error stems from the fact that the relations between the various loop momenta are written as 4-vectors which could at best be translated into bi-spinors. The bi-spinors have both left- and right-handed indices meaning that if we want to obtain the spinor form, we need to contract one of the indices in the following fashion $l_i\rangle [l_i \longrightarrow l_i\rangle [l_i k]$ with k being another label in our problem. To see the origin of the iteration problem let's suppose that the considered bi-spinor had an expression which we will just symbolically represent, one of its spinors would look like $l_i\rangle = (...) \frac{1}{[l_i k]}$ and it is written in term of the other spinor meaning that Mathematica will engage in an infinite loop trying to write each spinor in term of its chiral conjugate without succeeding to define any of them and trigger a max iteration limit error.

The work around I found was to force the loop momenta to appear within the chain through multiplication by 1. We can choose the ratio of anti-symmetric products in an arbitrary manner

since that multiplication will not mess up the count imposed by Little-group scaling. The freedom of choice leads us to annihilate all diagrams that presented this pathology leaving us with contributions from (1) only.

The final expression for the box-coefficient linked to a pure-gluon topology was built out of two contributions which shows the degree of simplifications induced by on-shell methods at level of intermediate calculations. This encourages for an algorithmic implementation once possible arising errors have been spotted and understood as to their nature and dealt with through contingent treatment (as illustrated by previous paragraphs).

Another error one can find especially for vanishing terms is that they are read to be divergent by Mathematica while in fact the expressions are made so that they vanish faster than they diverge. One way to explain it is that, when presented with a fraction Mathematica checks the denominator first and deliberates afterward on the status of the expression. A work around here would be to check the numerator first if it gives zero then the whole term is vanishing while if it is not, then we supplement with the denominator and save the whole expression as contributing.

We concluded our application with a numerical check where we solved for the cut-conditions numerically and verified if the obtained analytical expressions agree with the numerical results. Fortunately, the result was positive confirming the analytical solutions we employed for the massless cut-conditions. This confirmation is an important step, as we can consider the massless regime to be entirely spanned by these solutions in the case box-loops.

Conclusion

Throughout this thesis we formulated the answer as to the affinity of the Helicity method with NLO corrections starting from an insight that operated mainly at LO level, namely that in the absence of mass our amplitudes might be written entirely using Helicity spinors. These Helicity amplitudes have the advantage of reducing the workload by taking away the complexity of intermediate calculations.

In chapter 1, we started by giving an overview of the QCD sector of the Standard Model along with a list of its Feynman Rules. Then, we explored Helicity formalism in its massless case where we translated all quantities (arising in amplitudes) in term of Helicity spinors, starting from real 4-momenta down to external states (both bosonic and fermionic). The inconveniences we faced at this point were the varying conventions and notations between all the references we consulted, plus some notational inconsistencies when it comes to handling Dirac spinors. After ample reflection, the deliberation went in favor of adopting the convention given in Schwartz [6] then supplement it with the additions when needed. For the Dirac spinors we chose an embedding that respects their 4-dimensionallity and gives the correct contractions when put them with the Dirac matrix. The next step involved the inclusion of mass, where we first constructed massive 4-momenta and then worked on fermionic external states employing the Light Cone Decomposition procedure which was further tested to restore all properties linked to massive Dirac spinors. We again showed the relevance of adopting the previous embedding for the Dirac spinors and were able to generalize many of the identities found in the massless case to the massive one. QCD being a theory of massive spin one-half fermions interacting with massless spin one bosons, meaning that with much of what was presented earlier every quantity appearing in a QCD amplitude could be written only using Helicity spinors leading us to the notion of a Helicity amplitude. We concluded this chapter with the study of concepts like Maximum Helicity Violating amplitudes and crossing symmetries through an example. The application consisted in computing the cross-section of the $gg \longrightarrow gg$ process usually involving over 1000 terms in just few steps manually to show the powerful simplifications we have access to using the Helicity formalism.

Chapter 2 was marked by the introduction of Complex Momenta with the intention of using Helicity formalism on internal states by forcing them to be on-shell. Since unphysical states won't even appear in the final result meaning that they get simplified somewhere in the intermediate steps. An advantage of on-shell methods is that these states are automatically excluded from the get-go as they are always off-shell. The first important result we obtained from the usage of complex momenta was the amplitude expression of most relevant Kinematic 3-points (GGG & GQQ vertices). The second was a recursion rule enabling us to combine the 3-vertices in order to construct tree amplitudes. To put everything at work we implemented the usage of the recursion rules in two cases showing that we can construct tree-level amplitudes from basic Kinematic 3-points, a powerful alternative to Feynman-diagram based method. The implementation went smoothly as both S@M and SpinorsExtras have a function reproducing the BCFW-*shifts* on spinor expression for both massless and massive spinors. The massive case presented an increase in the workload of no significant difficulty as we had the ***RefSimplify[...]*** command finding the simplest

and most compact form for our expression containing reference momenta.

Chapter 3 represented the core of our work where we showed how the concept of Unitarity could link the NLO to LO via Cutkosky cut-rules then we fused it with on-shell ideas by solving the cut conditions for massless complex momenta leading us to the notion of Generalized Unitarity. Further additions came from perturbation theory where we noticed that any one-loop amplitude could be decomposed or at least reduced along a basis of *Master integrals* with associated coefficients obtained through cuts on loop propagators putting them on-shell. The one-loop formulation for Helicity amplitudes was based on determining these cut-coefficients being the product of tree amplitudes resulting from the cuts performed on a loop-topology. We first treated the box coefficients as they presented no difficulty since the system of massless cut conditions had exact solutions. The issues in the triangle case originated from the remaining degree of freedom in solving the conditions for the loop momentum. Finite singularities were present in the coefficients and identified as box-contributions (regions where the topology looked like a box one). We had to get rid of them by first finding the values at which they arise. The search for such poles was done by exposing a propagator (illustrated as "pinching") in order to generate a fourth condition to make use of our ability to exactly solve the box-case.

In the last chapter, we presented a detailed procedure for the extraction of box-coefficients relevant to the NLO correction for the $gg \longrightarrow gg$ process along with a detailed discussion about the various issues we encountered in our usage of the S@M package and how we made sense of them up to the final result.

All of the chapters were built around the simple logic of providing one asset at a time while making sense of its range of application and shortcomings. What we found at the end was that the determination of the coefficient defining the NLO problem was ultimately linked to the fundamental Kinematic 3-points written in term of Helicity spinors, meaning that all the calculations we do will be of use in determining the next ones.

Perspectives

Through this modest research work, we were able to gauge how large were our steps in covering the ground spanned by our topic so to suggest further directions of inquiry.

- Complete the massive case by treating bosonic external states (polarizations), then apply the Helicity formalism to the Electroweak sector.

- Study of remaining loop-topologies, their pole structure along with the extraction of their corresponding coefficients and the rational terms.

- Develop a package that combines both the philosophy of FeynCalc/FeynArt and the capabilities of S@M/SpinorsExtras.

Appendix A

Massive and massless Spinors

A.1 Dirac spinors

All of the relations that are given in this first section were taken from Schwartz book on QFT[6], while the rest has been derived.

Dirac equation,

$$(\not{p} - m)\, u(p) = 0. \tag{A.1}$$

Dirac spinors,

$$
\begin{aligned}
u_s(p) &= \begin{pmatrix} \sqrt{p\cdot\sigma}\,\xi_s \\ \sqrt{p\cdot\overline{\sigma}}\,\xi_s \end{pmatrix} \\
v_s(p) &= \begin{pmatrix} \sqrt{p\cdot\sigma}\,\eta_s \\ -\sqrt{p\cdot\overline{\sigma}}\,\eta_s \end{pmatrix}
\end{aligned}\ \ ., \tag{A.2}
$$

with $\xi_1 = \eta_1 = \begin{pmatrix} 1 \\ 0 \end{pmatrix}$ and $\xi_2 = \eta_2 = \begin{pmatrix} 0 \\ 1 \end{pmatrix}$. Their barred counter-parts are obtained through the prescription $\overline{\psi} = \psi^\dagger \gamma^0$.

Normalization,

$$
\begin{aligned}
\overline{u}_s(p) u_{s'}(p) &= 2m\delta_{ss'} \\
\overline{v}_s(p) v_{s'}(p) &= -2m\delta_{ss'}
\end{aligned}\ . \tag{A.3}
$$

Closure,

$$
\begin{aligned}
\sum_{s=1}^{2} u_s(p)\overline{u}_s(p) &= \not{p} + m \\
\sum_{s=1}^{2} v_s(p)\overline{v}_s(p) &= \not{p} - m
\end{aligned}\ . \tag{A.4}
$$

A.1.1 Diracology

Dirac matrix,

$$\gamma^\mu = \begin{pmatrix} & \sigma^\mu \\ \overline{\sigma}^\mu & \end{pmatrix}, \tag{A.5}$$

with $\sigma^\mu = \{1, \overrightarrow{\sigma}\}$ and $\overline{\sigma}^\mu = \{1, -\overrightarrow{\sigma}\}$.

The fundamental anti-commutation relation,

$$\{\gamma^\mu, \gamma^\nu\} = 2g^{\mu\nu}, \tag{A.6}$$

from which we can derive that $\gamma^\mu \gamma_\mu = 4$.

The trace of an odd product of $gamma's$ vanishes,

$$Tr\,(odd\#\gamma's) = 0. \tag{A.7}$$

The $gamma - 5$ matrix,

$$\gamma^5 = i\gamma^0\gamma^1\gamma^2\gamma^5, \tag{A.8}$$

with $\left(\gamma^5\right)^2 = 1$ and $\{\gamma^5, \gamma^\mu\} = 0$.

Its trace gives us,

$$Tr\left(\gamma^5\right) = 0.$$

The product of a $gamma-$matrix with a 4-vector object gives us its slashed version,

$$\gamma^\mu p_\mu = \not{p}. \tag{A.9}$$

The product of two slashed objects is given by this identity,

$$\{\not{a}, \not{b}\} = 2a \cdot b, \tag{A.10}$$

which in the case where $a^\mu = p^\mu$ and $b^\mu = p^\mu$, we get $\not{p}\not{p} = p^2$.

The traces involving the slashed objects reduce to traces over $gamma-$matrices with momentum factors, meaning that an odd product of slashed momenta will vanish (see above) leaving us only with even products,

$$\begin{aligned} Tr\,(\not{a}\not{b}) &= 4a \cdot b \\ Tr\,(\not{a}\not{b}\not{c}\not{d}) &= 4\left[(a \cdot b)\,(c \cdot d) - (a \cdot c)\,(b \cdot d) + (a \cdot d)\,(b \cdot c)\right] \end{aligned}. \tag{A.11}$$

A.2   Chirality, Helicity and Spin

Often misunderstood, Chirality in our context isn't related to the notion of mirror image. It refers to a theory being one that is not symmetric under the interchange of the (A, B) representations with the (B, A) representations where $A \neq B$ and the $(,)$ are Lorentz representations labeled with a combination of two integers or half-integers. Recalling that the Dirac spinor is a doublet of two Weyl spinors, one is left-handed and the other is right-handed, the handedness of a spinor is referred to as, "Chirality",

$$\begin{aligned} \gamma^5 &= i\gamma^0\gamma^1\gamma^2\gamma^3 \\ \gamma^5 &= \begin{pmatrix} -1 & 0 \\ 0 & 1 \end{pmatrix}, \end{aligned} \tag{A.12}$$

where the left- and right-handed spinors are eigenstates of γ^5 with eigenvalues ∓ 1.

The projectors are built as follows,

$$\begin{aligned} P_R = \frac{1+\gamma^5}{2} \qquad &\qquad P_L = \frac{1-\gamma^5}{2} \\ P_R \begin{pmatrix} \psi_L \\ \psi_R \end{pmatrix} = \begin{pmatrix} \psi_L \\ 0 \end{pmatrix}; \quad P_R &\begin{pmatrix} \psi_L \\ \psi_R \end{pmatrix} = \begin{pmatrix} 0 \\ \psi_R \end{pmatrix}. \end{aligned} \tag{A.13}$$

To go further and link this concept with the next one that is Helicity, we write the Dirac equation,

$$\begin{pmatrix} -m & i\sigma^\mu \partial_\mu \\ i\overline{\sigma}^\mu \partial_\mu & -m \end{pmatrix} \begin{pmatrix} \psi_L \\ \psi_R \end{pmatrix} = 0. \tag{A.14}$$

In Fourier space,

$$\begin{aligned} -i\sigma^\mu \partial_\mu \psi_R = \sigma^\mu p_\mu \psi_R = (E - \overrightarrow{\sigma} \cdot \overrightarrow{p})\psi_R = m\psi_L \\ -i\overline{\sigma}^\mu \partial_\mu \psi_L = \overline{\sigma}^\mu p_\mu \psi_L = (E + \overrightarrow{\sigma} \cdot \overrightarrow{p})\psi_L = m\psi_R \end{aligned} \ . \tag{A.15}$$

We see that the mass mixes left- and right-handed states. Dropping the mass term by setting $m = 0$, with $E = |\overrightarrow{p}|$,

$$(|\overrightarrow{p}| - \overrightarrow{\sigma} \cdot \overrightarrow{p})\psi_R = 0 \implies \frac{\overrightarrow{\sigma} \cdot \overrightarrow{p}}{|\overrightarrow{p}|}\psi_R = +\psi_R. \tag{A.16}$$

This makes left- and right-handed states eigen-vectors of the operator $h = \frac{\overrightarrow{\sigma} \cdot \overrightarrow{p}}{|\overrightarrow{p}|}$ with eigen-values ∓ 1 respectively, just as with the γ^5. The h projects the spin on the momentum direction, we call it, "Helicity".

The independent solutions to the free equations of motion for massless particles for any spin are the Helicity eigenstates.

For "any" spin we'll always find

$$\overrightarrow{S} \cdot \overrightarrow{p} \Psi_s = \pm s |\overrightarrow{p}| \Psi_s \tag{A.17}$$

where the $\overrightarrow{S}$ are the rotation generators in the Lorentz group for spin s. To summarize, in the free massless case, spin eigenstates are also Helicity eigenstates and Chirality eigenstates.

A.3 Helicity spinors

Knowing that momenta transform more naturally in $\left(\frac{1}{2}, \frac{1}{2}\right)$ representation of the Lorentz group, which involves both left- and right- handed representations implying that there is a decomposition we can apply on 4-vectors in general to obtain them in a more fundamental format[1]. Following from what was previously advanced, any four vector object can be converted into a bi-spinor. This conversion takes up the components of the vector and puts them in a compact format that is a 2x2 matrix, which also is made up of four elements. The integrity of the information isn't affected since we moved it from a container to another with the same capacity. A bi-spinor is an object with hybrid double spinor indices, where one is right-handed (dotted) and another is left-handed (undotted). Taking a four-vector p_μ we can find its bi-spinor representation through contraction with a sigma matrix,

$$\begin{aligned} p^{\alpha\dot\alpha} = \sigma^{\mu\alpha\dot\alpha} p_\mu \\ p_{\dot\alpha\alpha} = \overline{\sigma}^\mu_{\dot\alpha\alpha} p_\mu \end{aligned} \ . \tag{A.18}$$

Explicitly the bi-spinors are,

---

[1]In what follows I will use the same symbol for objects representing the same quantity, that is, the 4-vector, Weyl spinor and the bi-spinor representing the same quantity will have the same Latin symbol, while our way of telling them apart would focus on the index accompanying it. The 4-vectors will have mid-Greek letters $\{\mu, \nu, \xi, ..\}$, while the left-handed Weyl spinor would get "undotted" early-Greek letters $\{\alpha, \beta, \gamma, ...\}$ and the right-handed ones would get "dotted" early-Greek letters. As for the bi-spinor since they are hybrid of the outer-product (at least in our case) between a left- and right-handed Weyl spinor then we'll keep on using the same conventions for Weyl spinors individually.

$$p^{\alpha\dot{\alpha}} = \begin{pmatrix} p^0 - p^3 & -p^1 + ip^2 \\ -p^1 - ip^2 & p^0 + p^3 \end{pmatrix}$$
$$p_{\dot{\alpha}\alpha} = \begin{pmatrix} p^0 + p^3 & p^1 - ip^2 \\ p^1 + ip^2 & p^0 - p^3 \end{pmatrix} \quad . \tag{A.19}$$

The sigma objects are what encodes the information in this new format and it can retrieve them back to their original form. These are defined with spinor indices left implicit as $\sigma^\mu = (1, \overrightarrow{\sigma})$ and $\overline{\sigma}^\mu = (1, -\overrightarrow{\sigma})$ where $\overrightarrow{\sigma}$ are the Pauli matrices[2]. To get back the original 4-vectors from bi-spinor we use,

$$p^\mu = \tfrac{1}{2}\sigma^{\mu\alpha\dot{\alpha}} p_{\dot{\alpha}\alpha}$$
$$p^\mu = \tfrac{1}{2}\overline{\sigma}^\mu_{\dot{\alpha}\alpha} p^{\alpha\dot{\alpha}} \quad . \tag{A.20}$$

The norm of p^μ writes $p^2 = det(p^{\alpha\dot{\alpha}}) = det(p_{\dot{\alpha}\alpha})$, keeping in mind that we are using the west-coast convention Minkowski metric[3]. In the case, of a light-like four-vector $p^2 = 0 \Rightarrow det(p^{\alpha\dot{\alpha}}) = 0$, the bi-spinor can be written as an outer product of two commuting spinors, which are called, Twistors [27]or Helicity spinors,

$$p^{\alpha\dot{\alpha}} = p^\alpha p^{\dot{\alpha}}. \tag{A.21}$$

This consequence allows us to inject whatever information is contained in the bi-spinor into Helicity spinors enabling us to make use of their mechanisms.

To prove that this decomposition holds we set,

$$p^\alpha = \begin{pmatrix} a_1 \\ a_2 \end{pmatrix}$$
$$p^{\dot{\alpha}} = \begin{pmatrix} b_1 & b_2 \end{pmatrix}$$
$$p^\alpha p^{\dot{\alpha}} = \begin{pmatrix} a_1 \\ a_2 \end{pmatrix} \begin{pmatrix} b_1 & b_2 \end{pmatrix} = \begin{pmatrix} a_1 b_1 & a_1 b_2 \\ a_2 b_1 & a_2 b_2 \end{pmatrix} \quad . \tag{A.22}$$

We can check that $det(p^\alpha p^{\dot{\alpha}}) = a_1 b_1 a_2 b_2 - a_1 b_2 a_2 b_1 = 0$. And by identifying the explicit form of $p^{\alpha\dot{\alpha}}$ with the previous equation and solve for $\{a_1, a_2, b_1, b_2\}$ to get,

$$p^\alpha = \frac{z}{\sqrt{p^0 - p^3}} \begin{pmatrix} p^0 - p^3 \\ -p^1 - ip^2 \end{pmatrix}$$
$$p^{\dot{\alpha}} = \frac{z^{-1}}{\sqrt{p^0 - p^3}} \begin{pmatrix} p^0 - p^3 & -p^1 + ip^2 \end{pmatrix} \quad . \tag{A.23}$$

First we notice that in the case of massless real momenta, $p^\alpha = (p^{\dot{\alpha}})^\dagger$ implying that all the relevant information is held in just one of the Helicity spinors while for massless complex momenta p^α and $p^{\dot{\alpha}}$ are different. Second, the z can be arbitrary since what matter is their product which makes it vanish from the final form, we will later see that this freedom is the origin of an important constraint on the amplitudes at all orders[4].

Working with these objects requires us to know the ways in which we can construct meaningful quantities using them along with techniques to manipulate them. Since our method incites us to search for invariants and express everything in term of them, we will start by writing down the left- and right-handed Lorentz invariants,

---

[2]Explicitly, $\sigma^\mu = \left\{ \begin{pmatrix} 1 & 0 \\ 0 & 1 \end{pmatrix}, \begin{pmatrix} 0 & 1 \\ 1 & 0 \end{pmatrix}, \begin{pmatrix} 0 & -i \\ i & 0 \end{pmatrix}, \begin{pmatrix} 1 & 0 \\ 0 & -1 \end{pmatrix} \right\}$

[3]Space-time signature $(+, -, -, -)$is used in all our formulas in this document.

[4]The form of scaling transformation that z embodies is identified with, Little group scaling.

$$\begin{aligned}\epsilon^{\alpha\beta} p_\alpha q_\beta \\ \epsilon^{\dot{\alpha}\dot{\beta}} p_{\dot{\alpha}} q_{\dot{\beta}} \end{aligned} \quad . \tag{A.24}$$

The ϵ is the totally anti-symmetric 2x2 object with either two left- or right-handed indices, called Levi-Civita symbol. This object works much like the metric tensor g in space-time, that is, we use it to raise or lower spinor indices,

$$\epsilon^{\alpha\beta} = -\epsilon_{\alpha\beta} = \epsilon^{\dot{\alpha}\dot{\beta}} = -\epsilon_{\dot{\alpha}\dot{\beta}} = \begin{pmatrix} 0 & +1 \\ -1 & 0 \end{pmatrix}. \tag{A.25}$$

Here, the index ordering is important since ϵ is an anti-symmetric object, meaning $\epsilon^{\alpha\beta} = -\epsilon^{\beta\alpha}$.

There is one other object we can construct, which is the metric with one index up and one down that we use to change the index without affecting its position,

$$\epsilon_{\alpha\beta}\epsilon^{\beta\gamma} = \delta_\alpha^\gamma. \tag{A.26}$$

Keeping in mind that the $\sigma's$ and ϵ are linked via the following formulas,

$$\begin{aligned} \sigma^{\mu\alpha\dot{\alpha}} = \epsilon^{\alpha\beta}\epsilon^{\dot{\alpha}\dot{\beta}}\overline{\sigma}^\mu_{\dot{\beta}\beta} && \overline{\sigma}^\mu_{\dot{\alpha}\alpha} = \epsilon_{\alpha\beta}\epsilon_{\dot{\alpha}\dot{\beta}}\sigma^{\beta\dot{\beta}}_\mu \\ \sigma^{\mu\alpha\dot{\alpha}}\sigma^{\beta\dot{\beta}}_\mu = 2\epsilon^{\alpha\beta}\epsilon^{\dot{\alpha}\dot{\beta}} && \overline{\sigma}^\mu_{\dot{\alpha}\alpha}\overline{\sigma}_{\mu\dot{\beta}\beta} = 2\epsilon_{\alpha\beta}\epsilon_{\dot{\alpha}\dot{\beta}} \\ \epsilon_{\alpha\beta}\epsilon_{\dot{\alpha}\dot{\beta}}\sigma^{\mu\alpha\dot{\alpha}}\sigma^{\nu\beta\dot{\beta}} = 2g^{\mu\nu} && \sigma^{\mu\alpha\dot{\alpha}}\overline{\sigma}_{\mu\dot{\beta}\beta} = 2\delta^\alpha_\beta\delta^{\dot{\alpha}}_{\dot{\beta}} \end{aligned} \quad . \tag{A.27}$$

In term of these Helicity spinors, we write the "anti-symmetric inner products" as,

$$\begin{aligned} \langle pq \rangle = \epsilon^{\alpha\beta} p_\alpha q_\beta = p_\alpha q^\alpha \\ [pq] = \epsilon_{\dot{\alpha}\dot{\beta}} p^{\dot{\alpha}} q^{\dot{\beta}} = p^{\dot{\alpha}} q_{\dot{\alpha}} \end{aligned} \quad . \tag{A.28}$$

Under this form the angle-brackets refer to left-handed objects while the square-brackets to the right-handed ones, moreover the index format is important. We have linked $\langle AB \rangle \longrightarrow A_\alpha B^\alpha$ and $[AB] \longrightarrow A^{\dot{\alpha}} B_{\dot{\alpha}}$ while any change of the form $A^\alpha B_\alpha \longrightarrow A_\alpha B^\alpha$, would produce a minus $(-)$ sign with the same happening to the right-handed case. The origin of the minus sign cannot come from anywhere except the ϵ (anti-symmetry). We summarize our words in the following formulas,

$$\begin{aligned} \langle pq \rangle = - \langle qp \rangle \\ [pq] = - [qp] \end{aligned} \quad , \tag{A.29}$$

with a direct result from the previous being that,

$$\langle pp \rangle = [pp] = 0. \tag{A.30}$$

The mixed product $\langle |$ and $[\rangle$ vanishes identically because of the perpendicularity of the projectors $P_L P_R = P_R P_L = 0$.

We extend the new notation[5] for a usage that is independent of the explicit representation of the Helicity spinors in this fashion,

$$\begin{aligned} p\rangle = p^\alpha && \langle p = p_\alpha \\ p] = p_{\dot{\alpha}} && [p = p^{\dot{\alpha}} \end{aligned} \quad . \tag{A.31}$$

---

[5]Something to keep in mind is that his correspondence between the notation and the spinors is mainly dependent on how you define the anti-symmetric inner products.

Appendix B

Group theoretic technology

B.1 Little-Group

Poincare group, or the isometry group of Minkowski space, is the construction that account for two fundamental observation about our universe : (1) no place in space-time seems any different from any other place (Translation Invariance) and (2) physics should look the same whether we look to the left or to the right or observe from a moving object (Lorentz Invariance). Any physical theory that we build ought to respect these two symmetries, meaning that particles transform under irreducible unitary representations of the Poincare group [6]. Unfortunately the study of such group brings a complication being that unitary irreducible representation of the Poincare group are all dimensionally infinite[1].

The representation of the full Poincare group is induced by a representation of the sub-group of Poincare that holds a certain momentum fixed, called the Little-group. It has finite dimensional representations. In the massive case, the little-group, holding a certain massive 4-vector fixed is just the group of 3D rotations, SO(3), with finite irreducible representations of spin J with $2J + 1$ degrees of freedom. While in the massless case, the group that holds a massless 4-vector fixed is the isometry group of the 2D Euclidean plane, ISO(2), with finite irreducible representations of spin J with two degrees of freedom for each J.

A situation that illustrates the utility of the Little-group is the determination of solutions that satisfy a certain equation of motion e.g. Dirac solutions, for a specific momentum then generalize them to an arbitrary direction via a Lorentz transformation.

In term of Helicity spinors, the entire set of transformations that preserve the momentum $p\rangle\,[p$ are rescalings,

$$
\begin{aligned}
p\rangle &\longrightarrow z\,p\rangle \\
[p &\longrightarrow z^{-1}\,[p
\end{aligned} \quad ,
\tag{B.1}
$$

implying that the little group transformations must be rescalings of that form.

Each momentum has its associated little-group transformation preserving it. For real momenta, we require z to be a complex phase, but for general momenta z can be any nonzero complex number.

When it comes to polarizations, each gluon with momentum p will have its polarization scaling under the little group associated with p as,

$$
\begin{aligned}
\varepsilon_p^-(r) &\longrightarrow z^2\varepsilon_p^-(r) \\
\varepsilon_p^+(r) &\longrightarrow z^{-2}\varepsilon_p^+(r)
\end{aligned} \quad .
\tag{B.2}
$$

---

[1]One reason particles are naturally described by fields.

Since the reference momentum will be chosen to be another momentum in the problem, the scaling of the amplitude is entirely determined by the external polarizations which constraint the form of the amplitude at all orders enabling us sometimes to guess its form without computing it especially when the number of allowed forms is small[2].

Any amplitude involving polarizations must satisfy [17],

$$\mathcal{A}\left(...,\left\{i\rangle,i\right],h_i\right\},...\right) = z^{-2h_i}\mathcal{A}\left(...,\left\{i\rangle,i\right],h_i\right\},...\right),\qquad (B.3)$$

where h_i is the helicity of the i-*th* particle.

B.2   Handling Color

In writing the amplitude for a QCD process from Feynman rules we notice that, working while carrying along the algebra elements like, structure constants and generators arising from the vertices is just cumbersome. Most of the treatments that happen at first is on the spin part which doesn't affect the color part. Leading us at this point to decompose the amplitude into group-theoretical factors and functions of kinematical variables, we will term partial amplitude.

This division isn't superficial as it turns out that the bits we are separating have some interesting algebraic properties and exhibit interesting symmetries especially for pure gluonic processes [3]. Another benefit of this factorization is seen when it comes to the automation and writing efficient algorithm that work by exploiting our insights.

QCD is based on the gauge-group SU(3), while in common practice we use the generalization of it, that is SU(N) and substitute for N=3 at the end. This way of doing things means that the tricks and simplifications we use aren't just specific to QCD only, but general to any gauge theory based on SU(N). The physics described in our context involves gluons and quarks. The gluons carry an adjoint color index while the quarks and anti-quarks carry fundamental and anti-fundamental indices. All of the algebra involving these is already described in [4] along with the normalization we'll use for the generators.

Although doing group-theoretic calculus might look somewhat daunting at first due to its heavy reliance of indices and how to manage them, a graphical technology called Birdtracks is presented in [28][26] making the work much more intuitive. For the purposes of the next section we shall provide with two graphical identities [29] that will come in very handy.

---

[2]See chapter 2, about GGG-vertex.

[3]Section 27.4, [6].
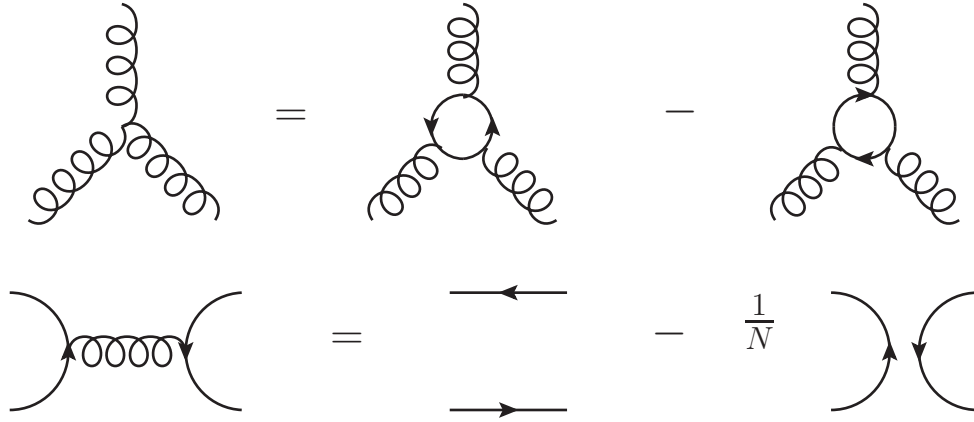
[4]Section 25.1 and 27.2.1, [6].

Figure B.1: Simplifying identities for $SU(N)$

The curly lines represent adjoint indices while oriented lines fundamental ones. The 3-vertex of curly lines represent structure constants and the vertex with one curly line and two oriented solid ones represent the generators of the algebra. As a conclusion before starting to put this interesting idea to practice, through this separation we somehow managed to add more meaning to diagrams representing a process as they are also representative of algebra structure and color interaction manageable via an elegant diagrammatic formalism thus elevating them above the status of just mnemonic graphics.

B.3 Color ordering

A generic Feynman diagram in QCD is composed by mainly three constituents, a pure gluon 3-vertex, a gluon-quark-quark 3-vertex and a pure gluon 4-vertex. Each of these vertices contribute with a color factor.

The identification of possible color structures that can be found along with rules for the construction of kinematic coefficients associated with each color structure is the objective of this section.

While we know that the possible color factor arising from each of the previously mentioned vertex are f^{abc}(structure constants), T^a_{ij}(generators) and $f^{abe}f^{cde}$, we can expose the underlying structure by applying,

$$f^{abc} = -2iTr\left\{\left[T^a, T^b\right]T^c\right\}. \tag{B.4}$$

That is represented by the first graphical identity in the previous section. At this point the generic color pattern we get looks roughly like,

$$Tr\left\{...T^a...\right\}Tr\left\{...T^a...\right\}Tr\left\{...\right\}(...)_{ij}. \tag{B.5}$$

where ... refers some string of T^a's. The traces comes from pure gluon vertices and the generators from the gluon-quark-quark vertex. Contractions of adjoint indices that appear can be reduced using a Fierz rearrangement,

$$\left(T^a\right)_{ij}\left(T^a\right)_{kl} = \frac{1}{2}\left(\delta_{il}\delta_{kj} - \frac{1}{N}\delta_{ij}\delta_{ij}\right), \tag{B.6}$$

represented in the second graphical identity.

These actions can all be carried away diagrammatically starting from the Feynman diagram then systematically apply the previous identities. The end product in the case of a pure gluon situation fully worked in section 27.4 of [6], is that any tree diagram of n-gluon reduces to a sum over single trace terms,

$$\mathcal{A}^{tree}(1,...n) = -2\left(\sqrt{2}ig_s\right)^{n-2}\sum_{\sigma\in S_n/Z_n} Tr\left\{\sigma(1)...\sigma(n)\right\}\widetilde{\mathcal{A}}^{tree}(\sigma(1)...\sigma(n)), \qquad (B.7)$$

where $\widetilde{\mathcal{A}}^{tree}(1,...n)$ is known as the "color-ordered partial amplitude". The determination of the partial amplitude is enough to construct the full amplitude. The Feynman rules here are slightly changed as each 3-vertex has been stripped from the factor $\sqrt{2}ig_s f^{abc}$.

For the case involving quarks we strip the factor $\sqrt{2}g_s T_{ij}^a$ from the gluon-quark-quark vertex. And the generic form of the tree amplitude for a process with two external quarks only and (n-2)-gluons is given in [29]with a slight adjustment to our normalization as,

$$\mathcal{A}^{tree}(1,...n) = \frac{1}{2}\left(\sqrt{2}g_s\right)^{n-2}\sum_{\sigma\in S_{n-2}}\left(T^{a_{\sigma(3)}}...T^{a_{\sigma(n)}}\right)_{i_1 j_2}\widetilde{\mathcal{A}}^{tree}(1_{\overline{q}},2_q,\sigma(3)...\sigma(n)). \qquad (B.8)$$

This method of treating the color part diagrammatically generalizes even to loop-diagrams [30].

Appendix C

Packages and Tools

C.1 S@M/SpinorsExtras

In order to handle the computation of spinor objects that arise throughout the parts of this manuscript both analytically and numerically, we used a combination of two packages that run under Mathematica [31] on top of each other. The first package is S@M [32], which allows the usage of complex spinor-algebra and implements a formalism that is essentially massless along with a possibility to perform BCFW-shift making it very suitable for on-shell techniques. The second package is SpinorsExtras [33] and it runs as an extension of S@M and builds on its functionalities. It adds the possibility to use massive spinors along with the introduction of polarizations and an update of the BCFW-shifts to apply on massive spinors.

The underlying mathematical structure behind these packages is exposed in two published papers [11, 12]. I should point out that the conventions of this manuscript slightly differ from the ones used to make these tools, so appropriate accommodations[1] have been performed in order to maintain consistency throughout the work. As for the installation one has to refer to the documentation and follow the steps. To load S@M we start by indicating the path to where we installed it and then use the **Get[...]** command.

In[72]:=
```
$SpinorsPath="C:\\Users\\Name\\Documents\\Spinors-1.0"
Get[ToFileName[{$SpinorsPath},"Spinors.m"]]
```

Out[72]=
```
C:\Users\Wise\Documents\Spinors-1.0
```

```
-------   SPINORS @ MATHEMATICA (S@M)   -------


              Version:   S@M 1.0 (3-APR-2007)


        Authors:
```

---

[1] *There is a swap between dotted and undotted objects, basically what they refer to as dotted is undotted in our side, which if we think about it could only happen if we swap between right-handedness and left-handedness.*

```
                    Daniel Maitre (SLAC),
                    Pierpaolo Mastrolia (University of Zurich)

           A list of all functions provided by the package
           is stored in the variable
                    $SpinorsFunctions
```

If you get this output, it means that you successfully loaded the package.

SpinorsExtras requires S@M to be already loaded in order to function as it uses most of its functionalities and adapts them for the massive case along with some new additions that we will expose in the latter subsections. Once installed and S@M loaded we only have to evaluate,

In[73]:=
```
           Needs["SpinorsExtras`"]
```

```
           -------  SpinorsExtras  -------

           Version:       1.0.2 (2014.06.18)
           Author:        Jakub Kuczmarski (University of Warsaw)
           Documentation:        Documentation Center    Online version
```

To have this output confirming that we indeed have access to the assets of the package.

Among the plethora of functionalities offered to us we choose to list down the most useful set from both packages to conduct most of the calculations. We separate the functionalities into those that are specific to each package keeping in mind that the architecture of the computational framework is pyramidal, meaning that higher-level packages (SpinorsExtras) build on lower-level ones (S@M) so that the access to functionalities is uni-directional meaning that only higher-level packages have access to lower-level functions and never the opposite.

C.1.1   Mathematica/S@M

The first three important commands are,

In[74]:= `DeclareSpinor[a,b,c]`

In[75]:= `DeclareLVector[p,q,s]`

In[76]:= `SmBA[b,a]`

DeclareSpinor grants the status of complex-spinors to the symbols we pass as arguments to it. Spinor objects are the smallest containers of information we can declare and are set to obey Weyl equation along with basic spinor properties making them eligible to be used in the construction of spinor chains and slashed matrices.

72

DeclareLVector grants the status of a Lorentz vector to the symbols we pass as arguments to it. Lorentz vectors are the biggest containers of information we can declare but they are massless and the meaningful information is reducible to spinor objects. Thus if we already declared a spinor object then all what can be construct using a spinor namely, the *Lorentz Vector* and *Slashed Matrix* is already understood using the same spinor symbol.

SmBA returns a slashed matrix object made of two different spinors (or the same one) passed as arguments. It is useful to note that the ***B*** refers to the box-bracket and the ***A*** to the angled-bracket.

The second set of commands is used in order to clarify how to interpret the symbol in the code when ambiguity arises.

In[77]:= Sp[a]

Sp forces the program to treat the symbol as a spinor object. Integers are built-in spinor objects and can be used without declaration.

In[78]:= Sm[a]

Sm forces the program to treat the symbol as a slashed matrix.

The Minkowski product and the norm of the Lorentz vectors are handled with the functions ***MP*** and ***MP2*** respectively.

In[79]:= MP[p,q]

In[80]:= MP2[p]

Now to the functionalities, we start by how to write various spinor products.

In[81]:= Spaa[a,b]

Out[81]= ⟨a|b⟩

The function ***Spaa*** can take two spinor-objects as an argument to return their anti-symmetric angled product. In case we have more than two arguments, the ones in-between are interpreted as slashed-matrices.

In[82]:= Spaa[a,c,d,b]

Out[82]= ⟨a|c|d|b⟩

The other types of products and spinor chains are given by its sister functions ***Spab***, ***Spba*** and ***Spbb***, where the ***a*** and ***b*** denote the position of the angle and box brackets.

Kinematic invariants are introduced using,

In[83]:= s[i,j]

Out[83]= s_{ij}

The conversion of a spinor product in term of Kinematic invariants and vice versa is implemented simply by double-slashing[2] your expression followed by either ***ExpandSToSpinors*** or ***ConvertSpinorsToS.***

When the expression contains a lot of spinor products and we want to have a compact form in term of spinor chains we use,

In[84]:= `SpClose[⟨1|2⟩ [2|3]]`

Out[84]= `⟨1|2|3]`

when ***SpOpen*** does the inverse.

The Shouten identity is implemented following three algorithm of search-and-replace depending on how many argument you supply it with,

In[85]:= `Shouten[expression,i,j,k,l]`

With four arguments it will search in *expression* for occurrences of the products $\langle ij\rangle\langle kl\rangle$ or $[ij][kl]$ and replace it using the other terms that appear in the identity.

In[86]:= `Shouten[expression,i,j,k]`

With just three it will search in *expression* for occurrences of the products $\langle ij\rangle$ or $[ij]$ and tries to use the identity to combine it with the spinor k.

In[87]:= `Shouten[expression,l]`

This will search for structure like this $\frac{\langle lu\rangle}{\langle ls\rangle\langle lt\rangle}$ and $\frac{[lu]}{[ls][lt]}$ and uses Shouten to split them into partial fractions.

There are two variants to this function that act selectively on either angled-brackets or box-brackets which are ***AShouten*** and ***BShouten.***

Our last and most important function is ***ShiftBA*** which allows us to perform a shift on a given expression with an induced complex parameter z.

In[88]:= `ShiftBA[b,a,z][expression]`

Another mention is that the package puts at our disposal the $\gamma - matrices$ and the projection operators via the the predefined variables ***Gamma0***, ***Gamma1***, ***Gamma2***, ***Gamma3***, ***ProjPlus*** and ***ProjMinus*** which are also treated as slashed-objects and can appear within spinor chains.

The numerical aspect relies on many functions that we will not mention here except one that generates massless momenta that add up to zero which is very convenient since we chose to take all momenta to be incoming.

In[89]:= `GenMomenta[{1,2,3,4}]`

Out[89]= `Momenta for the spinors 1, 2, 3, 4 generated.`

---

[2]expression // function

C.1.2 Mathematica/S@M/SpinorsExtras

The introduction of the massive spinors using the LCD method brings with it a multiplicity in the semantics of a Lorentz vector beyond what we had previously. We now have a reference and an associate vector along with the actual massive vector.

In[90]:= `SpRef[k]`

Out[90]= q_k

In[91]:= `SpAssoc[p,q]`

SpRef labels the reference spinor for the Lorentz vector given as an argument and ***SpAssoc*** labels the associate vector of the massive momentum p undergoing LCD with reference vector q.

In[92]:= `SpM[p,±1]`

SpM labels a u- or v-spinor for massive momentum p where the sign given as a second argument decides about its mass sign. Keeping in mind that in order to use the previous functions, one needs to declare the vectors beforehand using ***DeclareLVector***.

The second new object introduced in this package allows us to handle polarizations in a very clean manner while the implementation goes as far as to be of use even for massive polarization vectors we'll only bound ourselves with massless ones having two possible signs.

In[93]:= `PolVec[k,±1]`

As to the functionalities, we start by ***LightConeDecompose*** which perform LCD on the expression we feed it as a first argument, more control over the procedure is possible through a second argument where we tell it what to decompose exactly.

In[94]:= `LightConeDecompose[expr]`

Polarization can be expanded in term of their reference spinors using ***ExpandPolVec*** that we append to an expression containing polarization vectors by double-slashing it.

The shift suitable for massive spinors as described in [16] are implemented in the new updated function ***ShiftBA*** that we use as before we just feed it two massive vectors instead of massless spinors.

In[95]:= `ShiftBA[p1,p2,z][expression]`

To deal with expressions growing in the length due to reference spinors arising from both polarization and massive spinors the function ***RefSimplify*** helps us find the most compact form of the expression we feed it and can exhibit more complex behaviors suiting our needs since as most functions in this package, it has been coded in a flexible manner. It accepts more than one possible set of arguments and produces different behaviors as broad or as precise as we want it.

In[96]:= `RefSimplify[expr]`

We close this listing of functionalities with a replacement utility.

In[97]:= `ReplaceLVector[expr,x→y]`

In[98]:= `ReplaceSpinor[expr,x→y]`

C.2 Axo/JaxoDraw and Dia

In this section we'll briefly introduce the two technologies we used in creating the figures and diagrams present in this document. I will start by speaking about the program that is external to LaTeX and then turn to the one which actually has a TeX package.

Dia [34] is a multi-purpose diagramming tool with an easy to use interface. It comes with many packages for various types of diagrams and graphical components. This program was used in order to produce cut-diagrams using its fairly intuitive GUI[3] and then export the result in the *.eps* format to include it using *\includegraphics.* Unfortunately this tool can't produce Feynman diagrams and to that end we employed JaxoDraw [35] in conjunction with the TeX package AxoDraw [36]. The workflow is trickier, and for everything to work there are some important things we need to put in place.

JaxoDraw is a Java program that is platform independent and a tool for drawing Feynman diagram in click-and-drag fashion. The generated graphs can be exported in many formats while what interests us is the LaTeX format. After drawing your diagram and inserting equations you export into LaTeX and open the exported file to copy the code that corresponds to your diagram which would look like something like this after we change the *\begin{center}…\end{center}* into *\begin{equation}…\end{equation},*

```
\begin{equation}
\fcolorbox{white}{white}{
\begin{picture}(162,178) (15,-63)
\SetWidth{1.0}
\SetColor{Black}
\Gluon(96,82)(96,18){7.5}{5}
\Gluon(96,18)(48,-30){7.5}{5}
\Gluon(96,18)(144,-30){7.5}{5}
\Text(32,-46)[lb]{\Black{$\nu,b$}}
\Text(160,-46)[lb]{\Black{$\rho,c$}}
\Text(96,98)[lb]{\Black{$\mu,a$}}
\Text(160,18)[lb]{\Black{$\begin{alignedat}{1}= &  gf^{abc}
[g^{\mu\nu}\left(k-p\right)^{\rho}\\
+ & g^{\nu\rho}\left(p-q\right)^{\mu}\\
+ & g^{\rho\mu}\left(q-k\right)^{\nu}]
\end{alignedat} $}}
\end{picture}
}
\end{equation}
```

and we insert the previous code where we want our diagram to be.

The requirements for the compilation are to have the following preambles along with the *axodraw4j.sty* file in your main folder,

```
\usepackage{axodraw4j}
\usepackage{pstricks}
\usepackage{color}
```

and compile the file using *latex>dvips>ps2pdf* instead of *pdflatex* because the package isn't compatible with it.

---

[3]Graphical User Interface

```
latex filename.tex
dvips filename.dvi
ps2pdf filename.ps
```

If one has bibliography the usual workflow would go like,

```
pdflatex filename.tex
bibtex filename.aux
pdflatex filename.tex
pdflatex filename.tex
```

using ***axodraw*** requires that you change ***pdflatex*** to ***latex>...*** as shown earlier.

C.3   CellToTex/mmaCells

This last section of the Appendix is devoted to typesetting Mathematica code in a very faithful way. *CellToTex* [37] is a Mathematica package that provides us with a set of functions converting the cells appearing in the Mathematica notebooks to a specific TEX code compatible with the *mmaCells* [38] package. To use this combination one has to include in the preamble ***usepackage{mmacells}*** and put the ***mmacells.sty*** file[4] in the main folder.

Once the *CellToTex* package installed, we load it using **Needs** command and from there we have two ways of converting cells. The first converts one cell at a time using the following instructions,

```
Needs@"CellsToTeX'"
testCell = Cell[BoxData[MakeBoxes[... put your cell code here ...]],"Input"];
CellToTeX[testCell]
```

The second options converts a whole notebook and to do that we first create a notebook object corresponding to the file we want to convert and then pass it through a small algorithm[5] that convert each input and output,

```
nbObj = NotebookOpen["... path to the notebook.nb ..."]
SetOptions[CellToTeX, "CurrentCellIndex" −> Automatic];
ExportString[NotebookGet[nbObj]/.cell :Cell[_, __] :> Cell[CellToTeX[cell],
  "Final"],"TeX","FullDocument" −> False,
  "ConversionRules" −> {"Final" −> Identity}]
```

As an illustration of usage we give the following,

```
In[99]:=    testCell=Cell[BoxData[MakeBoxes[
            Subscript[x,1]==(-b±Sqrt[b^2-4 a c])/(2 a)]],
            "Input"];
            testCell//CellPrint
            CellToTeX[testCell]
```

$$In[100]:= \quad x_1==\frac{-b\pm\sqrt{b^2-4\ a\ c}}{2\ a}$$

```
Out[100]=  \begin{mmaCell}{Input}
           \mmaSub{x}{1}==\mmaFrac{-b\(\pmb{\pm}\)\mmaSqrt
           {\mmaSup{b}{2}-4a c}}{2 a}\end{mmaCell}
```

---

[4]Obtainable through a light search in internet using the keyword, *mmacells.*
[5]https://tex.stackexchange.com/questions/84748/fanciest-way-to-include-mathematica-code-in-latex

ACKNOWLEDGEMENT

I would first like to thank my thesis supervisor **DR. A. YANALLAH** and co-supervisor **DR. N. BOUAYED** of the Faculty of Sciences at the University of Blida, USDB-1. Both had shown trust in the continuation of my work even with the exceptional global pandemic situation. Their analysis and guidance were crucial to the redaction and completion of this manuscript.

Throughout the past three years both of my supervisors who also happened to be my lecturers had two complementary impacts on my development. The first came from my engaging discussions with DR. YANALLAH who always showed openness and confronted my arguments with constructive criticism. The second made me strive for discipline and consistency as DR. BOUAYED was an inspiring example for both of those qualities. I can't thank them enough for this beautiful opportunity.

I would also like to thank the experts who were involved in the validation survey for this research project: **DR M. SIDOUMOU** as the President of the Jury and **DR. S. A. YAHIAOUI** as the Examiner of this thesis. Without their input, the validation survey could not have been successfully conducted especially during these challenging times.

Bibliography

[1] R.Gastmans and T. T. Wu. *The Ubiquitous Photon Helicity Method for QCD and QED.* Oxford university press, 1990.

[2] M. Y. Benaida and El-M. Berbar. Tree level spinor helicity amplitude formalism for the standard model of electroweak and strong interactions. *Master thesis, USDB-1*, 2019.

[3] S.Glashow. Partial Symmetries of Weak Interactions. *Nuclear Physics*, 22:579–588, 1961.

[4] S.Weinberg. A Model of Leptons. *physical Review Letters 19 1264-1266*, 1967.

[5] A.Salam. Elementary Particle Theory. *367 edited by Svartholm N., Stockholm*, 1969.

[6] M. D. Schwartz. *Quantum Field Theory.* Cambridge University Press, United Kingdom, 2014.

[7] L.D.Faddeev and V.N.Popov. Feynman diagrams for the yang-mills field. *Physics Letters B*, 25:29–30, 1967.

[8] M. Srednicki. *Quantum Field Theory and the Standard Model.* Cambridge University Press, United Kingdom, 2007.

[9] S.Dittmaier. Weyl-van der waerden formalism for helicity amplitudes of massive particles. *Phys. Rev. D*, 59, 1998. arXiv: 9805445[hep-ph].

[10] R. Sattler S. Badger and V. Yundin. One-loop helicity amplitudes for ttbar production at hadron colliders. *Phys.Rev.D*, 83, 2011. arXiv:1101.5947 [hep-ph].

[11] D. Maitre and P. Mastrolia. S@m, a mathematica implementation of the spinor-helicity formalism. *Comput.Phys.Commun.*, 179, 2007. arXiv:0710.5559 [hep-ph].

[12] J. Kuczmarski. Spinorsextras - mathematica implementation of massive spinor-helicity formalism. *arXiv:1406.5612v1 [hep-ph]*, 2014.

[13] L. J. Dixon. A brief introduction to modern amplitude methods. *CERN-2014-008*, pages 31–67, 2013. arXiv:1310.5353 [hep-ph].

[14] F. Cachazo R. Britto and B. Feng. New recursion relations for tree amplitudes of gluons. *Nucl.Phys.*, B715:499–522, 2005. arXiv:hep-th/0412308.

[15] A. Hall. Massive quark-gluon scattering amplitudes at tree level. *Phys.Rev.D*, 77, 2008. arXiv:0710.1300 [hep-ph].

[16] C. Schwinn and S. Weinzierl. On-shell recursion relations for all born qcd amplitudes. *Journal of High Energy Physics*, 4, 2007. arXiv:hep-ph/0703021.

[17] K. Macey and M. Colwell. *Dualities, Helicity Amplitudes, and Little Conformal Symmetry.* Springer Theses, 2008.

[18] S. J. Parke and T. R. Taylor. Amplitude for n-gluon scattering. *Phys. Rev. Lett.*, 56, 1986.

[19] R. E. Cutkosky. Singularities and discontinuities of feynman amplitudes. *Journal of Mathematical Physics*, 1:429, 1960.

[20] F. Cachazo R. Britto and B. Feng. Generalized unitarity and one-loop amplitudes in n=4 super-yang-mills. *Nucl.Phys.*, B725:13, 2005. arXiv:hep-th/0412103.

[21] C. F. Berger et al. An automated implementation of on-shell methods for one-loop amplitudes. *Phys. Rev. D*, 78, 2008. arXiv:0803.4180 [hep-ph].

[22] W. B. Kilgore. One-loop integral coefficients from generalized unitarity. *arXiv:0711.5015 [hep-ph]*, 2008.

[23] D. Forde. Direct extraction of one-loop integral coefficients. *Phys.Rev.D*, 75, 2007. arXiv:0704.1835 [hep-ph].

[24] K.Melnikov R. K. Ellis, Z. Kunszt and G. Zanderighi. One-loop calculations in quantum field theory: from feynman diagrams to unitarity cuts. *Physics Reports*, 518, 2011. arXiv:1105.4319 [hep-ph].

[25] L. J. Dixon Z. Bern and D. A. Kosower. On-shell methods in perturbative qcd. *Annals Phys.*, 322, 2007. arXiv:0704.2798 [hep-ph].

[26] P. Cvitanovic. *Group Theory : Birdtracks, Lie's, and Exceptional Groups.* Princeton University Press, United States, 2008.

[27] R. Penrose. Twistor algebra. *Journal of Mathematical Physics.*, 8, 1967.

[28] S. Keppeler. Birdtracks for su(n). *SciPost Physics Lecture Notes*, 3, 2018. arXiv:1707.07280 [math-ph].

[29] L. Dixon. Calculating scattering amplitudes efficiently. *arXiv:hep-ph/9601359*, 1996.

[30] M. Sjodah and J. Thoren. Decomposing color structure into multiplet bases. *arXiv:1507.03814 [hep-ph]*, 2015.

[31] S. Wolfram. Wolfram mathematica 11.2.0.0. `www.wolfram.com/mathematica/`.

[32] D. Maitre and P. Mastrolia. S@m 1.0. `https://www.slac.stanford.edu/~maitreda/Spinors/`.

[33] J. Kuczmarski. Spinorsextras 1.0.2. `https://www.fuw.edu.pl/~jkuczm/SpinorsExtras/`.

[34] A. Larsson. diaw.exe 0.97.2. `http://dia-installer.de/`.

[35] C. Kaufhold D. Binosi, J. Collins and L.Theussl. Jaxodraw: A graphical user interface for drawing feynman diagrams. version 2.0 release notes. *Comput.Phys.Commun.*, 180, 2008. arXiv:0811.4113 [hep-ph].

[36] J. C. Collins and J.A.M. Vermaseren. Axodraw version 2. *arXiv:1606.01177 [cs.OH]*, 2016. `https://www.nikhef.nl/~form/maindir/others/axodraw2/axodraw2.html`.

[37] J. Kuczmarski. Cells to tex. `https://github.com/jkuczm/MathematicaCellsToTeX`.

[38] J. Kuczmarski. mmacells. `https://github.com/jkuczm/mmacells#installation`.